JOURNAL OF THE AMERICAN

ROCKET

SOCIETY

A journal devoted to rocket technology and the jet propulsion sciences

VOLUME 23 SEPTEMBER-OCTOBER 1953 NUMBER 5

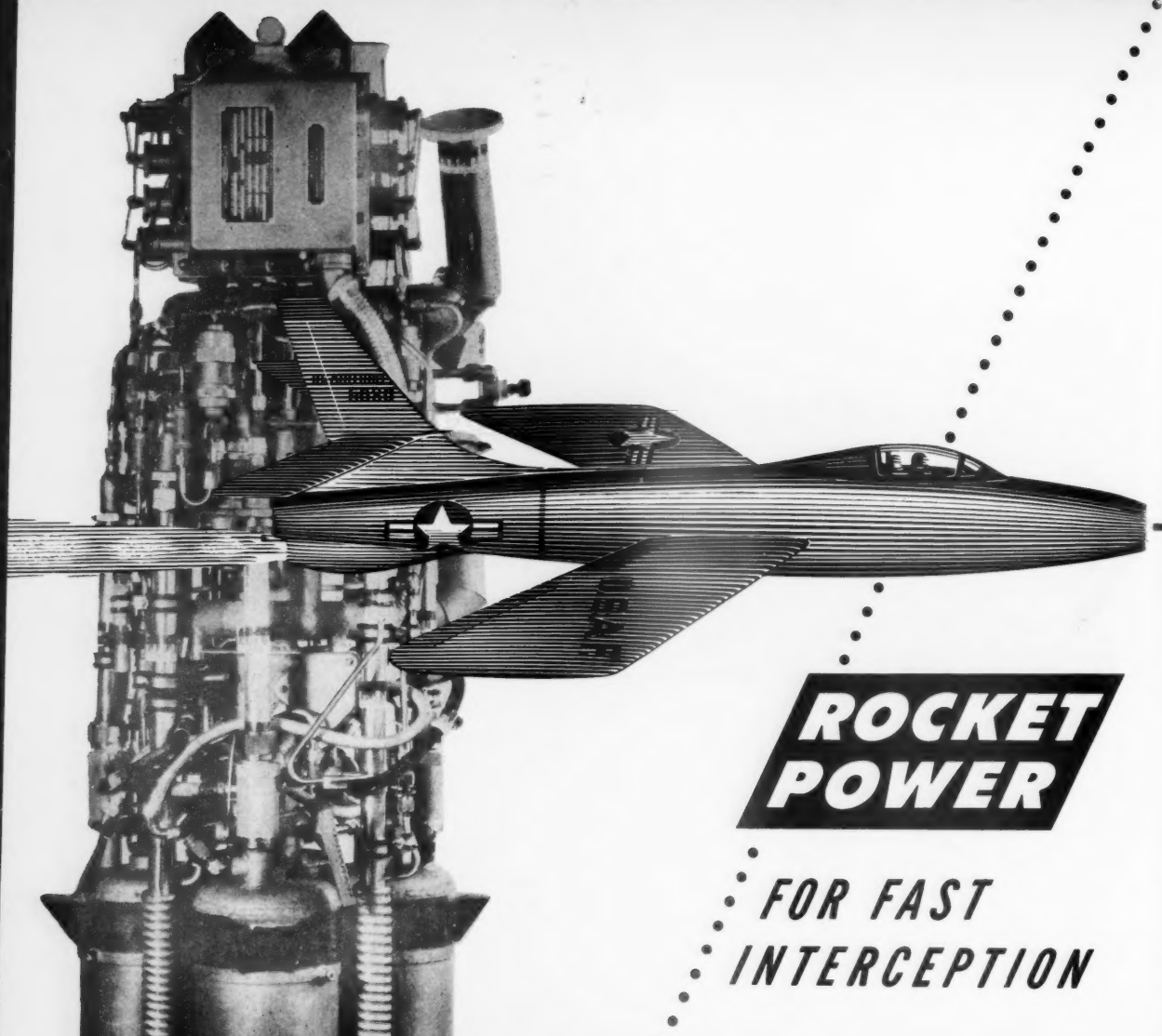

ROCKET POWER

FOR FAST INTERCEPTION

RMI ROCKET POWERED AIR FORCE XF-
INTERCEPTOR TYPE AIRCRAFT

First combat-ready interceptor aircraft
to fly at supersonic speeds in level flight.
RMI 6000 pound thrust rocket engine propels
turbojet-powered Republic XF-91 at Mach 1 plus.

RMI FOREMOST IN ROCKET POWER

REACTION MOTORS, INC., ROCKAWAY, NEW JERSEY

Scope of the Journal

The Journal of the American Rocket Society is devoted to the advancement of the field of jet propulsion through the publication of original papers disclosing new knowledge and new developments. The term "jet propulsion" as used herein is understood to embrace all engines that develop thrust by rearward discharge of a jet through a nozzle or duct, and thus includes systems utilizing atmospheric air and underwater systems, as well as rocket engines. The Journal is open to contributions, either fundamental or applied, dealing with specialized aspects of jet and rocket propulsion, such as fuels and propellants, combustion, heat transfer, high temperature materials, mechanical design analyses, flight mechanics of jet-propelled vehicles, astronautics, and so forth. The Journal endeavors, also, to keep its subscribers informed of the affairs of the Society and of outstanding events in the rocket and jet propulsion field.

Submission of Manuscripts

Manuscripts should be submitted in duplicate to the Editor-in-Chief, Martin Summerfield, Professor of Aeronautical Engineering, Princeton University, Princeton, N. J. See instructions on the following page.

Security Clearance

Manuscripts must be accompanied by written assurance as to security clearance in the event the subject matter of the manuscript is considered to lie in a classified area. Alternatively, written assurance that clearance is unnecessary should be submitted. Full responsibility for obtaining authoritative clearance rests with the author.

Limitation of Responsibility

Statements and opinions expressed in the Journal are to be understood as the individual expressions of the authors and do not necessarily reflect the views of the Editors or the Society.

Copyright

Subscription Rates

One year (six bimonthly issues)	$7.50
Foreign countries, additional postage	add .50
Single copies	1.25
Special issues, single copies	2.00
Back numbers	1.50

Subscriptions and orders for single copies should be addressed to the Secretary of the Society.

Change of Address

Notices of change of address should be sent to the Secretary of the Society at least 30 days prior to the date of publication.

Explanation of Numbering of Issues

The September 1951 issue was the first of a new series of expanded scope and contents. This series is numbered on an annual volume basis, beginning each year with the January issue as Number 1. Correspondingly, the September issue was Number 5, and since 1951 was the 21st year of publication the new series started with Volume 21, Number 5. This replaced Number 86 of the previous series.

Published Bimonthly by the American Rocket Society, Inc.

Journal of the American Rocket Society, published bimonthly by the American Rocket Society at 20th and Northampton Streets, Easton, Pa., U.S.A. The Editorial Office is located at the Engineering Societies Building, 29 West 39th Street, New York 18, N. Y. Price $1.25 per copy, $7.50 per year. Entered as second-class matter at the Post Office at Easton, Pa., under the Act of March 3, 1879.

THE AMERICAN ROCKET SOCIETY

AIMS The American Rocket Society is a professional engineering and scientific organization devoted to the encouragement of research and development of jet and rocket propulsion devices and their application to problems of transportation and communication. It is actively concerned with various technical aspects of space flight, and at the present time it is also interested in military applications of the reaction principle.

The Society carries out its aims by the following methods:

Represents the jet propulsion profession before the public, promotes interest in jet propulsion and its applications, encourages the formation of regional chapters and student branches where technical conferences may be held.

Publishes and disseminates news, experimental results, and technical information to its members, through the medium of its Journal.

Encourages and aids those actively working in this field by organizing national and regional technical meetings where contributed and invited papers are presented and discussed.

MEMBERSHIP Five types of membership are offered: MEMBER, shall consist of scientists, engineers, persons actively engaged in the field of jet propulsion and rocketry, and others who may be deemed eligible for membership by the Board of Directors; ASSOCIATE, for those interested in the development of jet propulsion and rocketry and who are deemed eligible for such membership by the Board of Directors; STUDENT, for persons not over 25 years of age, interested in the development of jet propulsion and rocketry, who are students of some recognized educational institution. CORPORATE membership shall consist of educational, scientific, industrial, or other corporations or associations interested in the development of jet propulsion and rocketry. Each corporate member shall be entitled to five representatives who shall have the rights and privileges of Members. AFFILIATE CORPORATE membership shall consist of scientific, industrial and other corporations or associations interested in the development of jet propulsion and rocketry to the extent that a part of their activities are directed to that end, directly or indirectly. Each affiliate corporate member shall be entitled to one representative who shall have the rights and privileges of an Associate Member. Furthermore, each affiliate corporate member shall be entitled to four advertisements per year in the JOURNAL in accordance with special advertising rates.

The American Rocket Society is an affiliate of The American Society of Mechanical Engineers. Annual dues, including Journal subscriptions, are: Member, $10.00; Associate, $10.00; Student, $5.00 per annum.

OFFICERS

President	F. C. Durant, III
Vice-President	Andrew G. Haley
Secretary	A. C. Slade
Treasurer	Robert W. Lawrence
General Counsel	Andrew G. Haley

BOARD OF DIRECTORS

Three-year term of office expiring on dates indicated

Kurt Berman, 1955	R. W. Porter, 1953
Noah S. Davis, 1955	C. C. Ross, 1953
Roy Healy, 1955	Martin Summerfield, 1954
G. Edward Pendray, 1954	Raymond Young, 1953
M. J. Zucrow, 1954	

COMMITTEES

Executive Committee	F. C. Durant, III, *Chairman*
Membership Committee	Roy Healy, *Chairman*
Finance Committee	Andrew G. Haley, *Chairman*
Program Committee	Noah S. Davis, *Chairman*
Publicity Committee	D. A. Anderton, *Chairman*

SECTIONS

NEW YORK	Paul F. Winternitz, *Pres.*
SOUTHERN CALIFORNIA	S. K. Hoffman, *Pres.*
INDIANA	M. Botje, *Pres.*
NEW MEXICO-WEST TEXAS	E. E. Francisco, Jr., *Pres.*
WASHINGTON-BALTIMORE	W. A. Webb, *Pres.*
NORTHEASTERN NEW YORK	G. E. Moore, *Pres.*
ALABAMA	G. Henderson, *Pres.*
CLEVELAND-AKRON	D. C. Romick, *Pres.*
ARIZONA	A. R. Tocco, *Pres.*
NORTHERN CALIFORNIA	F. G. Bollo, *Pres.*
CHICAGO	K. H. Jacobs, *Pres.*

INFORMATION FOR AUTHORS

Manuscripts must be double spaced on one side of paper only with wide margins to allow for instructions to printer. Submit two copies, original and first carbon. Include a 100–200 word abstract of paper. The title of the paper should be brief to simplify indexing. The author's name should be given without title, degree or honor. A footnote on the first page should indicate the author's position and affiliation. Include only essential illustrations, tables, and mathematics. References should be grouped at the end of the manuscript; footnotes are reserved for comments on the text. Use American Standard symbols and abbreviations published by the American Standards Association. Greek letters should be identified clearly for the printer. References should be given as follows: For Journal Articles: Title, Authors, Journal, Volume, Year, Page Numbers. For Books: Title, Author, Publisher, City, Edition, Year, Page Numbers. Line drawings must be made with India ink on white paper or tracing cloth. Lettering on drawings should be large enough to permit reduction to standard one-column width, except for unusually complex drawings where such reduction would be prohibitive. Photographs should be clear, glossy prints. Legends must accompany each illustration submitted and should be listed in order on a separate sheet of paper.

Send manuscripts to the Editor-in-Chief, Martin Summerfield, Professor of Aeronautical Engineering, Princeton University, Princeton, N. J.

Rates for Reprints and Covers

For quotations or orders not covered write to the Secretary
Reprints must be ordered when galley proof is returned to the Editor

	4 page	*8 page*	*16 page*	*Covers*
100 copies	$12.00	$20.00	$40.00	$15.00
200 copies	16.00	26.00	50.00	18.00
500 copies	28.00	44.00	80.00	27.00

from White Sands, N.M. to * * *
guided by–

STRATOPOWER
HYDRAULIC PUMPS

High on the list of vital components to home your guided missile to its destination are the STRATOPOWER Hydraulic Pumps. These "muscles" provide the power for guidance, scanning, tracking and control. STRATOPOWER Hydraulic Pumps are used more and more on Rockets, Guided Missiles and Launchers because they pack dependability, performance and power into a minimum of space. Apply these precise conveyors of power to your designs. The experience of years in the aircraft field is back of every STRATOPOWER Pump.

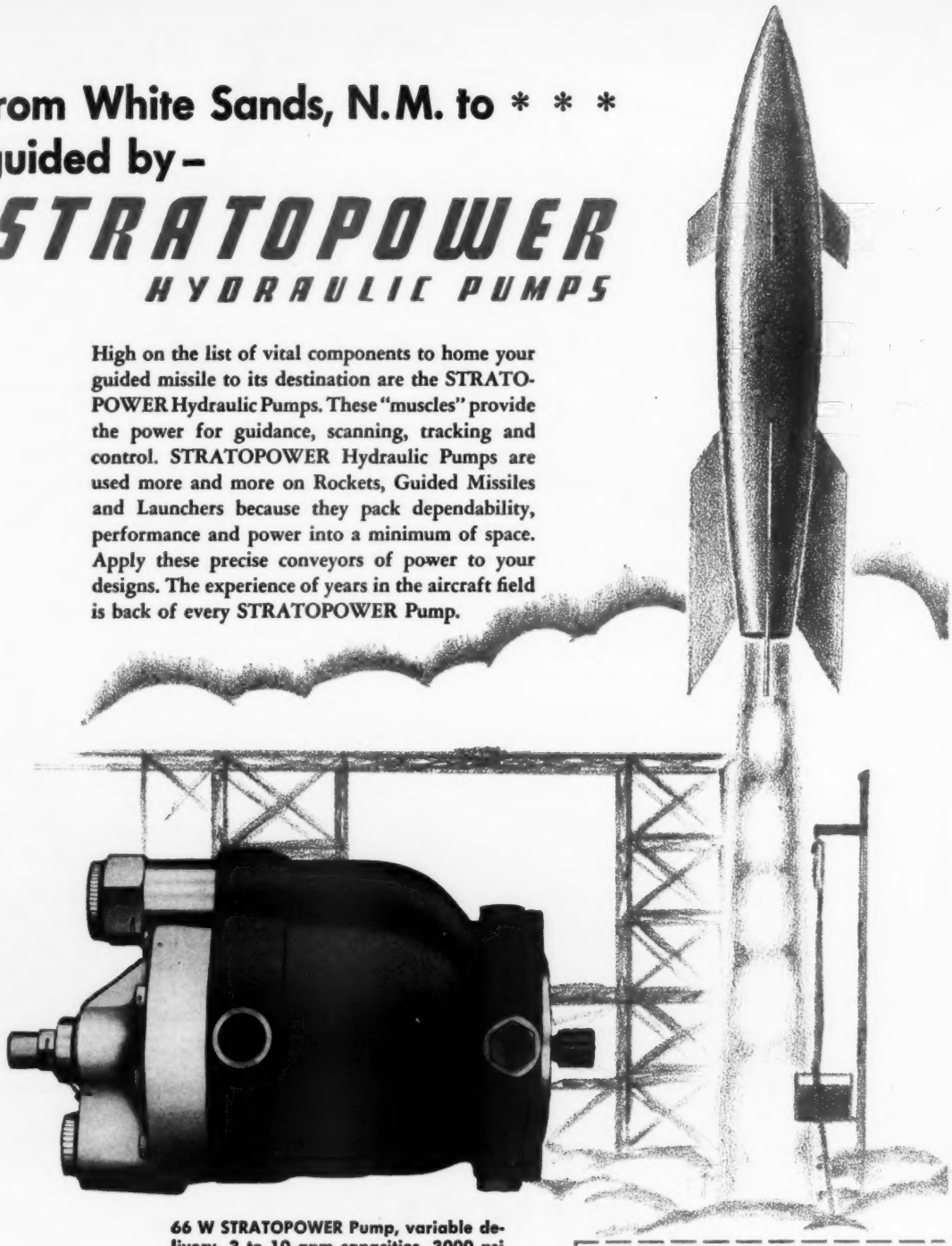

66 W STRATOPOWER Pump, variable delivery, 3 to 10 gpm capacities, 3000 psi at 1500 rpm. Other STRATOPOWER Pumps in constant and variable delivery types. Capacities .25 to 10 gpm provide pressures to 3000 psi.

Write for full information today

WATERTOWN DIVISION
THE NEW YORK AIR BRAKE COMPANY
STARBUCK AVENUE • WATERTOWN • N. Y.

THE NEW YORK AIR BRAKE COMPANY
730 Starbuck Avenue
Watertown, N.Y.

Please send me full particulars on your STRATOPOWER Hydraulic Pumps

Name_____

Company_____

Address_____

City_____ Zone____ State_____

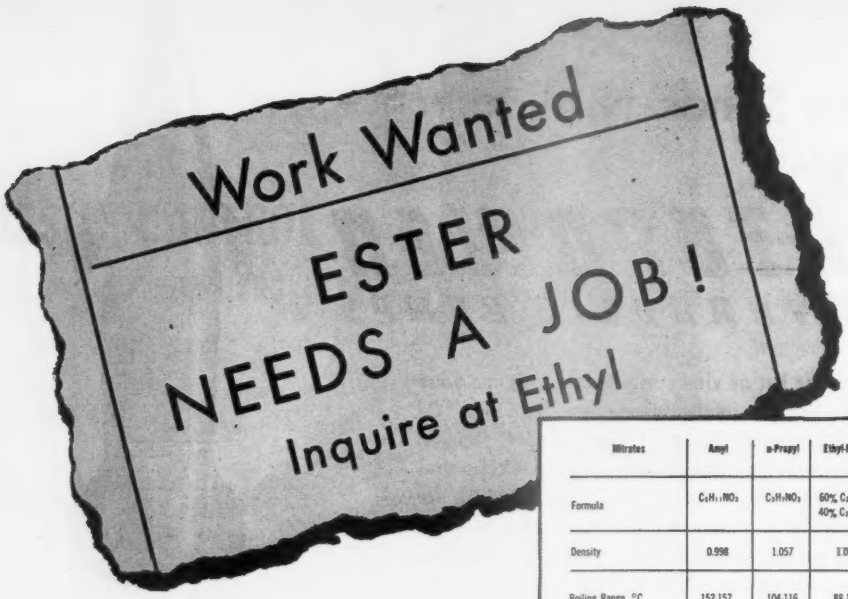

Nitrates	Amyl	n-Propyl	Ethyl-Propyl	Iso-octyl	Decyl	Tridecyl
Formula	$C_5H_{11}NO_3$	$C_3H_7NO_3$	60% $C_2H_5NO_3$ 40% $C_3H_7NO_3$	$C_8H_{17}NO_3$	$C_{10}H_{21}NO_3$	$C_{13}H_{27}NO_3$
Density	0.998	1.057	1.085	0.963	0.943	0.931
Boiling Range, °C	152-157	104-116	88-111	41-43 @ 1 mm	55-75 @ 1 mm	78-89 @ 1 mm
Freezing Point, °C	<-100	<-100	<-100	<-100	<-55	<-55
Flash Point, °F (Open Cup)	125	85	65	205	235	285
Viscosity in Centistokes @ 100°F	0.81	0.51	0.45	1.41	2.07	3.75
Coefficient of expansion per °C @ 20°C	0.00112	0.00095	0.00119	0.00094	0.00090	0.00090
Ref. Index n_D^{20}	1.413	1.397	1.390	1.431	1.438	1.446
Solubility in water (Parts/100) @ 20°C	0.028	0.33	0.567	<0.01	<0.01	<0.01
Impurities, wt. % Water Acid as HNO_3	<.05 <0.001	<.05 <0.001	<.05 <0.001	<.05 <0.001	<.05 <0.001	<.05 <0.001
Odor	Ethereal (Pleasant)	Same	Same	Same	Same (faint)	Same (faint)
Color	White to light straw	Same	Same	Same	Same	Same
Availability	Commercial quantities	Pilot plant quantities	Laboratory quantities	Laboratory quantities	Laboratory quantities	Laboratory quantities

AMYL NITRATE is now available in commercial quantities and NORMAL PROPYL NITRATE in pilot-plant quantities. Four other alkyl nitrates are available in laboratory quantities.

What can these new esters do in your field? They are characterized by low freezing point, favorable odor and color properties, very low water solubility, and low toxicity. They have high solvent power and are miscible with most organic solvents. They are stable in storage and can be shipped as non-explosive material in conventional steel drums.

Ethyl will be glad to work with you in evaluating these new compounds for your own needs, current or prospective. For specific data or samples of any of these new esters, please write us.

ETHYL CORPORATION
Chemicals for industry & agriculture
100 PARK AVENUE, NEW YORK 17, N.Y.

ATLANTA, BATON ROUGE, CHICAGO, DALLAS, DAYTON, DENVER, DETROIT, HOUSTON, KANSAS CITY, LOS ANGELES, NEW ORLEANS, PHILADELPHIA, PITTSBURGH, SALT LAKE CITY, SAN FRANCISCO, SEATTLE, TULSA, MEXICO CITY AND (ETHYL ANTIKNOCK, LTD.) TORONTO.

SEPTEMBER-OCTOBER 1953
VOLUME 23 NUMBER 5

JOURNAL OF THE AMERICAN ROCKET SOCIETY

Editor-in-Chief
MARTIN SUMMERFIELD

A Comparison of Propellants and Working Fluids for Rocket Propulsion

KRAFFT A. EHRICKE[1]

Guided Missile Development Group, Redstone Arsenal, Huntsville, Ala.

A series of chemical propellants and atomic working fluids, covering a wide range of density-specific impulse values, are compared with respect to vehicle performance and design parameters. The changing influence of density and specific impulse with increasing performance is discussed. Ranges for favorable application of different fluids are indicated and their respective limits of applicability shown for ascent in a gravity field as well as for space flight.

Introduction[2]

A CHEMICAL propellant or a working fluid for thermonuclear propulsion determines the mechanical performance of a rocket vehicle through its characteristic values of density and specific impulse. The interesting parameters describing the mechanical performance are cut-off velocity, attained upon termination of powered flight along a given trajectory, and payload weight carried.

The gross weight of a rocket vehicle can be subdivided into payload weight, propulsion fluid weight, and the residual weight which shall be called net weight, to be discussed below.

If, for a certain gross weight, the payload weight and cut-off velocity along a specific trajectory are given, then, by selecting a propulsion fluid, the fluid weight and consequently also the net weight are fixed. Comparison between different fluids will yield different fluid weights, depending on specific impulse and density, and therefore also different net weights. We shall designate this net weight as assigned net weight, since it results from the given gross weight and represents the maximum weight available for the items comprising the net weight. Whether or not the assigned net weight is sufficient for actual construction and flight depends on a more detailed design and project analysis with given fluid and purpose of project, since the fluid density influences the construction weight and the project purpose has a bearing on the weight of auxiliary devices. The net weight resulting from this analysis shall be designated as project net weight.

Received September 23, 1952.

[1] Chief, Gasdynamics Section. Member ARS.

[2] At the time of completion of this study, a paper by H. S. Tsien was published in the JOURNAL OF THE AMERICAN ROCKET SOCIETY, Vol. 22, No. 4, pp. 200–203, which compares the performance of different power plants by a method similar to the one derived in this paper.

If the project net weight becomes larger than the assigned net weight—for a given gross weight—it is technically not feasible to use this particular fluid, unless the cut-off velocity and/or payload weight are lowered.

Comparing several propulsion fluids, one can define an optimum fluid which requires a minimum of fluid weight *and* net weight per unit payload weight. Minimization of the net weight should be understood as reduction of the weight of those items which are influenced by the fluid selection; that is, mainly the power plant weight, determined by propulsion system and tank volume.

Obviously, this fluid is most desirable from a general performance viewpoint. Its rating for a particular project depends on additional considerations of great practical importance, such as economy, availability, handling, storage, transportation, effects on power plant development, and others. These viewpoints have been excluded intentionally in the aforesaid definition, in order to maintain its general validity.

This paper deals with the assigned net weight, or its dimensionless parameter, in relation to propulsion fluid and mechanical performance with the purpose of determining the approximate range of favorable applicability of individual fluids. The conclusions arrived at should be understood in the light of the above remark that, for practical reasons, a different fluid may be found preferable. It is believed, however, that the results may be found useful in that they show which propulsion fluids deserve greatest attention from the viewpoint of research and development in various performance ranges up to interplanetary flight.

General Analysis

For powered flight in a gravity field, vertical ascent only will be considered for the sake of simplicity.

From the fundamental equation of rocket motion, the cut-off velocity is then given by

$$v_1 = gI_{sp} \ln \frac{m_0}{m_1} - gt_1 \quad \ldots\ldots\ldots\ldots\ldots\ldots [1]$$

where v_1 denotes the cut-off velocity, g the gravitational acceleration at the surface, I_{sp} the specific impulse, m_0 and m_1 the over-all mass of the vehicle at take-off and cut-off, respectively, and t_1 designates the burning time, given by the relation

$$t_1 = \frac{I_{sp}A}{C_{a0}} \quad \ldots\ldots\ldots\ldots\ldots\ldots [2]$$

where Λ denotes the loading factor, that is, the ratio of propellant weight over gross weight of the vehicle, and C_{g_0} is the absolute acceleration at take-off in terms of g, defined by

$$C_{g_0} = \frac{F}{g m_0} \quad [3]$$

F is thrust.

The equation for the cut-off velocity can then be written in the form

$$v_1 = g I_{sp} \left(\ln \frac{m_0}{m_1} - \frac{\Lambda}{C_{g_0}} \right) \quad [4]$$

The mass ratio is connected with the propellant density by the relation

$$\frac{m_0}{m_1} = 1 + \gamma_p \phi \quad [5]$$

where γ_p denotes the mean specific weight of the propellant, and ϕ is the propellant capacity factor of the vehicle, defined as the ratio of available propellant container volume per unit empty weight

$$\phi = \frac{v_p}{W_1} = \frac{v_p}{W_0 - W_p} \quad [6]$$

W_p designates the propellant weight.

The loading factor can then be expressed in terms of propellant specific weight and capacity factor

$$\Lambda = \frac{W_p}{W_0} = \frac{\gamma_p \phi}{1 + \gamma_p \phi} \quad [7]$$

The cut-off velocity, as given in Equation [4], depends on specific impulse, mass ratio, loading factor, and initial acceleration. Since the last parameter is of minor interest for this discussion, a given value shall be assumed, say $C_{g_0} = 2$. Then, using Equations [5] through [7], the cut-off velocity becomes

$$v_1 = g I_{sp} \left[\ln (1 + \gamma_p \phi) - \frac{\gamma_p \phi}{2(1 + \gamma_p \phi)} \right] \quad [8]$$

This makes v_1 a function of the interesting parameters I_{sp}, γ_p, and ϕ only.

In order to be applicable for performance calculations, the propellant capacity factor has been defined in Equation [6] in terms of the empty weight of the vehicle. This includes not only the construction weight, but also the payload weight. Therefore, the capacity factor is not strictly a function of the design quality of the vehicle, but depends also on the payload weight carried. The capacity factor can be connected with a weight parameter by the following consideration. Let the net weight of the vehicle be defined by

$$W_N = W_0 - W_p - W_l \quad [9]$$

where W_l is the payload weight. The term W_N comprises the residual weight of the vehicle; that is, construction weight W_c, weight of the auxiliary fluids W_{AF} for energizing the prime mover of the feed system, and additional weight for equipment and installations which cannot be considered as payload and therefore are added to the construction weight to give the net weight. (The term net weight has been preferred to the term empty weight because the latter includes the payload weight.) Although the auxiliary fluid contributes to the overall thrust, its effect is comparatively small and shall be neglected in this case for the sake of simplicity.

Using net weight and propellant weight, a net weight factor can be defined as

$$f_N = \frac{W_N}{W_N + W_p} \quad [10]$$

Using the net weight factor, a simple relation can be derived for the payload factor, defined as ratio of payload weight over gross weight of the vehicle or of the stage under consideration

$$\frac{W_l}{W_0} = 1 - \frac{\Lambda}{1 - f_N} = 1 - \frac{\gamma_p \phi}{(1 - f_N)(1 + \gamma_p \phi)} \quad [11]$$

From Equation [11] the capacity factor follows as function of net weight factor, payload factor, and specific weight of the propulsion fluid

$$\phi = \frac{(1 - f_N)\left(1 - \frac{W_l}{W_0}\right)}{\gamma_p \left[1 - (1 - f_N)\left(1 - \frac{W_l}{W_0}\right)\right]} \quad [12]$$

Substituting the capacity factor in Equation [8] by expression [12], and making the cut-off velocity a dimensionless performance parameter by dividing it by $g I_{sp}$, yield

$$\frac{v_1}{g I_{sp}} = \ln \left(\frac{1}{1 - (1 - f_N)\left(1 - \frac{W_l}{W_0}\right)} \right) - \frac{(1 - f_N)\left(1 - \frac{W_l}{W_0}\right)}{C_{g_0}} \quad [13]$$

In Equation [8] a value of $C_{g_0} = 2$ was inserted.

General Discussion of Parameters

In the preceding analysis, Equations [8] and [13] define the relationship between the three sets of parameters describing the propulsion fluid (γ_p, I_{sp}), the vehicle performance (v_1, W_l/W_0), and the vehicle design (ϕ, f_N). Consequently, for a given performance a set of design parameters can be assigned to each propulsion fluid considered. These assigned values have a considerable practical bearing on the relative merits of the fluid and even on its applicability under given conditions.

The capacity factor indicates the vehicle size required for the particular fluid on account of its density and specific impulse. The net weight factor, in turn, is a function of capacity factor and fluid density if the payload factor is given. This is shown by Equation [11] which takes the influence of vehicle performance into account, since it contains the loading factor. Inspection of Equation [11] shows that for a given payload factor the assigned net weight factor becomes largest for the fluid which requires the smallest loading factor. Indeed, from the viewpoint of technical feasibility this fluid is most favorable, since a large assigned net weight factor facilitates design and construction of the vehicle.

However, the seeming advantage of this fluid over another fluid with smaller assigned net weight factor can be utilized in practice only if the increase in assigned net weight factor is larger than the increase in project net weight factor. This is not necessarily the case. Equation [10], which involves vehicle data only, shows that the net weight factor must increase when only the propellant weight is reduced. If, in addition, the absolute net weight becomes larger, for instance, if the alternate fluid is lighter (heavier feed system, plumbing, insulation, etc.), then the resulting increase of the project net weight factor is even greater. Comparison of the new values obtained from Equations [10] and [11] indicates in the first approximation whether or not the theoretical superiority of the alternate fluid can be made effective in practice In the same manner, different mixture ratios of a propellant combination can be compared.

These considerations apply also when a group of propulsion fluids is compared in the light of increasing vehicle performance. In this case the assigned net weight factors of all fluids will decrease as the performance is increased. In certain performance ranges they will not be within the limits of technical feasibility. These limits will be different for the various fluids. Their exact determination again requires a detailed design analysis. However, knowledge of the correlated capacity factors is useful for a preliminary estimate.

The Capacity Factor

For this reason, it is of interest to study the change of the capacity factor with density and specific impulse for a given cut-off velocity. For this purpose, a number of propellants and working fluids have been considered with the aim of covering a wide variety of values of specific impulse and density. The data as used here are taken from a previous publication in which the performance of various fluids was calculated for shifting equilibrium as function of mixture ratio and pressure ratio (1).[3]

The performance data of working fluids and additional pertinent data are summarized in Table 1. The calculations were based on a temperature before expansion of 3000° K and on a chamber pressure of 20 atm. Two exit pressures were chosen, representing operation at low and high altitude, respectively. For mercury, a higher chamber pressure of 40 atm was taken and the expansion limited to 1 atm, in order to avoid condensation. The mercury values should be considered as approximations only, since thermodynamic data at higher temperatures were not available. For heating up to 648° K a specific heat of 6.52 cal/mole was estimated (2). For mercury vapor, the specific heat of a monatomic gas was taken. This is certainly not correct in the lower vapor temperature range where real-gas corrections would lead to higher values. However, the performance of mercury is low and its application for propulsive purposes would hardly be considered, so that an approximation may be sufficient. Dissociation of diatomic gases was taken into account, except in the case of nitrogen.

The propellants considered are oxygen-hydrogen, a representative of light combinations, ozone-methane, oxygen-ammonia, oxygen-hydrazine, designating medium propellants, and hydrazine with the heavy oxidizers, nitric acid (RFNA), tetranitromethane, and chlorine trifluoride. Except in the combination with ozone, only hydrogen and hydrogen-nitrogen fuels were used, since they yield a higher specific impulse than most carbonaceous fuels and, in the case of hydrazine, show a favorably high density. Methane is especially useful in combination with ozone, since its boiling point lies 50 centigrades below that of ozone, but still above the freezing point of the latter. The main hazard in using ozone seems to be its explosive vapor rather than the liquid which appears to be stable if kept free from impurities which might act as catalysts (3). Arranging the ozone tank inside the methane tank would reduce the vapor pressure of ozone to 12 mm of mercury, using the vapor pressure data given in reference (4), when the vapor pressure of methane is 1 atm (5). In combination with methane the use of ozone might become practicable and therefore this oxidizer has been included in the comparison.

Fig. 1 presents the maximum theoretical specific impulse for different expansion ratios of propellants and working fluids, plotted against their mean density or density (working fluids), in liquid state. The mean density of the propellants increases slightly with decreasing exit pressure, since the mixture ratio for maximum specific impulse shifts toward the lean side.

The mixture ratio corresponding to maximum specific impulse is, in most cases, not the optimum mixture ratio for maximum flight performance, except when the densities of both propellant components are similar—as in the case of oxygen-hydrazine. For propellants with greatly different component densities, the mixture ratio for maximum flight performance is considerably closer to stoichiometric—the oxidizer being the heavier component—or even in the range of oxidizer excess. It is not the purpose of this paper to determine these optimum mixture ratios. However, for reasons of comparison, a particularly notable case, that of oxygen-hydrogen, is included. The performance of this propellant is shown in Fig. 1 for the mixture ratios yielding maximum spe-

[3] Numbers in parentheses refer to References on page 296.

TABLE 1 CHARACTERISTIC AND PERFORMANCE DATA OF WORKING FLUIDS FOR THERMONUCLEAR PILE PROPULSION

Working fluid	Formula	p_c (atm)	T_c (°K)	M_c (—)	H_c (kcal/kg)	p_e (atm)	T_e (°K)	M_e (—)	H_e (kcal/kg)	ΔH (kcal/kg)	$(\Delta H)^*$ (kcal/kg)	I_{sp} (sec)	$\gamma\rho$ (g/cm³)	I_d (kg sec/liter)
Hydrogen	H_2	20	3000	1.98	11,167	1.0	1616	2.016	4833	6334	12,125	742.3	0.071	52.7
						0.1	861	2.016	2043	9124	12,125	890.9	0.071	63.2
Helium	He	20	3000	4.003	3,384	1.0	903	4.003	782	2602	3,732	475.7	0.13	61.8
						0.1	360	4.003	108	3267	3,732	533.7	0.13	69.4
Nitrogen	N_2	20	3000	28.016	797	1.0	1506	28.016	334	463	892.7	200.7	0.812	163
						0.1	851	28.016	148	649	892.7	237.6	0.812	192.9
Oxygen	O_2	20	3000	31.568	786	1.0	1716	32	368	400	891.7	186.5	1.14	212.6
						0.1	1010	32	178	590	891.7	226.5	1.14	258.2
Argon	A	20	3000	39.94	373	1.0	906	39.94	112	261	435	150.7	1.59	239.6
						0.1	364	39.94	45	328	435	168.9	1.59	268.5
Mercury	Hg	40	3400	200.61	78.2	1.0	777	200.61	12.6	65.6	160.6	75.1	13.546	1017.3
Ammonia	NH_3	20	3000	8.399	2,650	1.0	1450	8.516	1007	1643	3,635	378	0.725	274
						0.1	787	8.516	424	2226	3,635	440	0.68	319
						0.01	412	8.516	93	2557	3,635	471.6	0.68	341.9
Hydrazine	N_2H_4	20	3000	10.534	2,117	1.0	1562	10.647	893	1224	2,080.6	326.3	1.011	329.9
						0.1	857	10.647	388	1729	2,080.6	387.8	1.011	392
						0.01	452	10.647	102	2015	2,080.6	418.7	1.011	423.3
Water	H_2O	20	3000	17.173	1,761	1.0	2179	17.85	1108	653	2,401	238	1.0	238
						0.1	1552	18.016	683	1078	2,401	306.2	1.0	306.2

p_c, T_c, M_c = pressure, temperature, molecular weight before expansion.
p_e, T_e, M_e = pressure, temperature, molecular weight after expansion.
H_c = enthalpy of gas before expansion.
H_e = enthalpy of gas after expansion.
$\Delta H = H_c - H_e$, enthalpy converted during expansion.
$(\Delta H)^*$ = heat energy required to convert liquid from state in tank to state before expansion.
I_d = density impulse = $\gamma_p I_{sp}$.

cific impulse at the respective pressure ratios and for stoichiometric ratio, $r = 7.94$, where r designates the weight ratio of oxidizer to fuel. This mixture ratio has a higher density, but it is not the correct optimum value which lies in the region of large oxygen excess and, therefore, has little practical interest.

The exhaust velocities gI_{sp} and the specific weights of all fluids are listed in Table 2 (see page 294), together with component densities and mixture ratios for the propellant combinations. As nitric acid, RFNA with 15 per cent NO_2 was taken.

The specific impulse of most working fluids is seen to be inferior to that of chemical propellants. The difference is so large in many cases that the gas temperature of the working fluids would have to be raised substantially, in order to obtain comparable values. Notable exceptions are, of course, hydrogen and helium, but also ammonia and hydrazine.

Figs. 2 and 3 show the cut-off velocity obtained as function of the capacity factor for the different propellants and working fluids. Most of the propellants show little difference with the exception of O_2 - NH_3 and O_2 - H_2, both mixture ratios, which require higher capacity factors for equal performance. Since the dimensions of a rocket vehicle are mainly dependent on its capacity factor, these graphs indicate the relative vehicle size required for different propulsion fluids as a function of flight performance. Among the propellants only oxygen-ammonia and oxygen-hydrogen yield a particular increase in vehicle dimensions. The capacity factor of the A-4 (V-2) rocket, using oxygen and diluted alcohol, is about 2.1 cu m per metric ton for a cut-off speed of about 5000 fps. For the same velocity, O_2 - H_2 for maximum specific impulse requires 3.5 cu m/t and $(O_2 - H_2)_{st}$, the stoichiometric mixture ratio, 2.7 cu m/t, which means that the vehicle would be about 70 per cent or 30 per cent larger, in spite of superior specific impulse. The heavy propellants which require the smallest capacity factor at low velocities are replaced gradually, with increasing performance, by combinations of medium density but higher specific impulse. Among the working fluids shown in Fig. 3, the dominant role of density for low-speed vehicles

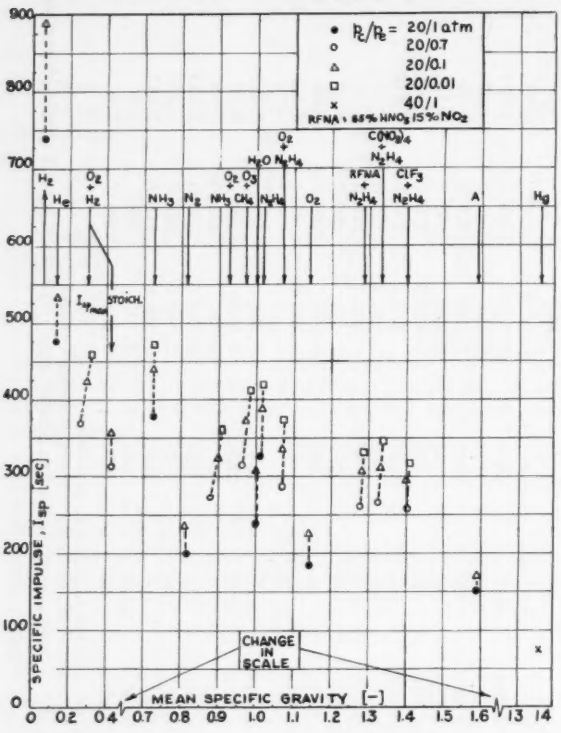

FIG. 1 SPECIFIC IMPULSE VS. DENSITY OF PROPULSION FLUIDS

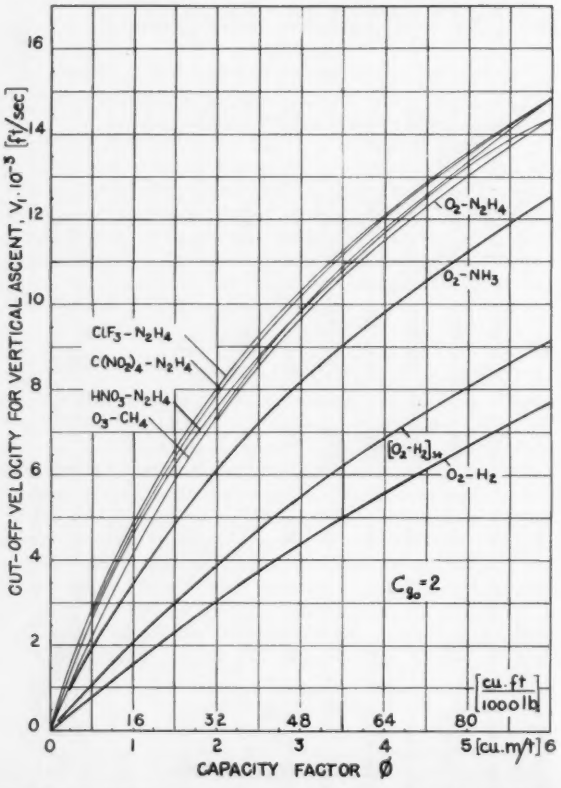

FIG. 2 INFLUENCE OF CAPACITY FACTOR ON CUT-OFF VELOCITY FOR DIFFERENT PROPELLANTS (EXPANSION RATIO 20/0.7 ATM)

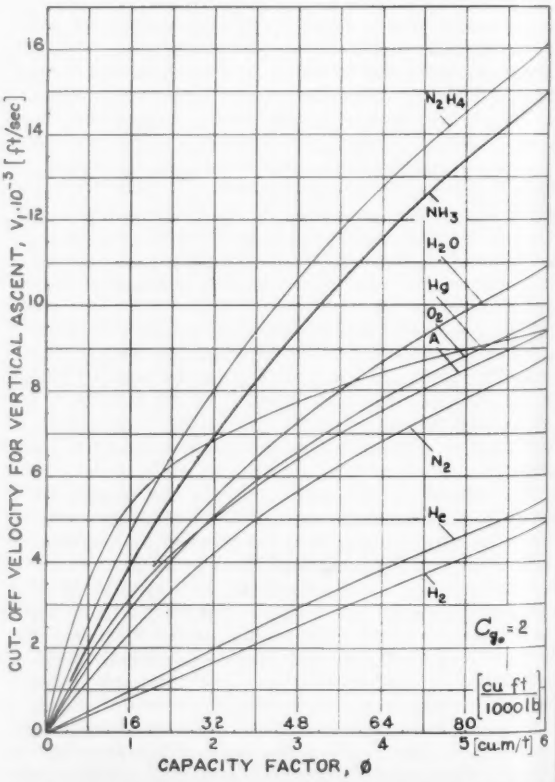

FIG. 3 INFLUENCE OF CAPACITY FACTOR ON CUT-OFF VELOCITY FOR DIFFERENT WORKING FLUIDS (EXPANSION RATIO 20/1 ATM)

and the growing importance of specific impulse are illustrated even more clearly in the case of mercury and argon. Figs. 2 and 3 are based on Equation [8]. The specific impulse corresponds to expansion from 20 to 0.7 atm for the propellants, and 20 to 1 atm for the working fluids.

A wider range of capacity factors is presented in Figs. 4 and 5 which are based on gravity-free powered flight, yielding the so-called ideal velocity at cut-off. This applies to horizontal propulsion in vacuo as, for instance, in the upper stage of satellite vehicles and propulsion of space ships. Due to the special construction of space ships, higher capacity factors will become feasible. The specific impulse and density used for computing Figs. 4 and 5 are based on 20 to 0.1 atm expansion ratio. Equation [8] has again been applied, putting the second term in the brackets equal to zero, since C_{φ_0} formally becomes infinite. The rapidly growing importance of ozone-methane is notable, while the denser propellants now require a larger capacity factor for the same performance. The largest factors still are needed for the oxygen-hydrogen mixtures. Among the working fluids, hydrazine and ammonia are outstanding, followed by water. The curves for hydrogen and helium show the steepest gradient, indicating the rapidly growing importance of high specific impulse.

The changes in Figs. 4 and 5, as compared to vertical ascent, are due to the fact that gravitational losses in Figs. 2 and 3 affect the fluids to a different degree, because constant initial acceleration rather than constant burning time has been assumed. This yields reduced burning time for the light fluids at small capacity factors and for the heavier fluids at large capacity factors. However, constant burning time would have involved a considerable variation of the initial acceleration for the different fluids. This hardly would be practicable in actual operation. Due to the differences in density, the same capacity factor corresponds to a different loading factor (Equation [7]). Therefore, the amount to be subtracted as gravitational loss at vertical ascent (the term Λ/C_{φ_0} in Equation [4]) is different. With increasing loading factor, the natural logarithm of the mass ratio grows more rapidly than the term Λ/C_{φ_0} in Equation [4]. Consequently, vehicles with a large loading factor, using dense propellants, are comparatively less affected. For gravity-free powered flight, in turn, light fluids become comparatively more efficient as far as small capacity factors are concerned.

Comparison between Figs. 2 and 3 and between Figs. 4 and 5 shows that most working fluids require larger capacity factors than the propellants for equal cut-off velocity. Exceptions are hydrazine and ammonia.

Fig. 6 shows the connection between capacity factor and mass ratio for the fluids under consideration. The little circles in this figure terminate the lines corresponding to mixture ratios for pressure ratio 20 to 0.7 atm, used in Fig. 2. The loading factors which correspond to the mass ratios indicated in Fig. 6 can be found immediately, since

$$\Lambda = \frac{(m_0/m_1) - 1}{m_0/m_1} \quad \ldots\ldots\ldots\ldots\ldots\ldots [14]$$

A comparison between Fig. 6 and the preceding performance diagrams reveals the significance of different density and specific impulse in terms of capacity factor and mass ratio. Take, for instance, ClF_3-N_2H_4 and O_2-H_2, both mixture ratios. Fig. 2 shows that for a cut-off velocity of 5000 fps the required capacity factors are, in cubic meters per metric ton

ClF_3-N_2H_4	$(O_2$-$H_2)_{st}$	O_2-H_2
1	2.7	3.5

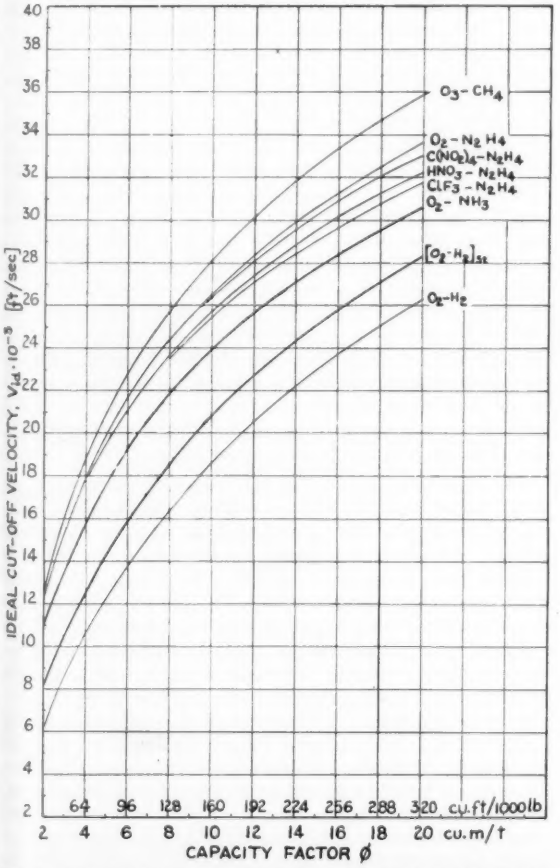

FIG. 4 INFLUENCE OF CAPACITY FACTOR ON IDEAL VELOCITY FOR DIFFERENT PROPELLANTS (EXPANSION RATIO 20/0.1 ATM)

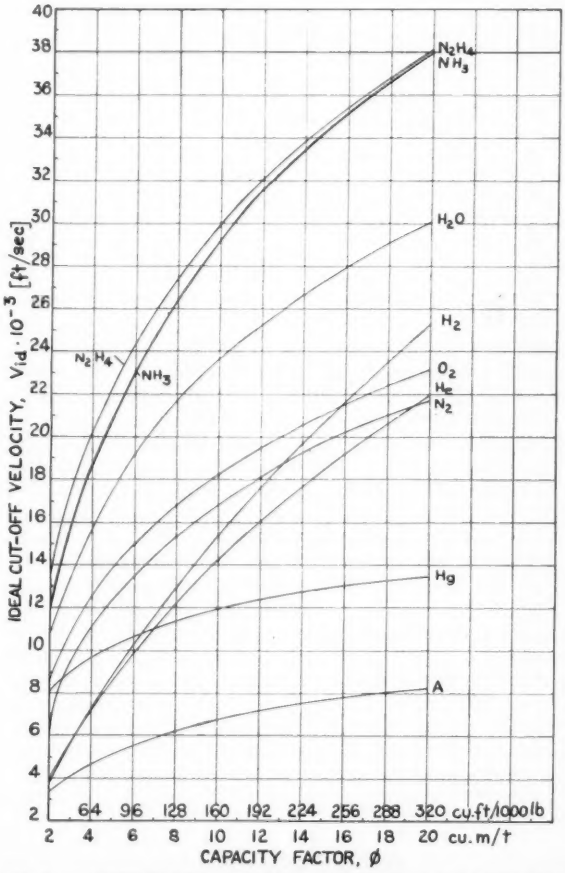

FIG. 5 INFLUENCE OF CAPACITY FACTOR ON IDEAL VELOCITY FOR DIFFERENT WORKING FLUIDS (EXPANSION RATIO 20/0.1 ATM)

The corresponding mass ratios are

2.4	2.14	1.93

In other words, oxygen-hydrogen requires slightly lower mass ratios, but much larger capacity factors.

Comparing this result with a high performance case, assuming, for instance, an ideal velocity of 26,000 fps, the required capacity factors and corresponding mass ratios are, according to Figs. 4 and 6

ClF_3-N_2H_4	$(O_2$-$H_2)_{at}$	O_2-H_2
10.6	16.4	19.6
15.8	8	6.9

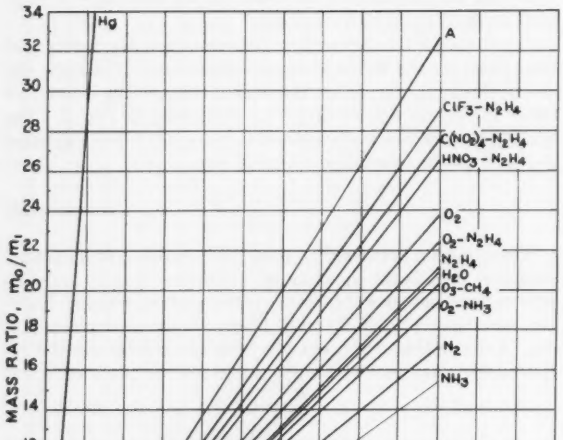

FIG. 6 MASS RATIO AS FUNCTION OF CAPACITY FACTOR

This ideal velocity corresponds approximately to the value required for circumnavigation of the moon, starting from a satellite at 2500 miles altitude and establishing a circular orbit at 30 miles above the surface of the moon.

These two examples illustrate the increasing superiority of lighter propellants of high specific impulse with increasing performance. The difference in mass ratio, hence in loading factor widens. Simultaneously the difference between the respective capacity factors is reduced. Still, the capacity factors indicate that the hydrogen vehicle would become considerably more bulky in either case, particularly in the first example. This would raise practical difficulties in terms of design and transportation. It also means that, in the first example, the oxygen-hydrogen vehicle gross weight will hardly be smaller than that of the ClF_3-H_2H_4 vehicle due to the very large difference in capacity factors. With increasing cut-off velocity the differences in gross weight will be reduced gradually, and eventually the light-propellant vehicle can be expected to have the lower gross weight for a given payload. However, even then this vehicle will have the higher construction weight.

The Net Weight Factor

As pointed out before, the net weight comprises the weight of construction, of the auxiliary fluids and additional weight, W_{ad}, depending on the project purpose. Therefore, the net weight, as defined in Equation [10] is, for a given propulsion fluid, not exclusively a function of the construction weight.

For a given propellant, the net weight factor depends on size and purpose of the vehicle. The factor will decrease with increasing vehicle size, because of the more favorable ratio between volume and surface area. For equal size, the purpose of the vehicle has a decisive bearing on the net weight factor. A ballistic rocket, for instance, can be expected to have a smaller factor than a glider rocket. The A-4 (V-2), a ballistic rocket, has a net weight factor of about 0.28. For its winged version, the A-4b which was fired at Peenemünde in 1944–1945, the net weight factor was about 0.31. Both vehicles were operated with liquid oxygen and diluted alcohol. Smaller net weight factors can be expected for future booster rockets in multistage vehicles. The large planned booster rocket A-10 with a thrust of about 200,000 kg and the A-4b or a similar vehicle as payload stage (13,400 kg) had a net weight factor of not more than 0.24 or 0.25. This version was supposed to use a combination of nitric acid (RFNA) and a heavy crude oil, the mean specific gravity being 1.33 as compared to about 1.0 for oxygen-alcohol.

If the vehicle size is given, the net weight factor decreases rapidly with increasing propellant density. As an example, the Peenemünde rocket project A-8 may be mentioned, which was laid out for nitric acid and crude oil. It had a gross weight of about 22,700 kg at 1000 kg payload. The propellant tank volume was 13 cu m (459 cu ft) and its net weight was about 4420 kg. This yields a net weight factor of roughly 0.2, mainly due to the large propellant weight of 17,300 kg. If the tanks were filled with oxygen-alcohol, keeping the net weight unchanged, the net weight factor would be raised to 0.25. If oxygen-hydrogen, at a mean specific gravity of 0.27, would be the propellant, the net weight factor would become 0.55, keeping the net weight constant. Using oxygen-hydrogen in stoichiometric mixture (mean specific gravity 0.424), the net weight factor would become 0.43, again at constant net weight. These are the effects of changing propellants without consideration of correlated changes in absolute net weight. A net weight increase of the order of 30 and 20 per cent for the lighter and heavier oxygen-hydrogen combination, respectively, would have to be expected, mainly due to increased propulsion system weight and additional insulation. This would raise the net weight to 5500 and 5100 kg, respectively, yielding net weight factors of 0.61 for the lighter and 0.48 for the heavier mixture. These values are considerably higher than the one required for the heavier propellant, although the influence of mixture ratio in the use of oxygen-hydrogen is quite strong.

These examples indicate the magnitude of net weight factors to be expected for present-day vehicles.

For very large vehicles of the future, a substantial net weight factor reduction can be expected. As an example, the weight study for a three-stage vehicle may be mentioned where a winged third stage is supposed to carry 11,000-lb payload into a circular orbit at 138 miles altitude. The main data are summarized in reference (6). In this reference the given propellant weight includes the propellant used for gas turbine feeding (2 per cent). If this propellant is added to the construction weight to obtain the net weight, the net weight factors become about 0.13 for the first stage and 0.11 for the second stage. The first stage was laid out for nitric acid (RFNA) and hydrazine, the second and third stage for oxygen and hydrazine. The absolute initial accelerations assumed were 1.5 g, 1.1 g, and 1.0 g, respectively, for the first, second, and third stage. The net weight factor for the third stage becomes about 0.4, although this vehicle is somewhat larger than the A-4b, having a factor of 0.31. The main reason for this increase in net weight is that the additional weight, due to pressurized cabin, cooling system, landing gear, etc.,

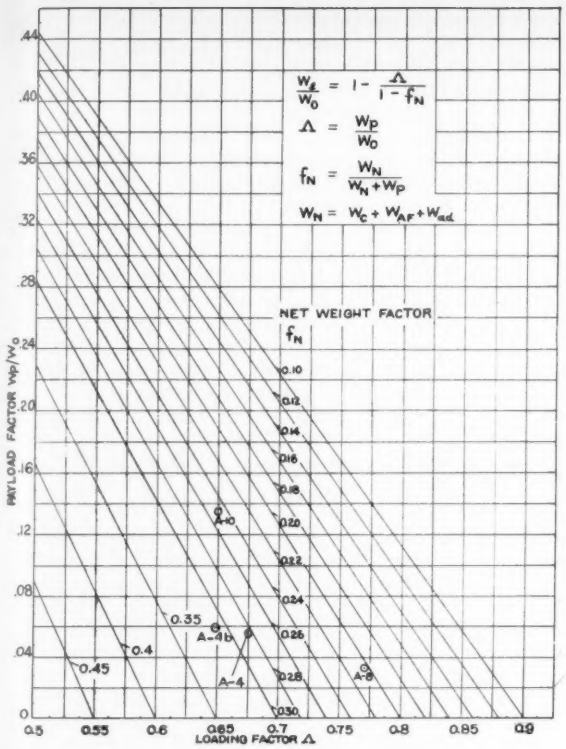

FIG. 7 PAYLOAD FACTOR AS A FUNCTION OF LOADING FACTOR FOR DIFFERENT NET WEIGHT FACTORS

is considerably larger than in an unmanned rocket glider of the guided missile type.

Equation [11], which is of general validity, shows that the payload factor decreases with increasing net weight factor. The exact amount of change depends on the loading factor. In Fig. 7 the payload factor is plotted as a function of the loading factor for different net weight factors. For a given cut-off velocity the loading factor may be decreased if the specific impulse can be increased, allowing for a higher payload factor and/or net weight factor. The plot shows that an increase in net weight factor by the amount mentioned before in connection with oxygen-hydrogen calls for a substantial decrease of the loading factor. That this is difficult to obtain with smaller vehicles was illustrated in the previous section. If the gross weight of the light fluid vehicle is lower than that of the heavy fluid vehicle, as is the case at very great vehicle size, then the payload factor must also be increased, if a given absolute payload weight is considered. This limits the permissible increase of the net weight factor.

Application

From Fig. 2 through Fig. 5 the capacity factor required for using a given fluid can be found as function of the cut-off velocity for vertical ascent. Similar curves can be drawn for ascent along any desired trajectory. A generalized representation, even for a given trajectory, is not possible due to the particular combination of density and specific impulse for each fluid.

The assigned net weight factor can be presented in general form as function of the dimensionless velocity parameter defined in Equation [13]. This is done in Fig. 8 for the two cases of vertical ascent and gravity-free powered flight, taking the payload as parameter. With the aid of Table 2, the assigned net weight factor for a given cut-off velocity and payload factor can then be found immediately for different propulsion fluids. The corresponding capacity factors follow from Fig. 2 through Fig. 5. Of course, for final conclusions the assigned net weight factor must be compared with the project net weight factor to determine the technical feasibility for a given application.

However, it has been seen in the previous sections that the net weight factor decreases with increasing capacity factor. Therefore, knowledge of assigned net weight factor and correlated capacity factor permits at least estimating the relative merits and the range of favorable application of different fluids. This shall be illustrated by a few examples.

A sounding rocket, ascending vertically at 2 g absolute initial acceleration and with a payload factor of 0.05, shall attain a cut-off speed of 7000 fps. The propulsion fluids considered are listed in Table 3. The upper part of this table shows the required capacity factors from Figs. 2 and 3, and from Equation [12], the velocity parameters v_1/gI_{sp}, using Table 2 (expansion ratio 20 to 0.7 or 1 atm, respectively) and finally the assigned net weight factor according to Fig. 8. Again, the application of light fluids appears difficult, since they require capacity factors which are considerably larger than those of heavier fluids, while their assigned net weight factors are not increased in proportion to offset this effect. Moreover, for vehicles using the dense propellants, a design analysis can be expected to yield project net weight factors which are smaller than the assigned values given in Table 3.

Comparing, for instance, $(O_2\text{-}H_2)_{st}$ with $O_3\text{-}CH_4$, it follows that the first propellant yields a vehicle about twice as large at half the mean fluid density of the ozone combination; but practically the same net weight factor is assigned to both ve-

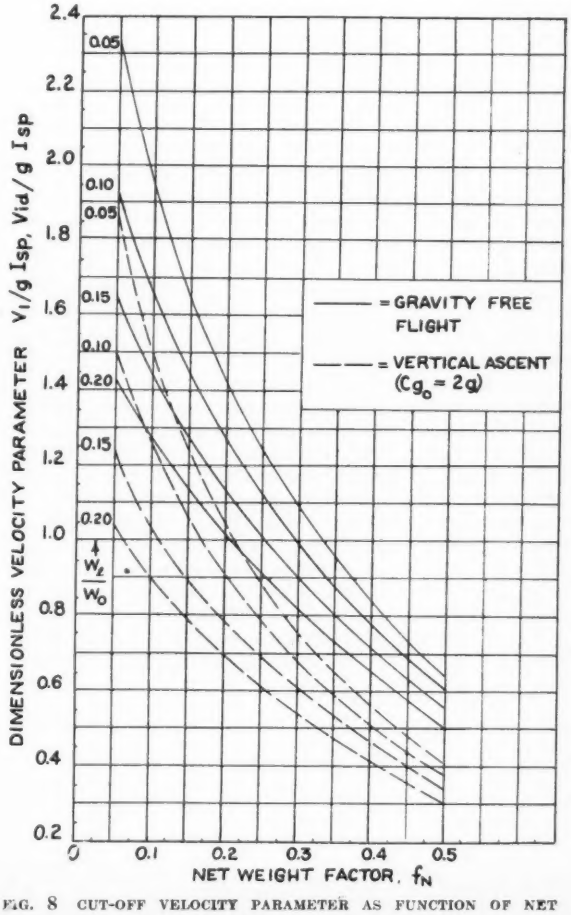

FIG. 8 CUT-OFF VELOCITY PARAMETER AS FUNCTION OF NET WEIGHT FACTOR AND PAYLOAD FACTOR

TABLE 2 CHARACTERISTIC DATA OF PROPULSION FLUIDS CONSIDERED

No.	Propulsion fluid	Expansion ratio (atm)	Mean specific gravity	Exhaust velocity (fps)	Mixture ratio O/F	Component specific gravity* Oxid.	Component specific gravity* Fuel
1	Hydrogen	20/1	0.071	23,902	...	...	...
		20/0.1		28,687			
2	Helium	20/1	0.13	15,317	...	...	...
		20/0.1		17,185			
3	Ammonia	20/1	0.68	12,272	...	...	...
		20/0.1		14,168			
4	Oxygen-hydrogen (max. spec. impulse)	20/0.7	0.266	11,914	3.6	1.14	0.071
		20/0.1	0.30	13,556	4.4		
4a	Oxygen-hydrogen (stoichiometric)	20/0.7	0.424	10,110	7.94	...	...
		20/0.1	0.424	12,560	7.94		
5	Hydrazine	20/1	1.01	10,507	...	...	...
		20/0.1		12,487			
6	Ozone-methane	20/0.7	0.96	9,963	2.9	1.71	0.424
		20/0.1	0.97	11,946	2.96		
7	Oxygen-hydrazine	20/0.7	1.065	9,177	0.8	1.14	1.01
		20/0.1	1.07	10,819	0.92		
8	Oxygen-ammonia	20/0.7	0.88	8,791	1.32	1.14	0.68
		20/0.1	0.90	10,401	1.4		
9	Tetranitromethane-hydrazine	20/0.7	1.32	8,501	1.42	1.65	1.01
		20/0.1	1.33	9,982	1.6		
10	RFNA-hydrazine (RFNA: 85HNO_3-15NO_2)	20/0.7	1.276	8,372	1.4	1.57	1.01
		20/0.1	1.28	9,821	1.44		
11	Chlorine trifluoride-hydrazine	20/0.7	1.4	8,275	1.9	1.76	1.01
		20/0.1	1.4	9,467	1.9		
12	Water	20/1	1.0	7,190	...	...	...
		20/0.1		9,860			
13	Nitrogen	20/1	0.812	6,462	...	...	...
		20/0.1		7,651			
14	Oxygen	20/1	1.14	6,005	...	...	...
		20/0.1		7,293			
15	Argon	20/1	1.59	4,852	...	...	...
		20/0.1		5,438			
16	Mercury	40/1	13.546	2,418	...	...	...

* For liquefied gases the density at 1 atm vapor pressure was used.

hicles. It is very obvious in this case that O_3-CH_4 would be preferable from the viewpoint of vehicle performance. Also, in comparison to the other propellants, oxygen-hydrogen would be inferior in the present example, even if its assigned net weight factor would technically be feasible, which is doubtful.

Comparing the propellants with the working fluids, it is rather obvious that, in this performance range, they cannot compete with the propellants. This applies to hydrogen in particular, since it appears very unlikely, in view of the supposedly heavy atomic propulsion system, that a net weight factor of 0.51 could be realized at all. Ammonia and hydrazine would impose less severe problems from the design viewpoint, but also in their case the assigned net weight factors seem inadequate for actual construction. Among the heavier propellants, ozone-methane would be outstanding, since its density is but slightly lower than that of oxygen-hydrazine, while its assigned net weight factor is comparatively much larger. The difference between the oxygen and nitric acid combination with hydrazine is small at this performance level. Preference of either one would be influenced by other factors.

As a second example, assume a space ship capable of attaining an ideal velocity of 20,000 fps with a payload factor of 0.10. The same fluids shall be compared. Their relevant data are listed in the lower portion of Table 3. The picture has changed greatly, as compared to the previous example. The increase in capacity factor for hydrogen is very small, since no gravity losses occur in this case. The net weight factor of the oxygen-hydrogen ships is now about one third and one fourth, respectively, of that of the hydrogen ship, while in the previous example they were better than one half of this value. The change is due to inferior specific impulse and to a larger payload factor. Nevertheless, the higher density of oxygen-hydrogen and the smaller propulsion system weight would make this propellant at least equivalent to hydrogen, let alone greater simplicity of design. The data also show that oxygen-hydrogen could compete with nitric-acid-hydrazine in this performance range. This was not the case in the previous example. However, it still would be inferior to ozone-methane and to oxygen-hydrazine, leaving these medium propellants in the highest bracket. As in the previous example, ozone-methane appears to be the best propellant because of its favorable combination of specific impulse and density. Oxygen-hydrazine and oxygen-hydrogen have gained in importance while nitric-acid-hydrazine has lost its high rating. Among the working fluids, ammonia and

TABLE 3 COMPARISON OF PROPULSION FLUIDS

Fluid→	H_2	NH_3	O_2-H_2	$(O_2$-$H_2)_{SI}$	N_2H_4	O_3-CH_4	O_2-N_2H_4	RFNA-N_2H_4
			v_1 (fps):	7000 (W_l/W_0 = 0.05)				
ϕ (cu m/sec)	9	2	5.3	4.13	1.66	1.85	1.89	1.77
v_1/gI_{sp}(−)	0.294	0.571	0.59	0.691	0.666	0.705	0.765	0.836
f_N(−)	0.59	0.394	0.38	0.33	0.345	0.325	0.297	0.27
			v_1 (fps):	20,000 (W_l/W_0 = 0.10)				
ϕ (cu m/sec)	14.25	4.6	11.4	9.3	3.95	4.5	5.0	5.3
v_1/gI_{sp}(−)	0.695	1.41	1.48	1.594	1.605	1.68	1.84	2.03
f_N(−)	0.447	0.16	0.14	0.113	0.11	0.095	0.065	<0.05

hydrazine probably are superior to hydrogen, in spite of lower assigned net weight factors, because of much higher density. Generally the position of the working fluids with regard to the chemical propellants is greatly improved in comparison to the previous example. Already the data of the heavy working fluids appear competitive when compared with nitric-acid-hydrazine or even oxygen-hydrazine, disregarding development problems. More detailed specifications depend on an exhaustive comparison of atomic and chemical propulsion system weight requirements, but the general tendency is apparent.

If interplanetary flight shall ever rise beyond the status of occasional scientific expeditions, it seems necessary, for instance, to exploit valuable deposits on other celestial bodies, preferably on satellites and asteroids which could be contacted directly by space ships. Their payload factor must be as high as possible for economic exploitation. If possible, no auxiliary ships should be needed, to avoid loss of costly engines, particularly if atomic piles are used. This means that still higher ideal velocities must be required for the individual space ship. For a trip to the inner moon of Mars, e.g., which requires about the lowest of all ideal velocities for interplanetary flights, the over-all value would be about 41,000 fps when leaving from an artificial satellite. Assume, as a third example, this ideal velocity and a payload factor of 0.2. Inspection of Fig. 8 shows that even a hydrogen atomic pile ship is allowed only a net weight factor of about 0.055 for accomplishing this performance. For all the other fluids considered, the net weight factor would be zero already, long before this ideal velocity could be attained, even at smaller payload factors. This means, if such a ship can ever be built at all, the working fluid would have to be hydrogen.

These three examples verify what was previously revealed tentatively in Figs. 2 through 5, namely, that high density is important and necessary for vehicles of comparatively low cut-off speeds. As the mechanical performance is increased, specific impulse gradually becomes more important and ultimately emerges as the decisive parameter.

Solving Equation [11] for f_N, the assigned net weight factor for a certain payload factor can be found if the loading factor or the capacity factor is determined for a given value of v/gI_{sp} from Equation [4] or [8]. Thus the significance of Fig. 8 can be specified for any desired propulsion fluid, as it has been done in the afore-mentioned three examples for a few selected fluids. The result can be plotted as net weight factor versus cut-off velocity. Such a graph is shown in Fig. 9 for vertical ascent and for a payload factor of 0.10. The highest net weight factors are assigned to the lightest fluids, since they yield the smallest loading factor. Those portions of the curves which are represented by solid lines indicate the favorable range of application; that is, the range in which the assigned net weight factor is likely to satisfy the technical requirements. Within the performance range covered in Fig. 9, the upper four fluids have little chance for favorable application. An atomic rocket using hydrazine might become applicable in the upper range of cut-off speeds considered in Fig. 9. For speeds between 7000 and 10,000 fps, ozone would be a favorable propellant A similar range applies for oxygen-hydrazine, while the heavier propellants may be applied more favorably in a somewhat lower range of speeds. Due to lower specific impulse and density and because of the presumably heavier weight of the atomic pile unit, working fluids such as water and nitrogen would require net weight factors of the order of 0.4 at least. This, in principle, would make these fluids eligible for a lower speed range between 2000 and 6000 fps. Actually, of course, this range is occupied by technically more preferable propellants such as oxygen-alcohol or acid-aniline, which are not considered in the graph. The specific impulse of nitrogen is similar to that of these two propellants which, however, have higher density and can be used in propulsion systems already developed. Mercury theoretically would fall in a similar velocity range. Its net weight factor would be extremely small. Fig. 9 shows that, with the possible exception of hydrazine as working fluid, atomic propulsion systems, in fact, would be of no advantage in this performance range, since chemical propellants are available which do as good or better. If may be emphasized that the solid portions of the curves are only very rough indications of favorable ranges of application and do not imply accurate limitations.

For velocities exceeding those considered in Fig. 9, either one of the upper five fluids would become eligible or, if heavier propellants are used, the vehicle must consist of more than one stage.

Considering the propulsion fluids as density-impulse points (Fig. 1), one can visualize these points sliding down on the net weight factor scale as the performance is increased. All points are high up when the vehicle performance is small. They cannot rise above $f_N = 1$, hence must be crowded at the upper end of the scale. Many fluids are available for selection to suit specific projects. In general, that fluid is most favorable, from the viewpoint of performance, which, for a given gross weight, yields the highest ratio of assigned net weight factor over project net weight factor. With increasing vehicle performance, the points slide down on the net weight factor scale and begin to spread, since the light fluids with high specific impulse drop less rapidly. Since there is a lower technical limit for the net weight factors connected with each fluid (namely, when the ratio of assigned over project net weight factor becomes less than one), the heavy propellants are the first to drop below this limit. They become principally inapplicable when they pass this limit at zero payload factor. This selective effect gradually leaves a higher percentage of light fluids for practical application as the performance is increased. Eventually only hydrogen remains, and thereafter either the multistage principle must be applied or

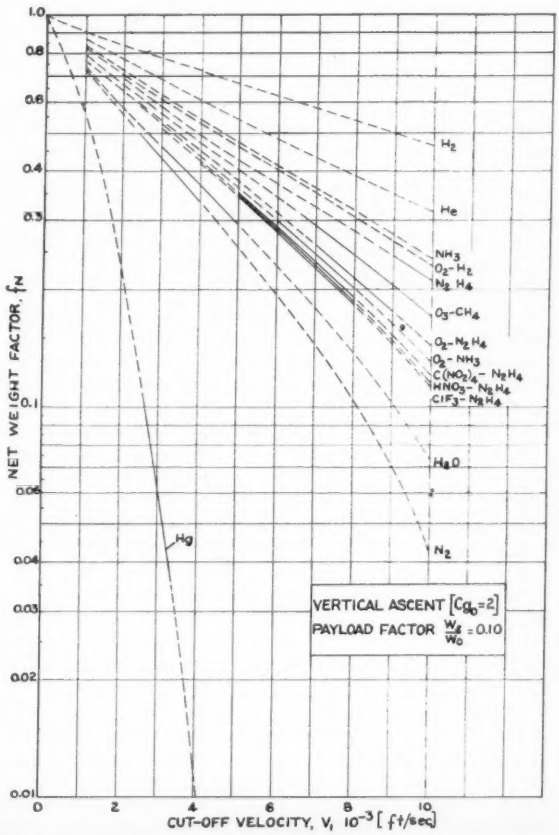

FIG. 9 NEW WEIGHT FACTOR AS FUNCTION OF CUT-OFF VELOCITY

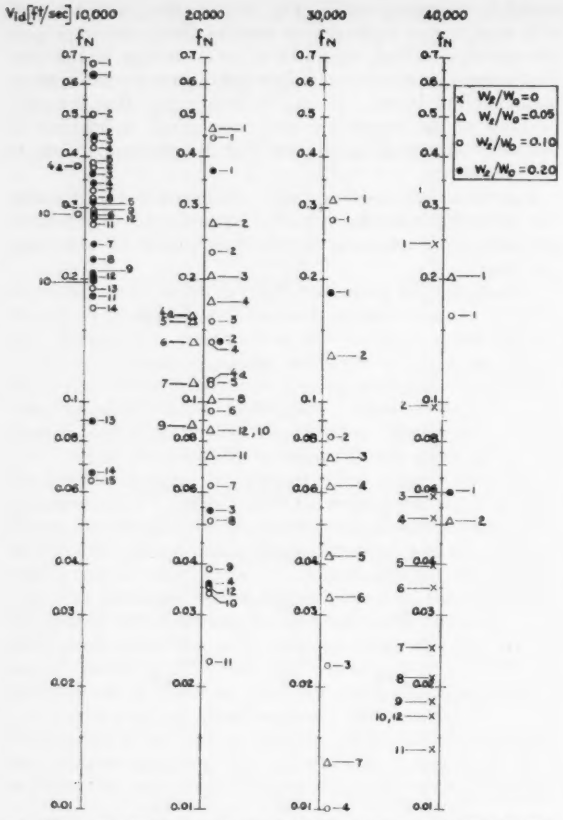

FIG. 10 NEW WEIGHT FACTOR FOR DIFFERENT IDEAL VELOCITIES

different methods of propulsion (for instance, high-speed ion jets) must be considered.

The process described before is illustrated in Fig 10 for space flight conditions. The fluids are designated by numbers in accordance with Table 2. In order to show the influence of the payload factor, three values, 0.05, 0.10, and 0.20, are represented. The assigned net weight factors corresponding to zero payload factor are indicated for several fluids. These points determine the highest possible loading factor for the space ship using the particular fluid at the given ideal velocity.

It can be seen that now, in contrast to Fig. 9, some working fluids, particularly hydrazine, ammonia, helium, and finally hydrogen become considerably superior to all propellants, including oxygen-hydrogen. While there is a wide variety of fluids available at 10,000 fps, their number is reduced considerably at 20,000 fps. At this ideal velocity, ammonia and hydrazine, at a payload factor of 0.1, possess the highest density among the fluids shown in the net weight factor range between 0.1 and 0.3. Ozone-methane and oxygen-hydrogen appear as favorable propellants and also oxygen-hydrazine may still be applicable. Between 20,000 and 30,000 fps, a range which comprises the energy requirements for circumnavigation of the moon when departing from an artificial satellite, most propellants cease to apply with the possible exception of ozone-methane and oxygen-hydrogen for small payload factors. At 30,000 fps, practically hydrogen and helium alone are available for payload factors above 0.05. At 40,000 fps, hydrogen alone can accommodate payload factors above 0.05. In other words, unless the payload factor is very small ($W_L/W_0 < 0.05$), chemical propellants apply for ideal velocities up to about 20,000 fps to be attained by a single ship or stage. In the region between 20,000 and 40,000 fps, working fluids definitely become superior to chemical propellants. Particularly between 30,000 and 40,000 fps, only working fluids allow for some net weight at all if the payload factor is above zero. Depending on the weight per unit thrust ultimately obtainable with thermonuclear propulsion systems, hydrazine and ammonia would be very promising working fluids also for terrestrial use in single or two-stage vehicles designed to attain cut-off speeds of the order of 15,000 to 20,000 fps.

Finally, it may be emphasized that the speed range between 35,000 and 41,000 fps represents about the lower speed limit required for interplanetary voyages (Mars) when taking off from an artificial satellite. Thus it is very unlikely that, in the foreseeable future, a single space ship can reach other planets in our solar system. However, by appropriate selection of propellants and especially by developing atomic propulsion, the number of supply ships could be reduced to a minimum, therewith simplifying space flight substantially.

Conclusions

The procedure outlined herein permits a rapid determination of the relative merits and of the range of applicability of propulsion fluids in rockets for different cut-off speeds and payload factors. This is accomplished by evaluating the characteristic capacity factor and net weight factor assigned to each fluid at given cut-off speed and payload factor. Knowing these assigned values, it can be determined by design analysis whether or not, for a given project, their realization is technically feasible.

The method has been applied to a general investigation of chemical propellants and working fluids for atomic propulsion over a wide range of vehicle performance. It was found that up to 10,000 fps cut-off velocity, that is, for most terrestrial applications as well as for satellite operations with multistage vehicles, a large number of propulsion fluids are available. Among them, working fluids are inferior to propellants or at least do not offer practical advantages, unless the payload factor is very high. Among the propellants, heavy and medium combinations appear preferable. If higher speeds are to be attained with single or two-stage vehicles, thermonuclear propulsion systems, preferably using hydrazine or ammonia, are advantageous.

For space flight, chemical propellants have competitive qualities, with emphasis on high specific impulse rather than density, up to ideal velocities of about 20,000 fps or somewhat higher, if payload factors of 0.05 or below are accepted. Aside from technical considerations, their range of applicability is extended, because, in space flight, the initial acceleration can be kept small so that high loading factors become feasible without yielding cut-off accelerations of physiologically prohibitive magnitude. The propellants applicable for these high ideal velocities are ozone-methane, oxygen-hydrogen, or similar combinations, and perhaps oxygen-hydrazine. Beyond 20,000 fps, working fluids become increasingly superior, particularly at payload factors greater than 0.05. Above 30,000 fps they are the only ones that appear technically applicable at all. Beyond ideal velocities of about 40,000 fps, thermal propulsion methods cease to apply unless the ship is refueled en route.

References

1 "Die Grundlagen des Interplanetaren Fluges, Pt. II, Treibstoffe und Arbeitsmedien fuer die Atomrakete," by K. A. Ehricke, *Forschungsreihe der NW Gesellschaft fuer Weltraumforschung*, No. 5, November 1951.

2 "Handbook of Chemistry and Physics," Chemical Rubber Publishing Co., Cleveland, 29th ed., 1945, p. 1724.

3 "Ozon," by E. H. Riesenfeld and G. M. Schwab, *Naturwissenschaften*, vol. 10, 1922, pp. 470–471. Cited in: "Ozone: Preparation and Stability in High Concentrations. Final Re-

(*Continued on page 300*)

The Evaluation of Competing Rocket Power Plant Components for Two-Stage Long-Range Vehicles

A. L. FELDMAN[1]

Consolidated Vultee Aircraft Corporation, San Diego, Calif.

A method for establishing the relative desirability of competing rocket power plant components is developed for long-range, two-stage rocket-powered vehicles. The measure of the desirability proposed is minimum net cost wherein missiles of the same class are required to perform identical functions; e.g., same range carrying the same payload. The relationships developed are derived from simple missile performance parameters and lend themselves to readily calculable results.

Characteristics of a hypothetical two-stage, long-range rocket vehicle are presented, and for this missile exchange rate curves are given which show the order of compromise allowable between weight and efficiency for any power plant component or between competing power plants. Several power plant arrangements are analyzed for this missile, and the proposed technique for establishing desirability is demonstrated.

Nomenclature

ΔF = difference in propellant weight, lb
ΔF_{1-2} = difference in first-stage propellant weight, lb
I = effective specific impulse, sec
m = mass ratio
n = portion of ΔT that is jettisoned
Δp = difference in component weight, lb
ΔP_j = difference in jettisoned component weight, lb
$\Delta R_{f_{3-4}}$ = difference in propellant flow rate required by component in second stage, lb/sec
ΔT = difference in tank weight, lb
t_{3-4} = second-stage burning time, sec
ΔV = difference in tank volume, cu ft
W_0 = gross weight at take-off, lb
W_B = weight at burnout, lb
W_2 = weight at end of first stage, lb
W_3 = weight at start of second stage, lb
$W_{f_{1-2}}$ = weight of propellant consumed during first stage, lb
α = ratio of ΔT to ΔV
ρ = propellant density, lb/cu ft

Introduction

ONE of the major recurrent problems in designing a rocket-powered vehicle is the selection of individual components to make up the power plant. In choosing a component, the missile designer gives consideration to availability, reliability, weight, efficiency, and cost. The first two of these yardsticks are dependent on market conditions and state of the art of the component in question and are outside the scope of this paper. If we limit consideration to quantity-produced vehicles, it would seem that the most sensible step would be to select the component which can perform its function satisfactorily for the minimum cost without affecting the basic missile function. Cost, in this sense, involves not only the price of the component but also the cost penalty of its weight. Some relationship is required which will describe the rate of exchange between component weight and efficiency as a function of the specific weight and performance characteristics of any missile. This relationship should also include terms to evaluate the penalties incurred if other than even exchanges between weight and performance are considered. The penalty could be considered in terms of extra propellant and structure required to permit the missile to carry out its design function when operating with heavier or less efficient components.

The general approach of the work presented in this paper is to consider the effect small changes in component weight and operating efficiency have on required propellant load when maintaining missile range and payload weight. It is assumed that for long-range vehicles, where the drag is small relative to the weight, a reasonable, though approximate measure of the range, for constant initial acceleration, is the parameter $I \ln m$, where I is the average effective specific impulse, and m is the mass ratio. On this basis, for any given missile to maintain constant range, $I \ln m$ must be held constant. If competing components having different operating efficiencies are considered, they will produce a change in the effective impulse and, in order to keep the $I \ln m$ parameter constant, the mass ratio will have to be adjusted. To some extent, it will be immediately adjusted by the change in component weight; but in order to balance the range parameter completely, some change in the weight of propellant carried will probably have to be made. If the costs of propellant and component per pound were known, the net costs of component and propellant differences can be compared to establish the cheapest system to carry the same payload the same distance. If the propellant weight change is greater than the component weight change, there will be a difference in the initial acceleration. For the comparatively small component variations considered in this paper, the results are not greatly affected.

Development of General Relationships

Two basically similar missiles, denoted by the subscripts A and B, will be considered. These missiles will be identical in all respects except for a power plant component which will differ in both weight and efficiency, where component efficiency is measured in terms of the over-all specific impulse. Both missiles will be two-staged and be required to carry the same payload over the same range.

To maintain the same range

$$I_A \ln m_A = \text{const} = I_B \ln m_B \quad [1]$$

which can be rewritten as

$$m_B = (m_A)^{I_A/I_B} \quad [2]$$

By definition

$$m = \frac{W_0}{W_2} \times \frac{W_3}{W_B} \quad [3]$$

Presented at the Seventh Annual Convention of the American Rocket Society, McAlpin Hotel, New York, N. Y., December 5, 1952.

[1] Thermodynamics Engineer. Member ARS.

where W_0 = gross weight at take-off
W_2 = weight at end of first stage
W_3 = weight at beginning of second stage
W_B = weight at burnout

The difference between W_2 and W_3 is the jettisoned weight, W_j, so Equation [3] can be written as

$$m = \frac{W_0}{W_B}\left(1 - \frac{W_j}{W_2}\right) \quad [4]$$

Combining Equations [2] and [4]

$$m_B = (m_A)^{I_A/I_B} = \frac{W_{0B}}{W_{B_B}}\left[1 - \frac{W_{jB}}{W_{2B}}\right] \quad [5]$$

In this case, the pertinent differences between missiles A and B are: (1) Some change in component weight ΔP and a corresponding change in jettisoned weight, ΔP_j; (2) some change in propellant weight, ΔF, required to operate the extra component weight and also to maintain the I ln m parameter constant; and (3) some change in tank and structural weight required to carry ΔF.

To evaluate this latter quantity, let ΔT represent the change in tank weight and structure incurred by ΔF, and assume that ΔT is proportional to the change in tank volume, ΔV. Then

$$\Delta T = \alpha \Delta V = \frac{\alpha}{\rho}\Delta F \quad [6]$$

where ρ = propellant density. Let

$$\Delta T_j = \frac{n\alpha}{\rho}\Delta F \quad [7]$$

On this basis, missile B weights can be expressed in terms of missile A weights in the following manner

$$W_{0B} = W_{0A} + \Delta P + \Delta F + \frac{\alpha}{\rho}\Delta F \quad [8]$$

$$W_{B_B} = W_{B_A} + (\Delta P - \Delta P_j) + \frac{\alpha}{\rho}\Delta F \quad [9]$$

$$W_{j_B} = W_{j_A} + \Delta P_j + \frac{n\alpha}{\rho}\Delta F \quad [10]$$

$$W_{2_B} = W_{0_B} - (W_{f_{A_{1-2}}} + \Delta F_{1-2})$$
$$= W_{0_A} + \Delta P + \Delta F\left(1 + \frac{\alpha}{\rho}\right) - (W_{f_{A_{1-2}}} + \Delta F_{1-2}) \quad [11]$$

Substituting Equations [8], [9], [10], and [11] into [4] yields

$$m_B = \frac{W_{0_A} + \Delta P + \Delta F\left(1 + \frac{\alpha}{\rho}\right)}{W_{B_A} + \Delta P - \Delta P_j + \frac{\alpha}{\rho}\Delta F}\left(1 - \frac{W_{j_A} + \Delta P_j + \frac{n\alpha}{\rho}\Delta F}{W_{0_A} + \Delta P + \left(1 + \frac{\alpha}{\rho}\right)\Delta F - (W_{f_{A_{1-2}}} + \Delta F_{1-2})}\right) \quad [12]$$

But

$$\Delta F_{1-2} + \Delta F_{3-4} = \Delta F \quad [13a]$$

$$\Delta F_{1-2} = \Delta F - \Delta F_{3-4} = \Delta F - \Delta R_{f_{3-4}}\, t_{3-4} \quad [13b]$$

where $\Delta R_{f_{3-4}}$ represents the difference in propellant consumption rate of the two missiles, due to the component change, and t_{3-4} equals the second-stage burning time. In Equation [13b] it has been assumed that all of the extra propellant in excess of that required to operate ΔP has been consumed in the first stage. Although this is not exact, it greatly simplifies the analysis and the resultant error is quite small.

Substituting Equation [13b] into [12] and equating the result to [5]

$$\left[\frac{W_{0_A}}{W_{B_A}}\left(1 - \frac{W_{j_A}}{W_{2_A}}\right)\right]^{I_A/I_B} = \frac{W_{0_A} + \Delta P + \Delta F\left(1 + \frac{\alpha}{\rho}\right)}{W_{B_A} + \Delta P - \Delta P_j + \frac{\alpha}{\rho}\Delta F}\left[1 - \frac{W_{j_A} + \Delta P_j + \frac{n\alpha}{\rho}\Delta F}{W_{0_A} + \Delta P + \frac{\alpha}{\rho}\Delta F - W_{f_{A_{1-2}}} + \Delta R_{f_{3-4}}\, t_{3-4}}\right] \quad [14]$$

Equation [14] can be solved for ΔF by setting

$$\Delta F = \left\{\left(W_{B_A} + \Delta P - \Delta P_j + \frac{\alpha}{\rho}\Delta F\right)\left[\frac{W_{0_A}}{W_{B_A}}\left(1 - \frac{W_{j_A}}{W_{2_A}}\right)\right]^{I_A/I_B} - \left[1 - \frac{W_{j_A} + \Delta P_j + \frac{n\alpha}{\rho}\Delta F}{W_{0_A} + \Delta P + \frac{\alpha}{\rho}\Delta F - W_{f_{A_{1-2}}} + \Delta R_{f_{3-4}}\, t_{3-4}}\right] - (W_{0_A} + \Delta P)\right\}\frac{1}{\left(1 + \frac{\alpha}{\rho}\right)} \quad [15]$$

and letting

$$A_0 = W_{B_A} + \Delta P - \Delta P_j \quad [16]$$

$$B_0 = \frac{\alpha}{\rho} \quad [17]$$

$$B_0' = \frac{n\alpha}{\rho} \quad [18]$$

$$C_0 = \left[\frac{W_{0_A}}{W_{B_A}}\left(1 - \frac{W_{j_A}}{W_{2_A}}\right)\right]^{I_A/I_B} \quad [19]$$

$$D_0 = W_{j_A} + \Delta P_j \quad [20]$$

$$E_0 = W_{0_A} + \Delta P \quad [21]$$

$$G_0 = -W_{f_{1-2}} + \Delta R_{f_{3-4}}\, t_{3-4} \quad [22]$$

Substituting Equations [16] through [22] into [15], the resulting relationship can be rewritten as

$$\Delta F^2[B_0(1 + B_0) + B_0'(1 + B_0) - C_0B_0^2] + \Delta F[E_0(1 + B_0) + G_0(1 + B_0) + E_0B_0 - D_0(1 + B_0) + B_0'E_0 - C_0A_0B_0 - C_0B_0E_0 - C_0B_0G_0] + [E_0^2 + E_0G_0 + D_0E_0 - C_0A_0E_0 - C_0A_0G_0] = 0 \quad [23]$$

This is in the form of a simple quadratic equation, the solution of which can be written as

$$\Delta F = \frac{-B_1 \pm (B_1^2 - 4A_1C_1)^{1/2}}{2A_1} \quad [24]$$

where

$$A_1 = B_0(1 + B_0) + B_0'(1 + B_0) - C_0B_0^2 \quad [25]$$

$$B_1 = E_0(1 + B_0) + G_0(1 + B_0) + E_0B_0 - D_0(1 + B_0) + B_0'E_0 - C_0A_0B_0 - C_0B_0E_0 - C_0B_0G_0 \quad [26]$$

$$C_1 = E_0^2 + E_0G_0 + D_0E_0 - C_0A_0E_0 - C_0A_0G_0 \quad [27]$$

Equation [24] essentially provides an exchange rate between component weight and efficiency as a function of missile performance. With the differences in component and required propellant weight of the proposed systems established, a cost comparison could be performed if dollars per pound of component and propellant were known. The most desirable system would be that whose combined cost of component and propellant to operate and carry the component is the least.

Detailed examination of the terms in Equation [24] indicates that for small changes in ΔF the terms representing tankage and structure incurred by changes in propellant load can be neglected with only slight effect on the resultant solution. If this were done, Equation [12] could be rewritten as

$$m_B = \frac{W_{0_A} + \Delta P + \Delta F}{W_{B_A} + (\Delta P - \Delta P_j)} \left[1 - \frac{W_{j_A} + \Delta P_j}{W_{0_A} + \Delta P - W_{f_{A_{1-2}}} + \Delta R_{f_{3-4}}\, t_{3-4}}\right] \quad [28]$$

and following the same procedure as before

$$\Delta F = \frac{\left[\frac{W_{0_A}}{W_{B_A}}\left(1 - \frac{W_{j_A}}{W_{2_A}}\right)\right]^{I_A/I_B} (W_{B_A} + \Delta P - \Delta P_j)}{\left[1 - \frac{W_{j_A} + \Delta P_j}{W_{0_A} + \Delta P - W_{f_{A_{1-2}}} + \Delta R_{f_{3-4}}\, t_{3-4}}\right]} - (WP_{0_A} + \Delta P) \quad [29]$$

Because of its relative simplicity, Equation [29] will be used throughout the remainder of this paper. It can be seen, from this relationship, that the actual magnitude of the exchange rate between ΔF, ΔP, and I_A/I_B is a function of the weight and performance characteristics of the missile in question. The "best" component and/or arrangement of components is not necessarily the lightest and, similarly, not necessarily the most efficient. Rather, a compromise is required, permitting the missile to perform its designated function reliably, at the minimum total operating cost. As might be expected, Equations [24] and [29] do not, in themselves, provide the basis for an absolute judgment as to component selection. The information they do provide is in the form of a measure of desirability which, when coupled with knowledge of relative cost, availability, and reliability, will provide a basis for choosing the most suitable configuration. These relationships may also be used to advantage when comparing components which do not affect the propellant consumption because of their efficiency characteristics but do present a problem in that they differ in weight and have varying portions of their weight jettisoned. In this case, I_A/I_B is equal to unity, and for the various combinations of ΔP and ΔP_j in question, the resultant ΔF's could be established. Relationships such as these can be developed, with relatively small effort, for missiles having any number of stages.

To illustrate the application of these relationships, consideration will be given to a hypothetical long range ballistic missile. Fig 1 is a sketch of this vehicle and Table 1 lists some of its pertinent characteristics. The two stages are parallel mounted, with five V-2 power plants, used in the boosters, set around the aft circumference of the missile. Detailed power plant data were obtained from Sutton (1)[2] and Kooy and Uytenbogaart (2). No attempt was made to design the best possible missile, and such detailed weight and performance changes as were made were done more to demonstrate the use of the techniques described in this paper than to adhere closely to realistic values. The missile will have a ballistic trajectory, a range of approximately 1750 nautical miles, carry a payload of 1000 lb, and have an over-all mass ratio of 15.8. Propellant combination, sea-level impulse, and general arrangement will be identical to those used on the V-2.

TABLE 1 WEIGHTS AND DIMENSIONS OF SAMPLE MISSILE

Weights

	lb
Missile	
Warhead (payload of 1000 lb)	2,050
Instrument compartment	1,350
Center section	5,385
Propulsion unit	2,775
Aft structure	1,116
Burnout weight	12,676
Booster	
Tank section (5)	6,805
Propulsion unit (5)	9,750
Aft structure (5) (including jettisoning mechanism and structure)	4,168
Jettisoned weight	20,723
Empty weight	33,399
Launching weight	269,000
Total propellant weight	235,600
Stage 1 propellant	188,480
Stage 2 propellant	47,120
Weight at end of stage 1	80,520

Dimensions

Over-all length, ft	82
Missile body diameter, in.	60
Booster length, ft	64
Booster body diameter (each of 5), in.	60

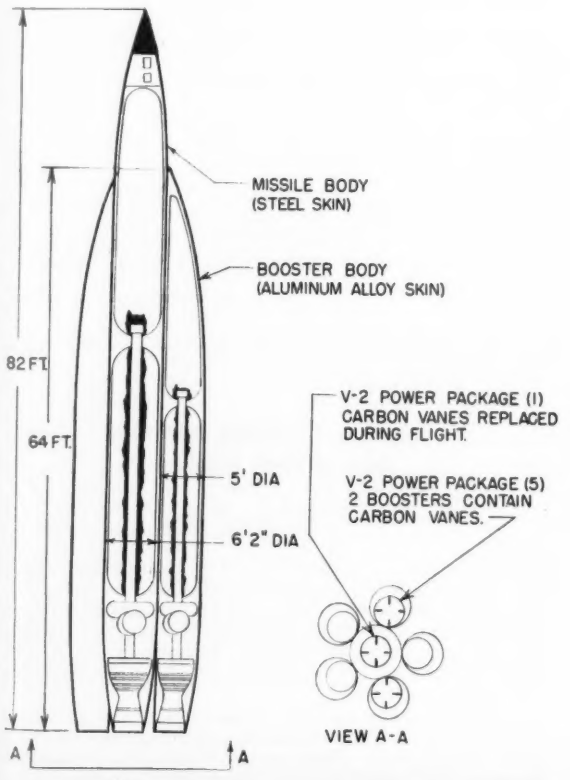

FIG. 1 SIX-MOTOR 1750 N. MI. BALLISTIC MISSILE, PARALLEL STAGE

Substituting values from Table 1 into Equation [29], a curve sheet such as Fig. 2 can be prepared showing the variation of ΔF with ΔP using I_A/I_B as a parameter. The intersepts and slopes of these curves are very much dependent on the weights and performance of the missile in question, and it follows that the exchange rate level for any component will be established quantitatively by these basic characteristics. For the case of zero efficiency change, where I_A/I_B is unity, a decrease in component weight is reflected by a corresponding decrease in the propellant load, corresponding with the mass ratio. As Φ, the ratio of ΔP_j to ΔP, is increased, the propellant weight-saving is seen to decrease. If component efficiency is decreased, producing an increase in I_A/I_B, the general level of the exchange rate curves is raised accordingly and greater component weight reductions are required to effect a comparable propellant weight-saving. Increases of range and performance requirements of the missile also tend to raise the level of the exchange rate curves.

[2] Numbers in parentheses refer to the References listed on page 300.

Fig. 3 is a plot of ΔP and I_A/I_B for the case of zero change in propellant weight, and indicates the component weight-saving required to compensate for reductions in efficiency while maintaining constant propellant load.

To illustrate the application of these curves, two selection problems that might arise will be investigated. The numerical values used in these examples were chosen primarily for their illustrative quality and are neither representative of any special design nor the result of detailed study aimed at modifying the power plant.

Consider first, the possibility of modifying the pumping plant. The original system uses six turbopumps weighing 350 lb each, five of which are jettisoned at the end of the first stage. As opposed to this, the proposed system will be lighter, each turbopump weighing only 300 lb, but will require 0.50 per cent more propellant per sec. Comparing these data yields $\Delta P = -300$ lb, $\Delta P_j = -250$ lb, $\Phi = 0.834$, and $I_A/I_B = 1.005$, where subscripts A and B represent the original and proposed systems, respectively. From Fig. 2, $\Delta F = +1500$ lb, which represents a 1500-lb increase in the quantity of propellant required if the new system is used. It can be seen from Fig. 3 that for the same component weight-saving, the minimum allowable I_A/I_B to maintain constant propellant weight is 1.0022. This is approximately equivalent to an increase in required propellant flow rate of 0.25 per cent. At first inspection, it would seem that the original system is best. However, considering production of a large number of vehicles, the actual selection should be made on a cost-per-missile basis, since it is apparent that with relatively minor modifications in structure, either configuration could be used without preventing the missile from completing its task. It will be arbitrarily assumed that machinery costs 55 dollars per pound, structure costs 25 dollars per pound, and propellant, 0.07 dollar per pound. From Equation [6] we know that $\Delta T = \alpha/\rho \cdot \Delta P$, and for the purposes of this example we can assume $\alpha/\rho = 0.043$. Using these values, the saving in

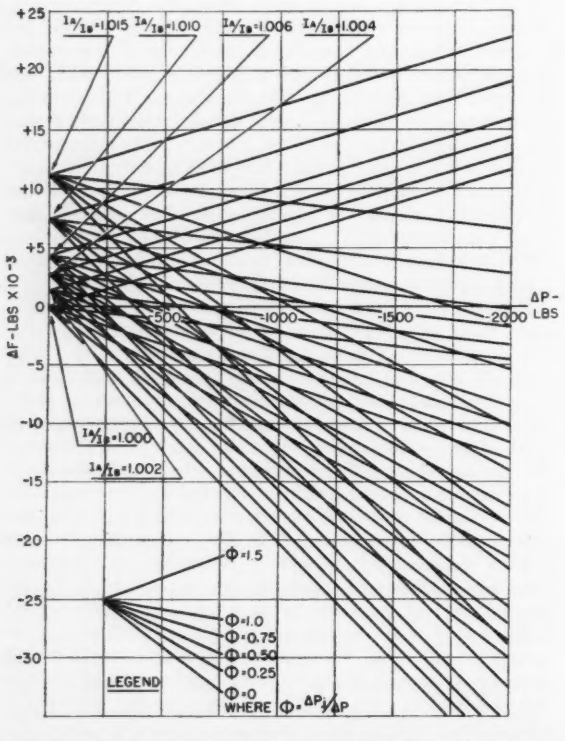

FIG. 2 EXCHANGE RATE CURVES. SIX-MOTOR CONFIGURATION RANGE = 1750 N. MI.

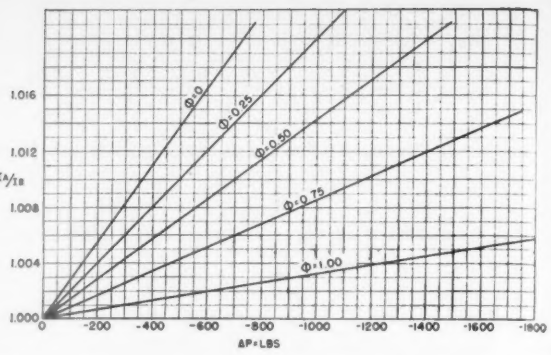

FIG. 3 EXCHANGE RATE CURVES FOR CASE OF $\Delta F = 0$. SIX-MOTOR CONFIGURATION RANGE = 1750 N. MI.

component cost is 16,500 dollars, while the cost of extra propellant and structure is 1717 dollars. If the assumed costs per pound are correct, the proposed system would be an economic improvement.

Another possible selection problem might be modification of the air bottle arrangement. The original system has an air bottle weight of 2070 lb and jettisons 1385 lb at the end of the first stage. The possibility will be considered of replacing this arrangement with one that has an initial weight of 500 lb more but jettisons 2000 lb, thereby reducing the final burnout weight. Using the proposed arrangment as a base, $\Delta P = -500$ lb, $\Delta P_j = -615$ lb, $\Phi = 1.23$, and since no efficiency change is involved, I_A/I_B is zero. From Fig. 2, $\Delta F = +1000$ lb, indicating that the proposed system would permit a 1000-lb propellant reduction. As before, the selection decision will be affected by the individual costs in question.

Acknowledgment

The author wishes to express his appreciation to Mr. Lloyd Curtis, also of Consolidated Vultee Aircraft Corporation, for his assistance in preparing the design data of the missile used as an example in this paper.

References

1 "Rocket Propulsion Elements," by G. P. Sutton, John Wiley & Sons, Inc., New York, 1949.

2 "Ballistics of the Future," by J. M. J. Kooy and J. W. H. Uytenbogaart, Technical Publishing Co., Haarlem, Holland.

A Comparison of Propellants and Working Fluids for Rocket Propulsion

(*Continued from page 296*)

port on Contract NObs 46845," Vol. II: Bibliography. Navy Dept. Bureau of Ships, Washington, D.C., 1951.

4 "Vapor Pressure of Pure Substances: Inorganic Compounds," by D. R. Stull, *Industrial and Engineering Chemistry*.

5 American Petroleum Institute, Research Project No. 44, Collection, Analysis and Calculation of Data on the Properties of Hydrocarbons, 1945.

6 "The Establishment of Large Satellites by Means of Small Orbital Carriers," by K. A. Ehricke. Paper presented at the Third International Astronautical Congress at Stuttgart, Germany, Sept. 1951, and at the 7th Annual Convention of the AMERICAN ROCKET SOCIETY, December 1952.

High-Frequency Combustion Instability in Rocket Motor with Concentrated Combustion[1]

LUIGI CROCCO[2] and SIN-I CHENG[3]

Nomenclature

τ_i = dimensionless instantaneous value of the time lag reduced by the characteristic time $\Theta/2 = \tau_i + \tau$

$\bar{\tau}_i$, τ_i = dimensionless steady-state value and instantaneous value of the part of the total time lag which is insensitive to the pressure oscillation

$\bar{\tau}$, τ = dimensionless steady-state value and instantaneous value of the other part of the total time lag which is sensitive to the pressure oscillation

n = exponent in the pressure dependence of the time lag = pressure index of interaction

$\dot{m}_i$ = rate of injection of the propellant per unit cross-sectional area of the combustion chamber

$\dot{m}_b$ = rate of the generation of the hot gas from the combustion of the propellant per unit cross-sectional area of the combustion chamber

L = combustion chamber length from injector end to the entrance of the de Laval nozzle = reference length scale for nondimensionalization

x^* = distance from injector end along the combustion chamber

t^* = dimensional time

u^* = dimensional mean flow speed of the gas along the combustion chamber axis

p^*, ρ^*, T^*, and c^* = dimensional instantaneous values of pressure, density, temperature, and speed of sound in the burned hot gas

p^*_0, ρ^*_0, T^*_0, and c^*_0 = values of p^*, ρ^*, T^*, and c^* at injector end = reference quantities for nondimensionalization

$\bar{p}^*$, $\bar{\rho}^*$, $\bar{T}^*$, and $\bar{c}^*$ = steady-state values of p^*, ρ^*, T^*, and c^*

$\Theta/2 = L/c^*_0$ = characteristic time = time required for a sound wave to travel the entire length of the combustion chamber filled with stagnant burned gas

$t = t^*/(L/c^*_0)$ = dimensionless time

$x = x^*/L$ = dimensionless length

u, $\bar{u} = u^*/c^*_0$ = dimensionless velocity of the gas in unsteady and steady-state operation

M, $\bar{M}$ = Mach number of the gas flow in unsteady and steady-state operation

p, ρ, T, and c = dimensionless instantaneous values of pressure, density, temperature, and speed of sound

$\bar{p}$, $\bar{\rho}$, $\bar{T}$, and $\bar{c}$ = dimensionless steady-state values of p, ρ, T, and c.

p', ρ', T', and c' = dimensionless instantaneous perturbations over their respective steady state values

$\alpha = \lambda + i\omega$ = root of the characteristic equation with the dimensionless time as the independent variable

λ = dimensionless amplification coefficient

ω = dimensionless angular frequency

Ω = absolute value of the angular frequency = $\omega(\Theta/2)$

γ = adiabatic index of the combustion gas

φ = $p' \exp(-\alpha t)$

δ = $\rho' \exp(-\alpha t)$

ν = $u' \exp(-\alpha t)$

ξ = dimensionless distance of the concentrated combustion front from the injector end expressed as a fraction of the characteristic length L

β = reduced angular frequency of the oscillation = angular frequency divided by the velocity gradient in de Laval nozzle

z = reduced velocity parameter = $\bar{u}^2(\gamma + 1)/2$

$I(\beta, \bar{u}) = \left[\frac{\nu/\bar{u}}{\delta/\bar{\rho}}\right]_{x=1}$ = the ratio of fractional variation of velocity to fractional variation of density at combustion chamber exit or entrance to de Laval nozzle

R, S = real and imaginary parts of $I(\beta, \bar{u})$

h, k = integers characterizing the modes of the oscillation

D/Dt = substantial derivatives along the path of a propellant element

$0(\ )$ = the order of magnitude of the quantity in the bracket

Subscripts

x or t = partial differentiation with respect to x or t

1 or 2 = the quantities evaluated in the flow field 1 or 2

1 Introduction

ROUGH combustion as a result of large pressure oscillations in the combustion chamber of a liquid propellant rocket motor has been observed under different circumstances in two distinct ranges of frequencies: the low-frequency range of less than 100 cps, and the high-frequency range of several hundreds or several thousands cps. Such rough combustion not only gives fluctuating performance but also shortens the life of the rocket motor. An understanding of the basic mechanism of producing unstable pressure oscillations that lead to rough combustion is therefore of great practical importance.

It has long been recognized that for unstable operations the oscillation of the chamber pressure and the oscillation of the rate of hot gas generation produced by the pressure oscillation must be properly out of time phase so that an increase of the rate of hot gas generation occurs at an overpressure period and further increases the overpressure in the combustion chamber. This time phase difference is originated from the fact that the propellant element does not burn immediately after being injected into the combustion chamber, but burns after a certain time interval, called the "time lag," during which the fuel and the oxidizer particles mix properly and absorb the necessary amount of activation energy. In (1, 2, 3),[4] the low-frequency oscillation has been analyzed based on the assumption that the time lag is constant and independent of the oscillations of the gas system in the combustion chamber. In these analyses, a pressure-sensitive feeding system which provides a varying injection rate under the pressure oscillation in the combustion chamber is assumed to be the self-exciting mechanism which creates the variation

Received February 9, 1953.

[1] This paper is based on Part I of the thesis submitted by the junior author in partial fulfillment of the requirements for the degree of Doctor of Philosophy from Princeton University, and has been presented at the VIII International Congress of Applied Mathematics and Mechanics, Istanbul, Turkey, August 1952.

[2] Robert H. Goddard Professor of Jet Propulsion, Daniel and Florence Guggenheim Jet Propulsion Center, Princeton University, Princeton, N. J. Member ARS.

[3] Instructor, Department of Aeronautical Engineering, Princeton University, Princeton, N. J.

[4] Numbers in parentheses refer to the References on page 313.

of the rate of hot gas generation. The senior author of the present paper has pointed out in (4) that the pressure sensitivity of the feeding system is not a necessary self-exciting mechanism for producing unstable pressure oscillations. By assuming a varying time lag τ which depends on the chamber pressure p in the manner

$$\int_{t-\tau}^{t} p^n(t')\, dt' = \text{const}$$

it is shown that unstable oscillations of both the low-frequency range and the high-frequency range can be produced even if the injection rate is constant. This kind of combustion instability cannot be eliminated by properly designing the feeding system but is intrinsic in the nature of the combustion processes.

The case of low-frequency intrinsic combustion instability is extensively studied by the senior author in (4), while the high-frequency case is only briefly discussed, using a simplified model of a single concentrated combustion front near the injector end and for the particular value of $n = 1/\gamma$ where γ is the adiabatic index of the burning gas. As n represents the extent of interaction between the pressure oscillation and the combustion processes, n must be an important parameter as a stability criterion. In practical cases, a large part of the combustion often takes place in a narrow region somewhere in the combustion chamber but usually not too close to the injector end. Therefore the analysis in (4) is extended in the present paper to the case with arbitrary location of the concentrated combustion front and for arbitrary values of n. The effect of distributing the combustion along the combustion chamber axis presents a more difficult problem and is analyzed in (5). The problem of shifting part of the concentrated combustion at the injector end to arbitrary axial location is briefly studied in the present paper with a view to some indication of the effect of distributing the combustion axially.

The unsteady supercritical flow in a de Laval nozzle with linear steady-state velocity profile in the subsonic portion has been studied in (6) and (7) from which the boundary condition for high-frequency oscillations can be deduced. This boundary condition will be used in several specific examples. In the limiting case of a very short nozzle, this boundary condition is equivalent to the boundary condition of constant flow Mach number at the entrance of the nozzle which is used in (4). This short nozzle boundary condition is simple and admits analytical solution of the characteristic value problem. The results with these two boundary conditions will be compared.

2 Formulation of the Problem

2.1 Assumptions and Simplified Models of Gas Flow System

The combustion chamber of a liquid propellant rocket motor is often a straight duct of constant cross-sectional area and is filled with the hot burned gas. The propellant elements injected into the combustion chamber are mostly in the form of atomized liquid droplets suspended in and carried along by the burned gas stream without occupying appreciable volume of the combustion chamber. The hot gas generated from combustion is recirculated actively to the region near the injector end where the hot gas supplies the activation energy to the unburned propellant elements. The recirculation and the mean flow patterns of the hot gas are extremely complicated, depending largely on the design and arrangement of the injectors. For the present analysis, we shall consider the gas flow inside the combustion chamber to be a one-dimensional flow of the hot gas only, with the unburned propellant elements suspended in and carried along by the hot gas. Oscillations in the transversal plane normal to the chamber axis is not being considered. The hot gases all over the combustion chamber are generated from the combustion of the same propellant under slightly different pressure, and thus are essentially at the same stagnation temperature. The combustion process in a liquid propellant rocket motor does not primarily increase the specific energy of the gas system. The heat released by the combustion of a propellant element is used to raise the temperature of the combustion products of this element to the temperature of the burned gas system. Therefore, from the point of view of the flow of the burned gas, the combustion process is essentially a process of generating or introducing new mass of the burned gas into the flow system, while the specific energy of the gas system remains substantially constant. As the combustion chamber is a duct of constant area, the mean flow velocity of the burned gas must increase whenever additional mass of burned gas is introduced into the flow system. The "new" burned gas and the "old" burned gas are assumed to mix intimately and accelerate together, carrying with them the suspended unburned propellant elements. This process of mixing and the process of accelerating the suspended particles give rise to an entropy variation in the gas flow field even if the specific energy release due to combustion is assumed constant. This entropy variation is shown in (5) to be a higher-order small quantity if the square of the Mach numbers of the gas flow system is negligibly small. Thus the gas flow system can be considered as isentropic to the proper order of approximation. A concentrated combustion front in such a gas flow system does not separate two regions of gases having significantly different thermodynamic states, but is only a sharp discontinuity of the mean flow velocity of the gas. The mean velocity distribution along the combustion chamber axis indicates the distribution of combustion, while the pressure, the density, and the temperature of the gas in steady-state operation are essentially uniform throughout the combustion chamber within the proper order of approximation.

The shape of the velocity profile or the distribution of combustion in a liquid propellant rocket motor varies considerably. It is often found that most of the combustion is concentrated in a narrow region. Therefore, as a rough approximation, we consider the combustion as a sharp discontinuous front. In (4), this concentrated combustion front is assumed to be near the injector end, which means the length of the combustion chamber is much longer than what is necessary. In the present paper we shall consider the concentrated combustion front to be located at arbitrary axial position, and the problem will be formulated for a model with two concentrated combustion fronts, one situated near the injector end, and the other at arbitrary axial position. Thus we have a two-step velocity profile which can be reduced to different simpler limiting cases of special interest.

Consider an idealized liquid propellant rocket motor whose injectors provide at a constant rate two uniform streams of propellant elements. The propellant elements in the first stream have a common small value of total time lag so that these elements that are injected into the combustion chamber at the same instant will burn simultaneously at a place very close to the injector end. The propellant elements in the second stream are assumed to have a uniform total time lag which is much larger than that of the elements in the first stream and will burn at a distance ξ from the injector end. In steady-state operation the hot gas generated from the first concentrated combustion front moves downstream with a velocity $\bar{u}^*_1$ in the region 1 bounded by the two concentrated combustion fronts. At the second concentrated combustion front a new mass of burned gas is introduced into the system and thoroughly mixed with the burned gas from region 1. They move downstream as a single unit with velocity $\bar{u}^*_2$ in the region 2 bounded by the second concentrated combustion front and the exit of the combustion chamber. Under the present simplified model there is no combustion taking place anywhere else except at the two concentrated combustion fronts. Thus $\bar{u}^*_1$ and $\bar{u}^*_2$ are constants in the two regions

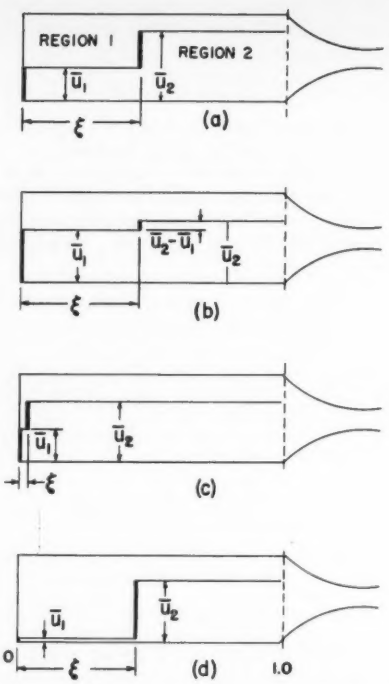

FIG. 1 SCHEMATIC DRAWING OF ROCKETS WITH CONCENTRATED COMBUSTION FRONTS

indicated by the subscripts 1 and 2 as shown in Fig. 1 (a). Both when $\bar{u}^*_1 \to \bar{u}^*_2$ and when $\xi \to 0$, as shown in Fig. 1 (b) and 1 (c), we have the case of a single concentrated combustion front at the injector end. When $\bar{u}^*_1 \to 0$, as shown in Fig. 1 (d), we have a single concentrated combustion front at arbitrary position ξ. The dimensionless velocities $\bar{u}_1$ and $\bar{u}_2$ obtained by dividing $\bar{u}^*_1$ and u^*_2 through the stagnation sound speed c^*_0 as a reference quantity are assumed to be so small that $\bar{u}_1{}^2$ and $\bar{u}_2{}^2$, coinciding practically with the square of the Mach numbers of the gas flow, are negligible compared to unity.

2.2 *The Time Lag and the Burning Rate*

It is explained in (4) that during the total time lag, the propellant elements undergo a series of complicated processes which ultimately lead to complete combustion of these propellant elements. Some of these processes, such as the atomization of the fuel and the oxidizer and the proper mixing of such atomized particles, are rather insensitive to the pressure and temperature oscillations of the burned gas in the combustion chamber. Many other processes, such as the vaporization of the propellant elements and the activation through ordinary heat transfer or other means, are rather sensitive to both the pressure and the temperature oscillations of the burned gas. The total time lag τ_i is therefore composed of a constant or insensitive part τ_i and a varying part τ which is sensitive to the oscillations of the burned gas in the combustion chamber. Without any precise knowledge of these processes taking place during the period of the time lag, we have to assume some form of the dependence of τ on the pressure and the temperature oscillations of the burned gas. For the case of small oscillations of the burned gas about the steady-state conditions, it will be assumed that the temperature and the pressure oscillations are correlated and that the effect of the temperature oscillations can be expressed in terms of the pressure oscillations. The average rate of the rates of the different local processes is assumed to be proportional to a constant power n of the local gas pressure acting on the propellant element. Thus, the relation defining the pressure sensitive time lag τ of the element burning at the instant t is given in (4) as

$$\int_{t-\tau}^{t} p^n[x'(t'), t']\, dt' = \text{const } C \quad \ldots\ldots [2.2.1]$$

where $p\,[x'(t'), t']$ is the gas pressure acting on the propellant element at the position $X'(t')$ and at the instant t'. Both the constant value C of the integral and the constant pressure index n of interaction are characteristic constants of the propellant under the operating steady-state chamber pressure. The index n is assumed to be constant throughout the time lag period and therefore represents the average extent of interaction between the combustion processes and the pressure oscillations. The effect of the temperature oscillations is also included in the index n. Our knowledge of the kinetics of the individual process is not sufficient for a theoretical prediction of such an over-all parameter. This constant n for given propellant can be determined through experiments only.

Now we shall see how this pressure-sensitive time lag can lead to varying burning rate in the simplified model as explained in the previous section. Consider for simplicity the case of a single concentrated combustion front. Let $m_i\,(t)$ be the total amount of the propellant injected from the beginning of the operation up to the instant t, and $m_b(t)$ be the total amount of the propellant burned up to the same instant t. At this instant t, the propellant injected into the combustion chamber during the interval $t - \tau_i$ to t has not burned. Therefore

$$m_b(t) = m_i(t - \tau_i) \quad \ldots\ldots [2.2.2]$$

The instantaneous burning rate is hence

$$\dot{m}_b(t) = \frac{dm_b}{dt} = \left(1 - \frac{d\tau_i}{dt}\right)\dot{m}_i(t - \tau_i) = \left(1 - \frac{d\tau}{dt}\right)\dot{m}_i(t - \tau_i) \quad [2.2.3]$$

As we are considering the intrinsic type of combustion instability in the idealized liquid propellant rocket as described in section 2.1, the injection rate $\dot{m}_i(t - \tau_i)$ is a constant equal to $\dot{m}_i$. Differentiate equation [2.2.1] with respect to t to obtain $1\text{-}(d\tau/dt)$ and substitute $1\text{-}(d\tau/dt)$ into equation [2.2.3]. The burning rate is thus given as

$$\dot{m}_b(t) = \dot{m}_i \frac{p^n[x(t),\, t]}{p^n[x(t - \tau,\, t - \tau)]} \quad \ldots\ldots [2.2.4]$$

Since the gas pressure varies with time and position, the burning rate is sometimes larger and sometimes smaller than $\dot{m}_i$, which is equal to the burning rate in steady-state operation. This variation of burning rate produced by the pressure oscillations in the combustion chamber is the self-exciting mechanism of producing the intrinsic combustion instability.

In the case of low-frequency oscillation, when the length of the combustion chamber is much smaller than the wave length of the pressure oscillation, the pressure in the combustion chamber is almost uniform at any instant. Thus $p[x(t-\tau), t-\tau]$ is approximately equal to $p[t-\tau]$. In the case of high-frequency oscillations, when the length of the combustion chamber is of the same order of magnitude as the wave length or several times larger than the wave length of the pressure oscillations, it is not obvious that $p[x(t-\tau), t-\tau]$ can be replaced by $p[x(t), t-\tau]$ as is done in (4). However, it is shown (5) that the spacewise variations of the pressure in the combustion chamber has a contribution which is a higher-order small quantity in the stability calculation compared with the contribution of the timewise variation of the chamber pressure at a given location if the pressure sensitive time lag τ is much smaller than the pressure insensitive time lag τ_i. In the simplified model which we are considering now, τ is much less than τ_i, and the spacewise distribution of combustion is

approximated. We shall hence put $p[x(t-\tau), t-\tau] \cong p[x(t), t-\tau]$, and the burning rate $\dot{m}_b(t)$ is given as

$$\dot{m}_b(t) = \dot{m}_i \frac{p^n(t)}{p^n(t-\tau)} \quad \text{[2.2.5]}$$

where both pressures are evaluated at the same location x where the propellant element burns. It should be noticed that when the total time lag varies with the gas pressure, the position where the propellant elements burn also varies. We shall neglect the oscillation of the concentrated combustion front about its steady-state position and evaluate $p(t)$ and $p(t-\tau)$ at the steady-state position of the concentrated combustion front.

2.3 *Small Perturbation Equations for the Gas System*

In analyzing the low-frequency oscillations, the combustion chamber pressure is assumed to be uniform at any instant but fluctuates as a whole. This is justifiable because the period of the low-frequency oscillation is very large compared to the time required for a pressure wave to travel the length of the combustion chamber, so that before the periodic oscillation of the gas has produced any appreciable changes in the gas properties, the pressure wave has traveled many times back and forth and has made the flow properties nearly uniform. Thus the consideration of mass balance is sufficient to formulate the low-frequency oscillation problem. In the case of high-frequency oscillations, the characteristic time for the pressure wave to travel the entire length of the combustion chamber is comparable to the period of the oscillations. Therefore the wave propagation phenomena will have to be considered along with the combustion process. The gas dynamic equations of continuity, momentum, and energy will then be used. From previous discussion in section 2.1 the energy equation will be replaced by the equation of isentropic change of state which is justified within the proper order of approximation. Thus we have

$$\left.\begin{aligned} &\rho^*{}_{t^*} + (\rho^* u^*)_{x^*} = 0 \\ &\rho^*[u^*{}_{t^*} + u^* u^*{}_{x^*}] = -p^*{}_{x^*} \\ &p^* \rho^{*-\gamma} = \text{const} \end{aligned}\right\} \quad \text{[2.3.1]}$$

where all quantities are dimensional and subscript t^* or x^* means the partial derivative with respect to the corresponding variable.

Use the following scheme to make all these quantities dimensionless

$$\rho = \frac{\rho^*}{\rho^*_0}, \quad p = \frac{p^*}{p^*_0}, \quad u = \frac{u^*}{c^*_0}, \quad x = \frac{x^*}{L}, \quad \text{and} \quad t = \frac{t^*}{\Theta/2} \quad \text{[2.3.2]}$$

with superscript * indicating that the quantity is dimensional, and subscript $_0$ indicating that the quantity is evaluated at the stagnation condition. C^*_0 is the sound speed in the stagnant gas and L is the length of the combustion chamber. The characteristic time $\Theta/2$ is defined as the time required for the sound wave to travel the combustion chamber length in a stagnant gas, i.e., $\Theta/2 = L/C^*_0$. This characteristic time is one half of the characteristic time defined in (4) under the approximation $\bar{u}^2 << 1$. Equations [2.3.1] when expressed in dimensionless quantities are

$$\left.\begin{aligned} &\rho_t + (\rho u)_x = 0 \\ &\rho(u_t + u u_x) = -\frac{1}{\gamma} p_x \\ &p \rho^{-\gamma} = 1 \end{aligned}\right\} \quad \text{[2.3.3]}$$

These equations govern the unsteady flow of the gas in region 1 and in region 2, respectively, separated from each other by the velocity discontinuity at the concentrated combustion front.

For the study of the small oscillations in the gas system, we shall consider the flow as a small perturbation over the steady-state flow. Thus define

$$\rho = \bar{\rho} + \rho', \quad p = \bar{p} + p', \quad \text{and } u = \bar{u} + u'$$

where the mean quantities $\bar{p}$ and $\bar{\rho}$ are practically unity in dimensionless form under the approximation $\bar{u}^2 << 1$. The mean velocity $\bar{u}$ is constant either in region 1 or in region 2. Both $\bar{u}_1$ and $\bar{u}_2$ are assumed to be small such that $\bar{u}^2$ is much less than unity. Introduce these perturbations into Equation [2.3.3] and linearize the equations with respect to small perturbations, and we have

$$\left.\begin{aligned} &\rho'_t + \bar{u}\rho'_x + u'_x = 0 \\ &u'_t + \bar{u}u'_x + \rho'_x = 0 \\ &p' = \gamma\rho' \end{aligned}\right\} \quad \text{[2.3.4]}$$

These equations are recognized as equivalent to the simple wave equations, and admit solutions of the type $u' = u'(\zeta)$ and $\rho' = \rho(\zeta)$ with $\zeta = t - ax$. Substituting these into Equation [2.3.4], one obtains

$$\left.\begin{aligned} (1 - \bar{u}a)u'_\zeta - a\rho'_\zeta &= 0 \\ -au'_\zeta + (1 - \bar{u}a)\rho'_\zeta &= 0 \end{aligned}\right\}$$

In order to have nonzero solutions of u'_ζ and ρ'_ζ, we must have $(1 - \bar{u}a)^2 - a^2 = 0$. Therefore only two values of a are possible, i.e., $a_r = \dfrac{1}{1+\bar{u}}$ and $a_s = -\dfrac{1}{1-\bar{u}}$ where $1/a_r$ is the speed of the downstream moving wave, and $1/a_s$ is that of the upstream moving wave as observed from the combustion chamber wall. Thus the general solution of Equations [2.3.4] is

$$\left.\begin{aligned} \rho' &= \rho'_r(t - a_r x) + \rho'_s(t - a_s x) \\ u' &= u'_r(t - a_r x) + u'_s(t - a_s x) \end{aligned}\right\} \quad \text{[2.3.5]}$$

Put Equations [2.3.5] into Equations [2.3.4], separate the upstream and the downstream moving waves, and integrate with the boundary condition that in steady state both ρ' and u' must vanish. We find the relations

$$\rho'_r = u'_r, \quad \rho'_s = -u'_s$$

Hence Equations [2.3.5] become

$$\left.\begin{aligned} \rho' &= u'_r(t - a_r x) - u'_s(t - a_s x) \\ u' &= u'_r(t - a_r x) + u'_s(t - a_s x) \end{aligned}\right\} \quad \text{[2.3.6]}$$

Let us investigate the stability of periodic solutions of exponential type

$$\left.\begin{aligned} u'_r &= c_r \exp[\alpha(t - a_r x)] \\ u'_s &= c_s \exp[\alpha(t - a_s x)] \end{aligned}\right\} \quad \text{[2.3.7]}$$

where c_r and c_s are integration constants, and $\alpha = \lambda + i\omega$ with λ = amplification coefficient and ω = angular frequency of the wave. For simplicity, let us also write the perturbations as

$$u' = \nu(x) \exp(\alpha t), \quad \rho' = \delta(x) \exp(\alpha t), \quad \text{and} \quad p' = \varphi(x) \exp(\alpha t)$$

Then the solutions for the functions $\nu(x)$ and $\delta(x)$ are

$$\left.\begin{aligned} \nu(x) &= c_r \exp(-a_r \alpha x) + c_s \exp(-a_s \alpha x) \\ \delta(x) &= c_r \exp(-a_r \alpha x) - c_s \exp(-a_s \alpha x) \end{aligned}\right\} \quad \text{[2.3.8]}$$

These solutions apply to regions 1 and 2 respectively. In region 1 the ratio of the two integration constants c_{r_1}/c_{s_1} can be determined by the boundary condition at the injector end. In region 2, the corresponding ratio can be determined by the boundary condition at the combustion chamber exit. The two sets of solutions in the two regions will have to be matched at the second concentrated combustion front as required by the boundary conditions at such front. This matching of the two sets of solutions defines completely the complex quantity $\alpha = \lambda + i\omega$. If λ is positive, the disturbance will grow exponentially with time and therefore is unstable.

If λ is negative, the disturbance will die out exponentially with time and is stable. The boundary between the stable and the unstable regions as a relation between the characteristic constants of the gas flow system, $\bar{\tau}$, n, ξ, $\bar{u}$ etc., is obtained if we put $\lambda = 0$. The determination of such stability boundary is one of the major objects of the present investigation.

2.4 *The Boundary Condition*

The boundary condition at a concentrated combustion front will be investigated first. As has been explained in section 2.1, the concentrated combustion front is not a discontinuity of pressure, density, and temperature but is only a discontinuity of velocity of the flow. Hence the boundary condition at a concentrated front consists of two parts:

1 The steady-state values as well as the small perturbation values of the gas pressure and the gas density are continuous at every instant across the concentrated combustion front. That is, $p'_2 = p'_1$ and $\rho'_2 = \rho'_1$. These are equivalent to the conditions

$$\left.\begin{aligned} &\varphi_2 = \varphi_1,\ \delta_2 = \delta_1 \\ \text{and} \\ &\alpha_1 = \alpha_2 = \alpha = \lambda + i\omega \end{aligned}\right\} \quad \ldots\ldots\ldots\ldots [2.4.1]$$

The last equality in Equations [2.4.1] indicates that the oscillation frequency and the amplification rate are the same on both sides of the concentrated combustion front.

2 The fractional increase of the difference of mass flow rates across the concentrated combustion front is equal to the fractional increase of the burning rate at the concentrated combustion front. The fractional increase of the burning rate $(\dot{m}_b - \dot{m}_i)/\dot{m}_i$ can be obtained from Equation [2.2.3]. But in the analysis of the simplified model, we shall use Equation [2.2.5]. Thus neglecting higher-order small quantities, we have

$$\frac{\dot{m}_b - \dot{m}_i}{\dot{m}_i} = -\frac{d\tau}{dt} = \frac{p^n(t)}{p^n(t-\tau)} - 1 = n[p'(t) - p'(t-\tau)]$$

The second boundary condition at the concentrated combustion front separating region 1 and region 2 is obtained by equating $(\dot{m}_b - \dot{m}_i)/\dot{m}_i$ to the fractional increase of the difference of the mass flow rates. Thus replacing the small perturbations by their periodic form and canceling the common factor $\exp(\alpha t)$, we obtain

$$\nu_2 - \nu_1 + (\bar{u}_2 - \bar{u}_1)(1 - \gamma n)\delta_1 + (\bar{u}_2 - \bar{u}_1)\gamma n \delta_1 \exp(-\alpha\bar{\tau}) = 0 \quad \ldots\ldots\ldots [2.4.2]$$

In Equation [2.4.2] we have replaced τ by $\bar{\tau}$ in the coefficient of the small perturbation δ_1, neglecting the difference $\bar{\tau} - \tau$ as a higher-order small quantity.

If the concentrated combustion front is located at the injector end, the upstream side of the combustion front has no oscillation. Hence the boundary condition at $x = 0$ is obtained by putting the disturbance and the mean velocity of the upstream flow in Equation [2.4.2] to zero.

$$\nu_1 + \bar{u}_1(1 - \gamma n)\delta_1 + \bar{u}_1\gamma n\delta_1 \exp(-\alpha\bar{\tau}) = 0 \ldots [2.4.3]$$

Now we come to the boundary condition at the combustion chamber exit where the gas enters the converging section of the de Laval nozzle. The reflection of a one-dimensional pulse at the entrance of the nozzle is essentially three-dimensional and will lead to a complicated problem somewhat like the problem of Mach reflection from a wedge. The result of such analysis, even if it could be obtained in reasonably simple form, is not suitable as a boundary condition for the one-dimensional flow in the combustion chamber. To be consistent the boundary condition must be obtained from one-dimensional consideration, neglecting completely the two-dimensional effects. The physical boundary condition at the nozzle entrance is that there are no discontinuities of the gas flow properties at this station. In other words, the unsteady one-dimensional motion of the gas in the combustion chamber and that in the nozzle must be joined continuously at this entrance. In (6) the unsteady flow in a de Laval nozzle with linear steady-state velocity in the subsonic portion is determined for arbitrary frequency, and the boundary condition at the entrance to the nozzle is presented in graphical form as the ratio of the fractional variations of velocity and density at the entrance. This boundary condition, when $\gamma = 1.20$, is reproduced in Fig. 2 with $I = (\nu/\bar{u})/(\delta/\bar{\rho}) = R + iS$ plotted against the reduced frequency $\beta = \omega \cdot l_{sub}/(\sqrt{2/(\gamma+1)} - \bar{u})$ where l_{sub} is the length of the subsonic portion of the nozzle as a fraction of the combustion chamber length.

If the length of the subsonic portion is very small, i.e., $l_{sub} \cong 0$, the values of β corresponding to the fundamental or the first few modes of oscillation are very close to zero. Hence for very short nozzle, one has

$$I(0, \bar{u}) = \left(\frac{\nu/\bar{u}}{\delta/\bar{\rho}}\right)_{\beta=0} = \frac{\gamma - 1}{2} \quad \ldots\ldots\ldots [2.4.4]$$

if the one-dimensional result holds good in such limiting case. This boundary condition has been shown in (6) and (7) to correspond to constant Mach number of the gas flow at the entrance of the nozzle.

2.5 *Final Formulation*

Having established the boundary conditions for the solutions in different flow regions, we can proceed to formulate the equation for the determination of the complex quantity $\alpha = \lambda + i\omega$ for a given system.

For region 1, the boundary condition at the injector end as given in Equation [2.4.3] can be used to determine the ratio of c_{r_1} and c_{s_1}. Call this ratio $-A$.

$$-A = \frac{c_{r_1}}{c_{s_1}} = -\frac{1 - \bar{u}_1(1 - \gamma n) - \bar{u}_1\gamma n \exp(-\alpha\bar{\tau})}{1 + \bar{u}_1(1 - \gamma n) + \bar{u}_1\gamma n \exp(-\alpha\bar{\tau})} \ldots [2.5.1]$$

The solution in region 1 can hence be written as

$$\left.\begin{aligned} \nu_1(x) &= c_{s_1}\exp(-\alpha a_s x)[1 - A\exp\{-\alpha(a_r - a_s)x\}] \\ \delta_1(x) &= -c_{s_1}\exp(-\alpha a_s x)[1 + A\exp\{-\alpha(a_r - a_s)x\}] \end{aligned}\right\} \ldots [2.5.2]$$

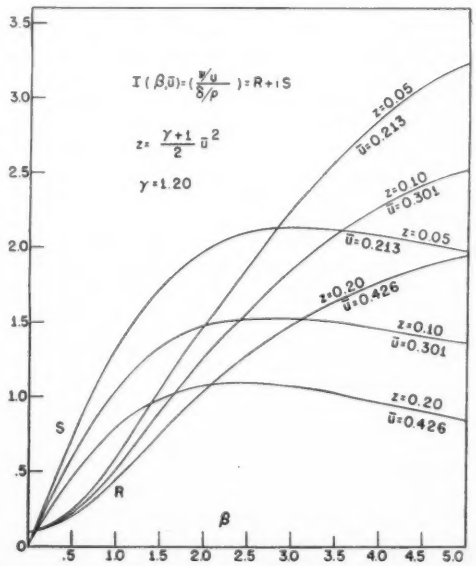

FIG. 2 RECIPROCAL OF NOZZLE IMPEDANCE FOR OSCILLATORY FLOW OF FREQUENCY $\omega = \pi\beta$

In a similar manner the boundary condition at the combustion exit $X = 1$ can be used to determine the ratio

$$C_{r_2}/C_{s_2} = -B \exp [\alpha(a_r - a_s)] \quad [2.5.3]$$

When the nozzle is very short the boundary condition given as Equation [2.4.4] is used, and we have

$$B(0, \bar{u}) = \frac{1 + (\gamma - 1)\bar{u}/2}{1 - (\gamma - 1)\bar{u}/2} \quad [2.5.4]$$

When the nozzle is long, B is a fraction of β and $\bar{u}$ with $I(\beta, \bar{u})$ given in Fig. 2.

$$B(\beta, \bar{u}) = \frac{1 + I(\beta, \bar{u})\bar{u}}{1 - I(\beta, \bar{u})\bar{u}} \quad [2.5.5]$$

In general, we can write the solutions in region 2 as

$$\left.\begin{aligned} \nu_2(x) &= c_{s_2} \exp(-\alpha a_s x)[1 - B \exp\{\alpha(a_r - a_s)(1 - x)\}] \\ \delta_2(x) &= -c_{s_2} \exp(-\alpha a_s x)[1 + B \exp\{\alpha(a_r - a_s)(1 - x)\}] \end{aligned}\right\} \quad [2.5.6]$$

Now the two sets of solutions [2.5.2] and [2.5.6] are to be matched at the second concentrated combustion front $x = \xi$. The oscillation of the second concentrated combustion front about the mean steady state position ξ is neglected. Equating $\delta_1(\xi)$ and $\delta_2(\xi)$ as given in Equations [2.5.2] and [2.5.6], we have

$$\frac{c_{s_2}}{c_{s_1}} = \frac{1 + A \exp[-\alpha(a_r - a_s)\xi]}{1 + B \exp[\alpha(a_r - a_s)(1 - \xi)} \cong \frac{1 + A \exp(-2\alpha\xi)}{1 + B \exp[2\alpha(1 - \xi)]} \quad [2.5.7]$$

where $a_r - a_s = 1/(1 + \bar{u}) + 1/(1 - \bar{u}) = 2/(1 - \bar{u}^2) \cong 2$ has been substituted.

By introducing Equation [2.5.2], [2.5.6], and [2.5.7] into Equation [2.4.2] and dividing the resulting expression with δ_1, we have

$$\frac{1 - B \exp[2\alpha(1 - \xi)]}{1 + B \exp[2\alpha(1 - \xi)]} - \frac{1 - A \exp[-2\alpha\xi]}{1 + A \exp[-2\alpha\xi]} = (\bar{u}_2 - \bar{u}_1)[(1 - \gamma n) + \gamma n \exp(-\alpha\bar{\tau})] \quad [2.5.8]$$

This is the final form of the equation for determining the complex quantity $\alpha = \lambda + i\omega$ of a combustion system with two steps of concentrated combustion, one at the injector end and the other at ξ. For the determination of the stability boundary, we put $\lambda = 0$ or $\alpha = i\omega$, then separate the real and the imaginary parts in Equation [2.5.8] to get two real equations from which we can eliminate ω. The eliminant is the equation defining the stability boundary. We see that in Equation [2.5.8] both A and B are, in general, complex quantities. The separation of the real and the imaginary parts of Equation [2.5.8] is quite laborious and the resulting real equations cannot be handled easily.

For the case of a single concentrated combustion front at arbitrary position ξ (Fig. 1 (d)), we put $\bar{u}_1 = 0$ in Equation [2.5.8]. Thus

$$\frac{1 - B \exp[2\alpha(1 - \xi)]}{1 + B \exp[2\alpha(1 - \xi)]} - \frac{1 - \exp(-2\alpha\xi)}{1 + \exp(-2\alpha\xi)} = \bar{u}_2[(1 - \gamma n) + \gamma n \exp(-\alpha\bar{\tau})] \quad [2.5.9]$$

where A becomes unity. When the nozzle is short, $B(0, \bar{u})$ is a real constant given by Equation [2.5.4]. Thus α is the only complex quantity in Equation [2.5.9]. The solution of the problem is therefore greatly simplified algebraically. When the nozzle is long the value of B is given by Equation [2.5.5] where I is a complex function given in Fig. 2. Then the determination of the stability boundary will have to be done graphically. If $\xi = 0$, Equation [2.5.9] becomes

$$(1 - \gamma n)\bar{u}_2 + \gamma n \bar{u}_2 \exp(-\alpha\bar{\tau}) = \frac{1 - B \exp(2\alpha)}{1 + B \exp(2\alpha)} \quad [2.5.10]$$

This case corresponds to a single concentrated combustion front at the injector end. This Equation [2.5.10] can also be obtained from Equation [2.5.8] by taking the limit of either $\xi = 0$ or $\bar{u}_2 = \bar{u}_1$ (Figs. 1 (b) and 1 (c)). When $\gamma n = 1$, Equation [2.5.10] reduces to a form identical with Equation [12.15] in (4).

3 Solution with Short Nozzle

3.1 *Single Concentrated Combustion Front at Injector End*

Rewrite Equation [2.5.10] and drop the subscript 2.

$$\gamma n \bar{u} \exp(-\alpha\bar{\tau}) - (\gamma n - 1)\bar{u} = \frac{1 - B \exp(2\alpha)}{1 + B \exp(2\alpha)} \quad [3.1.1]$$

where

$$B = \frac{1 + (\gamma - 1)\bar{u}/2}{1 - (\gamma - 1)\bar{u}/2} \quad [2.5.4]$$

Putting $\alpha = i\omega$ for the neutral oscillations and separating the real and the imaginary parts of Equation [3.1.1] we have

$$\left.\begin{aligned} \gamma n \bar{u} \cos \omega\bar{\tau} &= -(1 - \gamma n)\bar{u} + \frac{1 - B^2}{1 + B^2 + 2B \cos 2\omega} \\ \gamma n \bar{u} \sin \omega\bar{\tau} &= \frac{2B \sin 2\omega}{1 + B^2 + 2B \cos 2\omega} \end{aligned}\right\} \quad [3.1.2]$$

with the approximation $\bar{u}^2 << 1$ we can write

$$\frac{1 - B^2}{1 + B^2} = -\frac{(\gamma - 1)\bar{u}}{1 + [(\gamma - 1)\bar{u}/2]^2} \cong -(\gamma - 1)\bar{u} \quad [3.1.3]$$

$$\frac{2B}{1 + B^2} = \frac{1 - [(\gamma - 1)\bar{u}/2]^2}{1 + [(\gamma - 1)\bar{u}/2]^2} \cong 1$$

Thus Equation [3.1.2] become

$$\left.\begin{aligned} \gamma n \cos \omega\bar{\tau} &= -(1 - \gamma n) - \frac{\gamma - 1}{2 \cos^2 \omega} \\ \gamma n \bar{u} \sin \omega\bar{\tau} &= \tan \omega \end{aligned}\right\} \quad [3.1.4]$$

When γn is of the order of unity, $\tan \omega$ is of the order of $\bar{u}$; therefore we can neglect $\tan^2 \omega$ as compared to unity. Thus the first relation in Equation [3.1.4] immediately gives

$$\cos \omega\bar{\tau} = -\frac{\gamma + 1 - 2\gamma n}{2\gamma n} \quad [3.1.5]$$

and

$$\sin \omega\bar{\tau} = \pm\left[1 - \left(1 - \frac{\gamma + 1}{2\gamma n}\right)^2\right]^{1/2} \quad [3.1.6]$$

Thus

$$\tan \omega = \pm\gamma n \bar{u}\left[1 - \left(1 - \frac{\gamma + 1}{2\gamma n}\right)^2\right]^{1/2} \quad [3.1.7]$$

From Equation [3.1.6] or [3.1.7] we see that only when

$$n \geq \frac{\gamma + 1}{4\gamma} \quad [3.1.8]$$

can we have real solutions of $\omega\bar{\tau}$ and ω for neutral oscillations. Therefore the index n must be bigger than the minimum value $(\gamma + 1)/4\gamma$ if the combustion system is to have unstable pressure oscillations. As the values of γ for most of the combustion products of the common rocket propellants are usually close to 1.2 or 1.3, the minimum value of n is about 0.45 and is the same for all modes of the high-frequency oscillations when the constant Mach number boundary condition is used.

From Equation [3.1.7] we obtain the frequency of the neutral oscillations as

$$\omega = k\pi \pm \gamma n\bar{u}\left[1 - \left(1 - \frac{\gamma+1}{2\,\gamma n}\right)^2\right]^{1/2} \quad \ldots\ldots [3.1.9]$$

where $k = 1, 2, 3, \ldots\ldots$ The fundamental mode of the high-frequency oscillation is obtained when $k = 1$; solution with $k = 0$ is identified to be the low-frequency solution in (4) and is therefore discarded in the present investigation. Equation [3.1.9] shows that the frequencies of the neutral oscillations are close to the integral multiples of π which in dimensional form are the natural organ-pipe frequencies of the gas system. The fractional deviations of the neutral frequencies from the corresponding natural organ-pipe frequencies are of the order of magnitude of the Mach number of the gas flow.

Now we shall demonstrate on which side of the stability boundary is the oscillation unstable. Taking $B \cong 1$ and differentiating Equation [3.1.1] with respect to $\bar{\tau}$, we have on the stability boundary

$$\frac{d\alpha}{d\bar{\tau}} = \frac{d\lambda}{d\bar{\tau}} + i\frac{d\omega}{d\bar{\tau}} = -i\omega\left[\bar{\tau} - \frac{\cos\omega\bar{\tau}}{\gamma n\bar{u}\cos^2\omega\bar{\tau}} - i\frac{\sin\omega\bar{\tau}}{\gamma n\bar{u}\cos^2\omega\bar{\tau}}\right]^{-1}$$

or

$$\frac{d\lambda}{d\omega} = -\frac{\sin\omega\bar{\tau}}{\bar{\tau}\gamma n\bar{u}\cos^2\omega - \cos\omega\bar{\tau}} \quad \ldots\ldots [3.1.10]$$

When $n < (\gamma + 1)/2\gamma$, then $\cos\omega\bar{\tau} < 0$, thus the sign of $d\lambda/d\omega$ is the same as the sign of $-\sin\omega\bar{\tau}$ or the sign of $-\tan\omega$. When $d\lambda/d\omega$ is positive on the stability boundary, the region which is reached by increasing ω from the boundary is the unstable region. (From the usual argument of continuity, this statement would be expected to hold good for $n > (\gamma + 1)/2\gamma$ without making an effort for detailed proof.) Therefore, the unstable range of the frequencies is

$$k\pi - \gamma n\bar{u}\left[1 - \left(1 - \frac{\gamma+1}{2\,\gamma n}\right)^2\right]^{1/2} < \omega < k\pi + \gamma n\bar{u}\left[1 - \left(1 - \frac{\gamma+1}{2\,\gamma n}\right)^2\right]^{1/2} \quad [3.1.11]$$

It is therefore concluded that all the frequencies of the unstable oscillations are very close to the natural organ-pipe frequencies.

The corresponding ranges of the values of $\bar{\tau}$ for such unstable oscillations are given as

$$\frac{(2h+1)\pi - \left[\frac{\pi}{2} - \sin^{-1}\left(\frac{\gamma+1}{2\,\gamma n} - 1\right)\right]}{k\pi + \gamma n\bar{u}\left[1 - \left(1 - \frac{\gamma+1}{2\,\gamma n}\right)^2\right]^{1/2}} < \bar{\tau} < \frac{(2h+1)\pi + \left[\frac{\pi}{2} - \sin^{-1}\left(\frac{\gamma+1}{2\,\gamma n} - 1\right)\right]}{k\pi - \gamma n\bar{u}\left[1 - \left(1 - \frac{\gamma+1}{2\,\gamma n}\right)^2\right]^{1/2}} \quad [3.1.12]$$

where $k = 1, 2, 3, \ldots$ indicates the successive modes of the high-frequency oscillations, and $h = 0, 1, 2 \ldots$ indicates the successive higher ranges of the values of $\bar{\tau}$ for unstable oscillations of a given mode. The unstable range is shaded as given in Fig. 3 (a) for $\bar{u} = 0.213$. We see that the unstable ranges of the values of $\bar{\tau}$ for a given set of values of h and k increases with increasing n.

When n equals the minimum value $(\gamma + 1)/4\gamma$, Equations [3.1.11] and [3.1.12] give

$$\left.\begin{aligned}\omega &= k\pi \\ \omega\bar{\tau} &= (2h+1)\pi\end{aligned}\right\} \quad \ldots\ldots [3.1.13]$$

The oscillation is neutral and the range of the unstable values of $\bar{\tau}$ vanishes at this minimum value of n.

3.2 *Single Concentrated Combustion Front at Arbitrary Axial Position*

Rearrange Equation [2.5.9] and drop the subscript 2.

$$\gamma n\bar{u}\exp(-\alpha\bar{\tau}) = -(1 - \gamma n)\bar{u} + \frac{2[1 - B\exp(2\,\alpha)]}{[1 + \exp(2\,\alpha\xi)][1 + B\exp\{2\,\alpha(1-\xi)\}]} \quad [3.2.1]$$

Separate the real and the imaginary parts of Equation [3.2.1] for the neutral oscillation with $\alpha = i\omega$

$$\left.\begin{aligned}\gamma n\bar{u}\cos\omega\bar{\tau} &= -(1 - \gamma n)\bar{u} + \frac{1 - B^2}{1 + B^2 + 2B\cos[(1-\xi)2\,\omega]} \\ \gamma n\bar{u}\sin\omega\bar{\tau} &= \frac{2B\sin(2-\xi)\omega + (1+B^2)\sin\xi\omega}{\cos\xi\omega[1 + B^2 + 2B\cos[(1-\xi)2\,\omega]]}\end{aligned}\right\} \quad [3.2.2]$$

Using Equations [3.1.3] we have

$$\left.\begin{aligned}\gamma n\bar{u}\cos\omega\bar{\tau} &= -(1 - \gamma n)\bar{u} - \frac{(\gamma - 1)\bar{u}}{2\cos^2(1-\xi)\omega} \\ \gamma n\bar{u}\sin\omega\bar{\tau} &= \frac{\sin\omega}{\cos\xi\omega\cos(1-\xi)\omega}\end{aligned}\right\} \quad [3.2.3]$$

By squaring and adding the two equations in [3.2.3], one obtains an equation from which we can solve for the frequencies of the neutral oscillations. For qualitative discussion of the

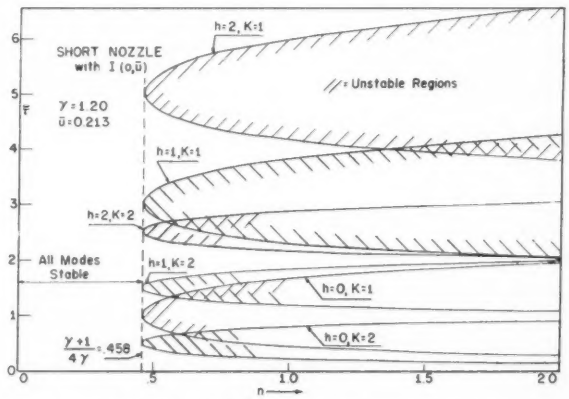

FIG. 3A STABILITY DIAGRAM, $\bar{\tau}$ VS. n, FOR COMBUSTION CONCENTRATED AT INJECTOR END

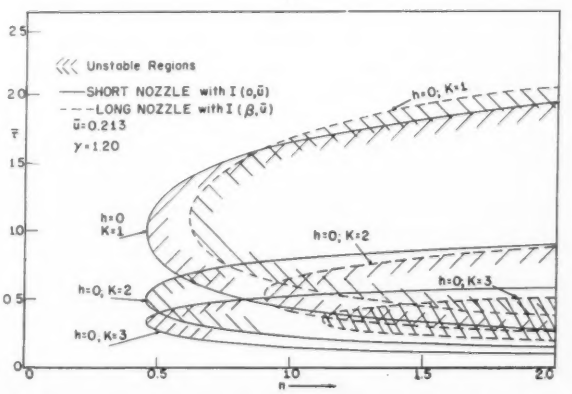

FIG. 3B STABILITY DIAGRAM, $\bar{\tau}$ VS. n, FOR COMBUSTION CONCENTRATED AT INJECTOR END

results, we write this equation as a quadratic of $2\cos^2(1-\xi)\omega$ and solved for $2\cos^2(1-\xi)\omega$. Thus

$$2\cos^2(1-\xi)\omega = \left[\frac{\sin^2\omega}{\cos^2\xi\omega}\cdot\frac{1}{2\gamma n-1}\cdot\frac{1}{\bar{u}^2}+\frac{(1-\gamma n)(\gamma-1)}{2\gamma n-1}\right]+\left\{\left[\frac{\sin^2\omega}{\cos^2\xi\omega}\cdot\frac{1}{2\gamma n-1}\cdot\frac{1}{\bar{u}^2}+\frac{(1-\gamma n)(\gamma-1)}{2\gamma n-1}\right]^2+\frac{(\gamma-1)^2}{2\gamma n-1}\right\}^{1/2} \quad [3.2.4]$$

The minus sign before the square root is dropped because $\cos^2(1-\xi)\omega$ is non-negative. Introducing the following two inequalities

$$2 \geq 2\cos^2(1-\xi)\omega \geq 0, \quad \text{and} \quad \frac{\sin^2\omega}{\cos^2\xi\omega}\cdot\frac{1}{2\gamma n-1}\cdot\frac{1}{\bar{u}^2} \geq 0$$

into Equation [3.2.4] we obtain the following necessary condition for any possible real solutions of ω

$$\frac{(1-\gamma n)(\gamma-1)}{2\gamma n-1}+\left\{\left[\frac{(1-\gamma n)(\gamma-1)}{2\gamma n-1}\right]^2+\frac{(\gamma-1)^2}{2\gamma n-1}\right\}^{1/2} \leq 2 \quad [3.2.5]$$

or

$$n \geq \frac{\gamma+1}{4\gamma}$$

which checks with the minimum value of n as given in Equation [3.1.8].

From Equation [3.2.4] we have another necessary condition for real solutions of ω if only the inequality $2 \geq 2\cos^2(1-\xi)\omega$ is introduced into Equation [3.2.4]

$$\sin^2\omega \leq \left\{\gamma[\gamma n+n-1]-\left(\frac{\gamma-1}{2}\right)^2\right\}\cos^2\xi\omega\cdot\bar{u}^2 \quad [3.2.6]$$

As n is of the order of unity, we must have

$$\sin\omega = \pm\,\bar{u}\cdot 0(1)$$

or

$$\omega = k\pi \pm \bar{u}\cdot 0(1) \quad [3.2.7]$$

Since the unstable regions of ω for the case of $\xi = 0$ is defined in Equation [3.1.11], we conclude that the frequencies of the neutral and the small unstable oscillations for all possible values of ξ are always close to the natural organ-pipe frequencies $k\pi$.

The right-hand side of Equation [3.2.6] vanishes when $n = (\gamma+1)/4\gamma$ or when $\cos\xi\omega = 0$. When either of the two conditions is satisfied, $\sin\omega$ must be zero. The results with $n = (\gamma+1)/4\gamma$ are the same as the result obtained from Equation [3.2.5]. The case $\cos\xi\omega = 0$ leads to an important restriction on the regions of ξ that admit real solutions of ω. When both $\sin\omega$ and $\cos\xi\omega$ are zero, $\cos(1-\xi)\omega$ must vanish; then Equations [3.2.3] cannot admit any real solutions for $\omega\bar{\tau}$.

From Equation [3.2.7] we know ω is approximately $k\pi$; therefore the zeros of $\cos\xi\omega$ are approximately $\xi = 1/2k$, $3/2k\ldots$ so long as $\xi \leq 1$. These positions correspond to the nodes of the pressure oscillations of the kth mode. Around each of these nodes there is a range of positions ξ of the combustion front which is always stable. The critical positions ξ_c which define such stable range around each node are those where the oscillations are neutral with $\omega = k\pi$ and zero unstable ranges of $\bar{\tau}$. Equation [3.2.4] then gives ξ_c as

$$1 \geq \xi_c = 1-\frac{1}{2k\pi}\cos^{-1}\left(\frac{\gamma-1}{2\gamma n-1}-1\right) \geq 0. \quad [3.2.8]$$

For the fundamental mode, $k = 1$, there are two values of

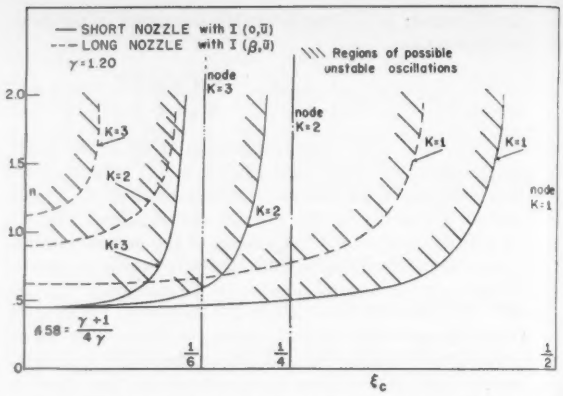

FIG. 4 MINIMUM VALUE OF INTERACTION INDEX n COMPATIBLE WITH UNSTABLE COMBUSTION CONCENTRATED AT ξ_c

ξ_c lying between 0 and 1 symmetric with respect to $1/2$. For the kth mode, we have $2k$ values of ξ_c between 0 and 1, defining k stable regions about the k nodes of the kth mode of oscillations. The results are plotted in Fig. 4 with n vs ξ_c for $k = 1, 2$, and 3, and $\gamma = 1.20$. It is observed that if $n = (\gamma+1)/4\gamma$, the critical values of ξ_c are 0, $2/2k$, $4/2k$, etc., and the entire region of ξ from 0 to 1 are stable except at those critical positions where the oscillations are neutral; and that if $n < (\gamma+1)/4\gamma$, no real values of ξ_c exist. This result agrees with Equations [3.1.8] and [3.2.5], and in addition reveals the fact that if the combustion is concentrated at the injector end $\xi = 0$, the combustion system is most liable to have unstable high-frequency oscillations. The positions 0, $2/2k$, $4/2k$, etc., are approximately the antinodes of the kth mode of pressure oscillations where the amplitude of the pressure oscillations is the largest.

Equation [3.2.4] can be used to solve the frequency of the neutral oscillation for arbitrary values of ξ. But with Equation [3.2.7], a rapidly converging iteration procedure can be used to solve the critical values of $\bar{\tau}$ and ω from equations [3.2.3] and [3.2.4]. By replacing $(1-\xi)\omega^{(0)}$ and $\xi\omega^{(0)}$ with $(1-\xi)k\pi$ and $\xi k\pi$, we can calculate $\sin\omega$ from Equation [3.2.4] and get $\omega^{(1)} = k\pi \pm l^{(1)}\cdot\bar{u}$. Using $\omega^{(1)}$ in the place of $\omega^{(0)}$, we can determine $\omega^{(2)} = k\pi \pm l^{(2)}\cdot\bar{u}$ and repeat the process until the necessary accuracy is acquired. Then Equation [3.2.3] gives the values of $\omega\bar{\tau}$. For the cases calculated, two iterations are sufficient. Calculation is carried out for $k = 1, 2$, and 3 and $h = 0, 1$, and 2 with $n = 1/\gamma = 0.833$, and $\bar{u} = 0.20$. The results are plotted as given in Fig. 5. These curves are not symmetric. The shaded regions for a given mode of oscillation represent the values of $\bar{\tau}$ and ξ that make this mode unstable. We see that there are only a few spots where all the three modes are stable.

From this calculation, it is clear that the position of the concentrated combustion front along the combustion chamber axis has considerable importance. If the combustion is mostly concentrated in a narrow region whose width is only a small fraction of the distance between two adjacent positions ξ_c of a given mode of oscillation, the stability behavior of this mode can be analyzed with the simplified model of concentrated combustion. If the width of the combustion zone is larger than the distance between two adjacent ξ_c of a given mode, it is hardly possible that the simplified model could be used satisfactorily. As the distance between two adjacent positions ξ_c decreases rather fast when k increases, the approximate simplified model becomes less satisfactory for the higher modes of oscillation. Consequently, if most of the combustion in a liquid propellant rocket motor is concentrated in a narrow region, for example, one tenth of the length of the combustion chamber, the stability behavior of the fundamental and the second mode of the high-frequency oscillations can be determined by using the simplified model of concentrated combus-

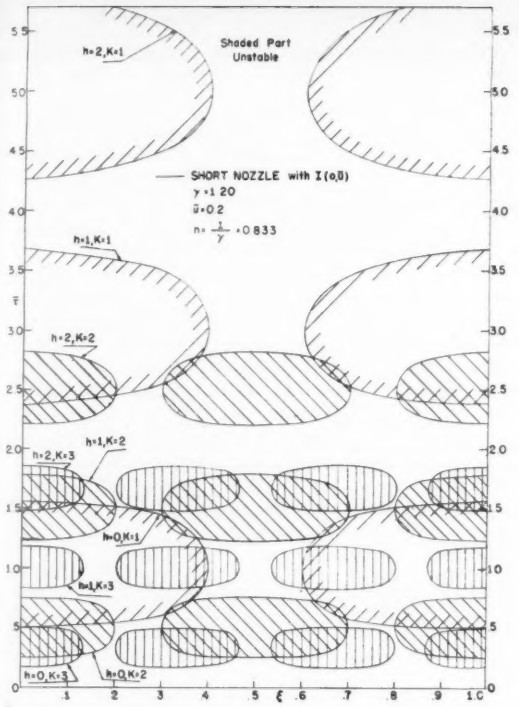

FIG. 5 STABILITY DIAGRAM, $\bar{\tau}$ VS. ξ, FOR PROPELLANTS HAVING $n = 1/\gamma = 0.833$

tion. But the stability behavior of the higher modes as analyzed by using the simplified model should not be considered too seriously.

3.3 *Two-Step Concentrated Combustion with $n = 1/\gamma$*

For the study of the nature of the solution of the two-step concentrated combustion with one at the injector end. we shall consider the representative case of $\gamma n = 1$ for the purpose of simplicity. Equation [2.5.8] becomes

$$\frac{1 - B\exp[2\alpha(1-\xi)]}{1 + B\exp[2\alpha(1-\xi)]} - \frac{[1 + \bar{u}_1\exp(-\alpha\bar{\tau})] - [1 - \bar{u}_1\exp(-\alpha\bar{\tau})]\exp(-2\alpha\xi)}{[1 + \bar{u}_1\exp(-\alpha\bar{\tau})] + [1 - \bar{u}_1\exp(-\alpha\bar{\tau})]\exp(-2\alpha\xi)} = (\bar{u}_2 - \bar{u}_1)\exp(-\alpha\bar{\tau}) \quad [3.3.1]$$

This equation can be rearranged in the form

$$2\exp(-2\alpha\xi)[1 - B\exp(2\alpha)] - 2\exp(-2\alpha\xi)[1 + B\exp(2\alpha)](\bar{u}_2 + \bar{u}_1)\exp(-\alpha\bar{\tau}) = [1 + B\exp[2\alpha(1-2\xi)] + [1 + B\exp[2\alpha(1-\xi)]]\{1 - \exp(-2\alpha\xi)\}\bar{u}_1\exp(-\alpha\bar{\tau})](\bar{u}_2 - \bar{u}_1)\exp(-\alpha\bar{\tau})$$

The coefficient of $\exp(-2\alpha\bar{\tau})$, which is of the order of $(\bar{u}_2 - \bar{u}_1)\bar{u}_1$, will be considered as negligibly small compared with the coefficient of $\exp(-\alpha\bar{\tau})$. Thus

$$\exp(\alpha\bar{\tau}) = [{}^1/_2(\bar{u}_2 + \bar{u}_1)[1 + B\exp(2\alpha)] + {}^1/_2(\bar{u}_2 - \bar{u}_1)[\exp(2\alpha\xi) + B\exp\{2\alpha(1-\xi)\}]][1 - B\exp(2\alpha)]^{-1} \quad [3.3.2]$$

Let $\alpha = i\omega$ for the neutral oscillations and separate the real and the imaginary parts of Equation [3.3.2] with the approximation of Equations [3.1.3]

$$\left.\begin{aligned}\cos\omega\bar{\tau} &= -(\gamma-1)\bar{u}_2[{}^1/_2(\bar{u}_2+\bar{u}_1) + {}^1/_2(\bar{u}_2-\bar{u}_1)\cos 2\xi\omega]/[1-\cos 2\omega]\\ \sin\omega\bar{\tau} &= [{}^1/_2(\bar{u}_2+\bar{u}_1)\sin 2\omega + {}^1/_2(\bar{u}_2-\bar{u}_1)\{\sin 2\xi\omega + \sin 2(1-\xi)\omega\}]/[1-\cos 2\omega]\end{aligned}\right\} \quad [3.3.3]$$

The equation for determining the frequencies of neutral oscillations of the system is obtained as

$$4\sin^4\omega = {}^1/_4(\bar{u}_2+\bar{u}_1)^2[(\gamma-1)^2\bar{u}_2^2 + 4\sin^2\omega\cos^2\omega] + {}^1/_4(\bar{u}_2-\bar{u}_1)^2[(\gamma-1)^2\bar{u}_2^2\cos^2 2\xi\omega + 4\sin^2\omega\cos^2(1-2\xi)\omega] + {}^1/_2(\bar{u}_2^2-\bar{u}_1^2)[(\gamma-1)^2\bar{u}_2^2\cos 2\xi\omega + 4\sin^2\omega\cos\omega\cos(1-2\xi)\omega] \quad [3.3.4]$$

It is not easy to solve for ω from Equation [3.3.4] directly. But a method of successive approximation, analogous to the method used in section 3.2 can be used. From Equation [3.3.4] we see that if $\bar{u}_2 - \bar{u}_1$ is small compared to $\bar{u}_2 + \bar{u}_1$, we have as a zero-th approximation $\omega^{(0)} = k\pi \pm u_1$ which is the solution given in (4). Introducing $\omega^{(0)}$ into the right-hand side of Equation [3.3.4], we can calculate $\omega^{(1)}$ from

$$4\sin^4\omega^{(1)} \cong 4\bar{u}_2^4 - \left(\frac{\bar{u}_2-\bar{u}_1}{2}\right)^2 4\bar{u}_2^2\sin^2(1-2\xi)\omega^{(0)} - \frac{\bar{u}_2^2-\bar{u}_1^2}{2}[1-\cos\omega^{(0)}\cos(1-2\xi)\omega^{(0)}]4\bar{u}_2^2 \quad [3.3.5]$$

The solution of the frequency of the neutral oscillations can thus be written as

$$\omega = k\pi \pm l\bar{u}_2 \quad [3.3.6]$$

where l is a function of ξ and $\bar{u}_2/\bar{u}_1$. From Equation [3.3.5] it is obvious that the coefficient l will be less than unity. At the nodes of the kth mode of pressure oscillations, i.e., $\xi \cong 1/2k, 3/2k, \ldots$ etc., Equation [3 3.4] gives the minimum value of $\sin\omega$ as $\pm(\bar{u}_1\,u_2)^{1/2}$ provided u_1 is not too small. Consequently, the frequencies of the neutral oscillations of the system are not significantly different from the natural organ-pipe frequencies when a small fraction of the concentrated combustion is shifted from the injector end to arbitrary location along the axis.

Having determined ω, we can obtain $\omega\bar{\tau}$ from Equation [3.3.3.]. The result of such calculation is given in Fig. 6. It is noticed that when the second concentrated combustion front is located at the nodes of the kth mode of oscillations,

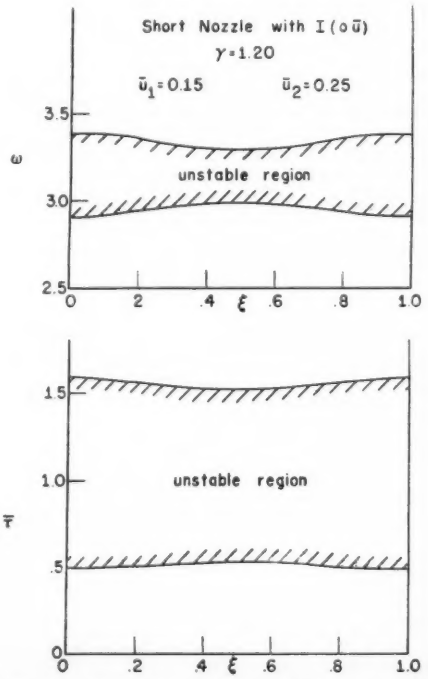

FIG. 6 EFFECT OF SHIFTING A SMALL FRACTION OF COMBUSTION FROM INJECTOR END TO ξ

i.e., $\xi = 1/2k, 3/2k$, etc., $\cos \omega\bar{\tau} \cong -(\gamma-1)\frac{u_2 u_1}{2\bar{u}_2\bar{u}_1} = -\frac{\gamma-1}{2}$, or $\omega\bar{\tau} = (2h+1)\pi \mp \left(\frac{\pi}{2} - \frac{\gamma-1}{2}\right)$. This is identical with the result for the case of a single concentrated combustion located at the injector end. However, owing to the slight decrease of the value of $\sin\omega$, the ranges of the values of $\bar{\tau}$ for producing unstable oscillations when the second concentrated combustion front is located at the nodes are slightly decreased as compared with that of the combustion system having a single concentrated combustion front at the injector end.

From Fig. 6 we see that the shift of a small fraction of the concentrated combustion from the injector end to any arbitrary locations along the axis is slightly stabilizing. The stabilizing effect is most significant when the small fraction is shifted to the node. Even in this case this shift does not give rise to unduly large effect on the stability behavior of the system. It may be inferred that the distribution of a small fraction of combustion from a given concentrated combustion front will not change the qualitative picture of the stability behavior of the system as analyzed with the single concentrated combustion front.

4 Solutions with Long Nozzle

4.1 The Boundary Condition at Combustion Chamber Exit

The proper boundary condition at the combustion chamber exit is, as mentioned in a previous section, the continuity of the disturbances in the combustion chamber and the disturbances in the de Laval nozzle. When the steady-state velocity distribution in the nozzle is linear from the entrance to the sonic throat, the ratio I of the fractional variation of the velocity to the density disturbance at the nozzle entrance is obtained in (6). The real and the imaginary parts of I when $\gamma = 1.20$ are plotted against the reduced frequency parameter β for different values of the reduced steady-state velocity parameter $Z = ((\gamma+1)/2)\, u^2$ (Fig. 2). The reduced frequency β is defined as the angular frequency of the oscillation divided by the steady-state velocity gradient in the subsonic part of the nozzle, i.e., $\beta = \omega \cdot l_{sub}/(\sqrt{2/(\gamma+1)} - u)$. Here l_{sub} is the length of the subsonic part of the nozzle as a fraction of the combustion chamber length.

For the fundamental mode of high-frequency oscillation, we know ω is about π. The value of β corresponding to the

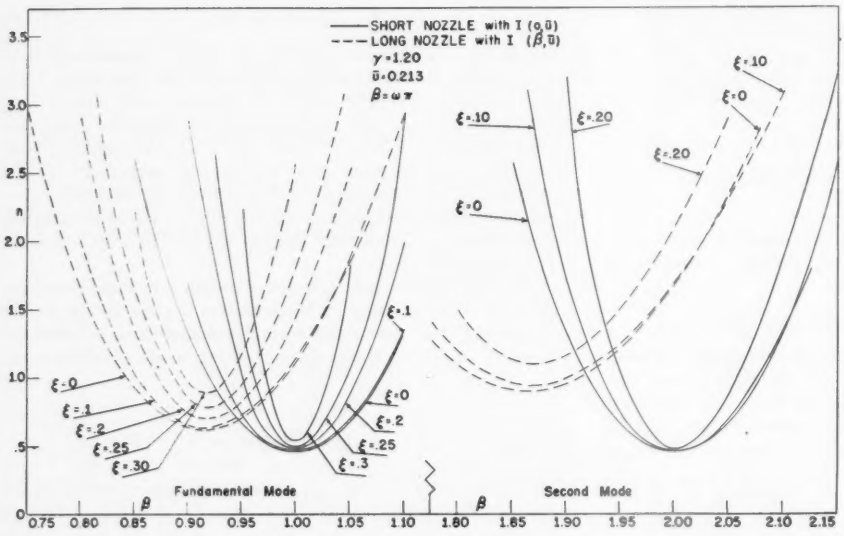

FIG. 7A

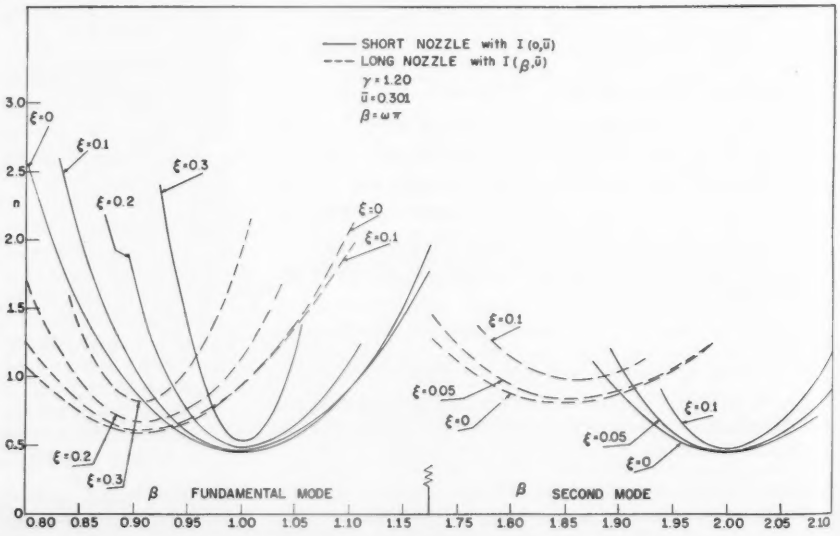

FIG. 7B

FIGS. 7A, 7B INTERACTION INDEX n CORRESPONDING TO NEUTRAL OSCILLATION OF FREQUENCY $\omega = \beta\pi$ FOR COMBUSTION CONCENTRATED AT ξ

fundamental mode is approximately $\pi l_{sub}/[\sqrt{2/(\gamma+1)} - \bar{u}]$. Since $\bar{u}$ is relatively small, the value of β for the fundamental mode depends primarily on the value of l_{sub}. In practical cases l_{sub} is often close to $1/3$. If l_{sub} of the nozzle is very small, the value of β corresponding to fundamental mode is very small. Therefore, if the one-dimensional picture could be extrapolated to such limiting case, the boundary condition of constant Mach number would apply satisfactorily to the case of a nozzle with a very short subsonic part. On the other hand, if l_{sub} is reasonably long, the stability behavior of the fundamental mode can be considerably different from that determined by the constant Mach number boundary condition.

We shall consider a practical example with $l_{sub}/[\sqrt{2/(\gamma+1)} - \bar{u}] = \pi$ such that $\omega = \beta\pi$. Thus the fundamental mode of acoustical oscillation corresponds to $\beta = 1$ and the kth mode corresponds to $\beta = k$. It should be noted that for different values of $\bar{u}$, the condition $\omega = \beta\pi$ requires that nozzles of different lengths are used with the combustion chamber.

4.2 *Solution for the Case of a Single Concentrated Combustion Front*

Equation [2.5.9.] can be rewritten as

$$\left[\frac{1 - B\exp\{2\alpha(1-\xi)\}}{1 + B\exp\{2\alpha(1-\xi)\}} - \tanh\alpha\xi\right]\frac{1}{u} =$$

$$(1 - \gamma n) + \gamma n \exp(-\alpha\tau) \ldots\ldots [4.1.1]$$

with $\alpha = i\omega$ for the neutral oscillations and $B = (1 + I\bar{u})/(1 - I\bar{u})$ where $I = R + iS$ is given graphically in Fig. 2 for $\gamma = 1.20$ as a function of z(or $\bar{u}$) and β (or ω). The stability boundary is determined numerically for two particular cases

$$z = 0.05 \text{ and } 0.10$$

corresponding to

$$\bar{u} = 0.213 \text{ and } 0.301$$

For a given value of ξ and a series of values of ω, the left-hand side of Equation [4.1.1] is calculated. Call this quantity

$$X + iY = \frac{1}{\bar{u}}\left[\frac{1 - B\exp\{2i\omega(1-\xi)\}}{1 + B\exp\{2i\omega(1-\xi)\}} - \tanh i\omega\xi\right] \ldots [4.1.2]$$

Then the values of n corresponding to the series of values of ω are given by

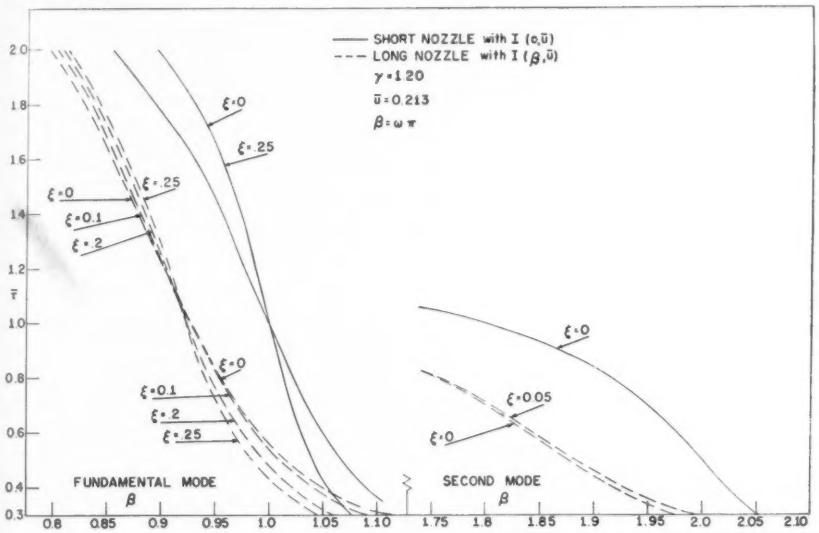

FIG. 8A

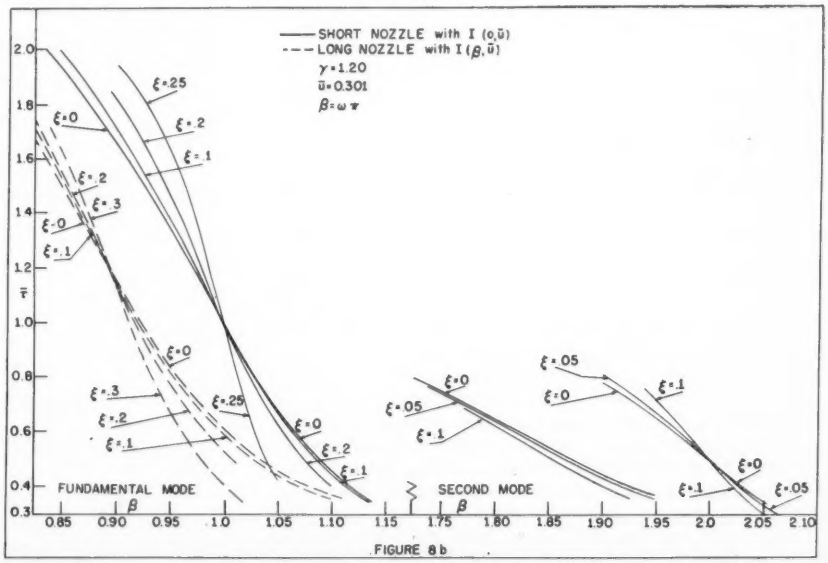

FIG. 8B

FIGURE 8b

FIGS. 8A, 8B CRITICAL VALUES OF $\bar{\tau}$ CORRESPONDING TO NEUTRAL OSCILLATION OF FREQUENCY $\omega = \pi\beta$ FOR COMBUSTION CONCENTRATED AT ξ

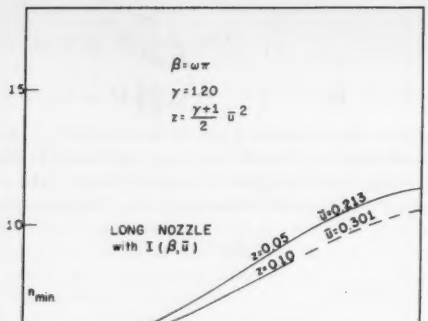

FIG. 9 MINIMUM VALUE OF INTERACTION INDEX n COMPATIBLE WITH UNSTABLE OSCILLATION OF FREQUENCY $\omega = \pi\beta$

$$n = \frac{1 - X}{2\gamma} + \frac{Y^2}{2\gamma(1 - X)} \quad \text{..... [4.1.3]}$$

and the corresponding critical values of $\bar{\tau}$ by

$$\bar{\tau} = \frac{1}{\omega} \sin^{-1}\left[\frac{-Y}{\gamma n}\right] \quad [4.1.4]$$

The value of $\sin^{-1}(-Y/\gamma n)$ is taken in the quadrant consistent with $\cos \omega\bar{\tau} = 1 - ((1-X)/\gamma n)$. The calculated results are plotted as shown in Figs. 7, 8, 9, 10, 11. For the purpose of comparison, these curves are also calculated and plotted when the boundary condition $I(0, u) = (\gamma-1)/2$ is used.

It is noticed in Figs. 7 (a) and 7 (b) that curves of n vs. β with the two different boundary conditions are of similar shape and vary with the same trend. The curve with the boundary condition $I(\beta, u) = [(v/\bar{u})/(\delta/\bar{p})]_{x=1}$ for long nozzle is shifted toward larger values of n and smaller values of β as compared to the corresponding curve with the constant Mach number boundary condition for very short nozzle. As a result, there are many apparent but important results with respect to the effect of changing the ratio of the length of the subsonic portion of the nozzle to the combustion chamber length.

1 The minimum value of n compatible with any unstable pressure oscillations determined by the long nozzle boundary condition increases rapidly with increasing β or ω. This is shown in Fig. 9. When the constant Mach number or short nozzle boundary condition is used, the minimum value of n for all the different modes of oscillation is the same constant $(\gamma+1)/4\ \gamma$, slightly less than $1/2$, which is the minimum value of n for the unstable low-frequency oscillation corresponding to $k = 0$.

2 When ξ increases, the rate of increase of the minimum value of n determined by the long nozzle boundary condition is larger than the corresponding rate determined by the short nozzle boundary condition. Both results are plotted in Fig. 4 as the dotted and the solid curves, respectively.

3 For a given value of n, the unstable region of $\bar{\tau}$ and ξ as determined by the long nozzle boundary condition are smaller than the corresponding unstable region as determined by the short nozzle boundary condition. Owing to the rapid increase of the minimum value of n for increasing ω, there is an upper limit of the frequency of possible unstable oscillation as determined from Fig. 9 for given value of n. This is quite different from the result given in section 3.2 and Fig. 5, where there is no such upper limit. Calculation for the case of

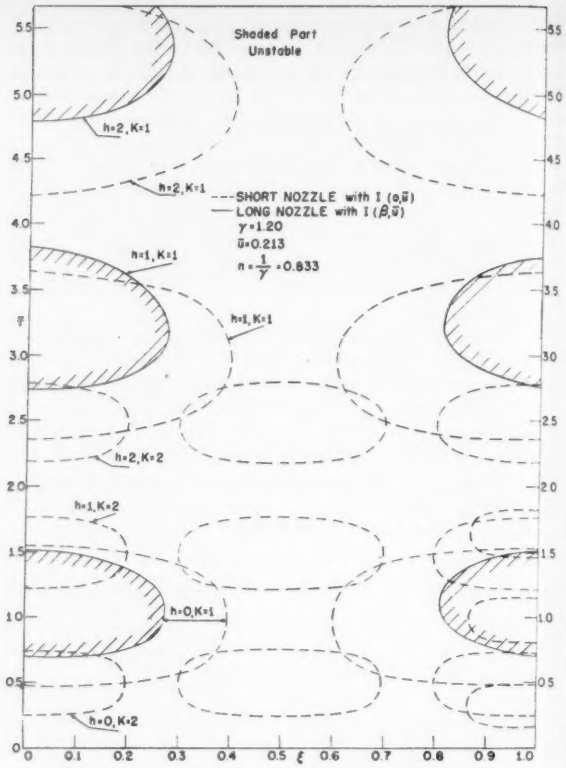

FIG. 10 STABILITY DIAGRAM, $\bar{\tau}$ VS. ξ, FOR PROPELLANTS HAVING $n = 1/\gamma = 0.833$

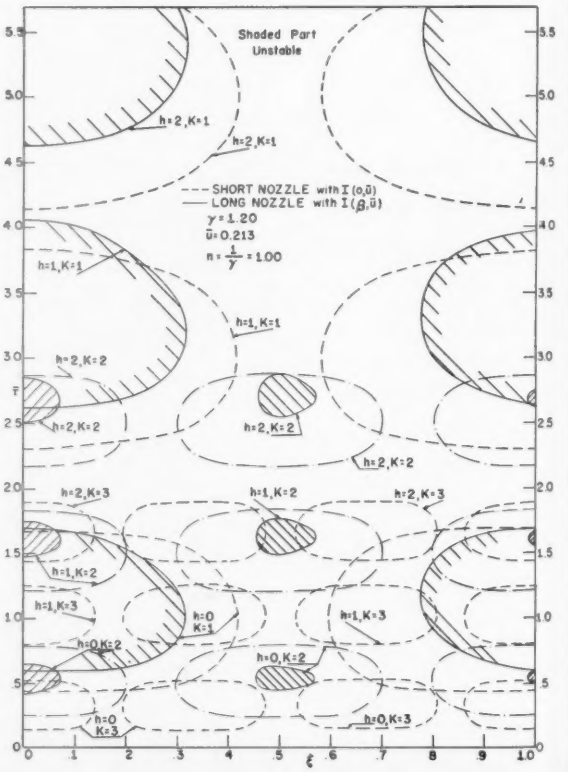

FIG. 11 STABILITY DIAGRAM, $\bar{\tau}$ VS. ξ, FOR PROPELLANTS HAVING $n = 1.00$

$n = 1/\gamma = 0.833$ and $\bar{u}_1 = 0.213$, using the long nozzle boundary condition, shows that the fundamental mode will be unstable when the values of $\bar{\tau}$ and ξ are in certain ranges while all the other modes are always stable (Fig. 10). For the case of $n = 1$, both the fundamental and the second mode may be unstable but not the higher modes (Fig. 11).

Consequently, in every respect, the combustion system with long nozzle is more stable than the one with very short nozzle.

It should be noticed that the rate of increase of the minimum value of n compatible with unstable kth mode of oscillation increases rather fast as k increases. The actual magnitude of n of the common liquid propellants is not known. However, being an exponential index, n is not likely to be much larger than unity. Therefore, for practical cases the higher modes of pressure oscillations are expected to be stable. Furthermore, even if these higher modes become unstable, they are not likely to build up rough combustions owing to the more effective viscous damping of the high-frequency components. It is the unstable fundamental and the first few high-frequency modes that result in rough combustion and hence are of practical interest.

A comparison of the results in Figs. 7 (a) and 7 (b) and in Fig. 9 for the two cases with different $\bar{u}$ shows that by increasing $\bar{u}$ from 0.213 to 0.301 while the nozzle is so modified as to maintain the relation $\omega = \beta\pi$, the minimum value of n compatible with unstable oscillations are slightly decreased; that is, the system becomes a little more unstable. The change is, however, rather small as produced by 40 per cent increase of the flow Mach number. Whether the effect of increasing $\bar{u}$ is destabilizing or stabilizing is as yet uncertain, because this small difference in n can be easily compensated by the terms of the order of $\bar{u}^2$ which have been neglected in the present analysis. It seems, however, that the stability behavior is rather insensitive to the change of flow velocity in the combustion chamber when $l_{sub}/[\sqrt{2/(\gamma+1)} - \bar{u}]$ is kept unchanged.

As has been mentioned in section 3, if the combustion is reasonably concentrated, the simplified model of concentrated combustion front can be used to analyze the stability behavior of the fundamental and the first few high-frequency modes of oscillation, but cannot be used to analyze the stability behavior of the higher modes with the constant Mach number boundary condition at $x = 1$. Now with the boundary condition for long nozzle at $x = 1$, all that we are interested in is the stability behavior of the fundamental and the first few high-frequency modes, because all the higher modes are expected to be stable. Consequently, the simplified model of concentrated combustion is a convenient model for analyzing the stability of the high-frequency oscillation if the combustion zone lies in a region which is small compared to the combustion chamber length.

From the calculated results with $\gamma = 1.20$, we see that if the combustion zone lies either between $\xi = 0.32$ and $\xi = 0.45$, or between $\xi = 0.57$ and $\xi = 0.78$, all the high-frequency modes are stable for any values of $\bar{\tau}$ when n is not larger than 1. Quantitative results as obtained in this calculation will be somewhat different when the steady-state velocity profile in the subsonic portion of the nozzle is not linear; but the qualitative results as shown in the present calculation is expected to remain unchanged.

5 Summary of Conclusions

From the previous results, we can draw in general the following qualitative conclusions:

1 The frequencies of the unstable pressure oscillations in the combustion chamber excited by the interaction between the combustion process and the pressure oscillations are close to the natural frequencies of the combustion system.

2 For a given configuration of the concentrated combustion unstable pressure oscillations are possible when the pressure index n of interaction is sufficiently large and when the value of the pressure sensitive time lag $\bar{\tau}$ of the system lies in certain ranges which are functions of n. These ranges of $\bar{\tau}$ for unstable pressure oscillations of a given mode increases if n increases from its minimum value.

3 There is an absolute minimum value of n which is $(\gamma +)/4\gamma$. If a combustion system has a value of n less than $(\gamma+1)/4\gamma$, all the high-frequency oscillations are stable no matter what the value of $\bar{\tau}$ is, where the combustion is concentrated, and what boundary condition at the exit of the combustion chamber is used.

4 The minimum value of n compatible with unstable pressure oscillations of a given mode increases when the concentrated combustion front is further away from the nearest antinode of the pressure oscillations of that mode. This minimum value of n for a given mode becomes "infinite" if the concentrated combustion approaches any of the nodes of that mode of pressure oscillation. The injector end is an antinode of all the modes of oscillations and the configuration with concentrated combustion front at the injector end is most liable to become unstable.

5 When the concentrated combustion front is at the injector end, the minimum value of n for the kth mode to be unstable increases rapidly with increasing k except when the nozzle is very short and the constant Mach number boundary condition is to be used at the axial exit. The higher modes of oscillations are relatively more stable than the lower modes in practical cases.

6 Rockets with very short nozzles are more unstable than similar rockets with long nozzle. A rocket with short nozzle has lower minimum value of n and larger unstable ranges of $\bar{\tau}$. The qualitative stability behavior of the two rockets are, however, similar and the results as determined by short nozzle boundary condition are a helpful qualitative guide in the numerical determination of the stability boundary with long nozzle boundary condition.

7 The stability behavior of a system with concentrated combustion is rather insensitive to the change of the flow Mach number of the gas in the combustion chamber if the velocity gradient in the subsonic portion of the nozzle is not changed.

8 If the combustion is mostly concentrated in a region whose width is only a small fraction of the combustion chamber length, the stability behavior of the fundamental and the next few higher modes of oscillations can be satisfactorily analyzed by using the simplified model of concentrated combustion front. The higher modes of oscillations are expected to be stable when the long nozzle boundary condition is used at the combustion chamber exit. If the combustion is distributed so that the combustion zone covers considerable portion of both the stable region and the unstable region of ξ of the fundamental mode, there is no obvious position of the concentrated combustion front in the simplified model which can be satisfactorily used for the analysis of the stability behavior of the actual system.

Since the analysis is made on a one-dimensional basis in the axial direction, all results apply to longitudinal oscillations only.

References

1 "Stability of Flow in a Rocket Motor," by D. F. Gunder and D. R. Friant, *Journal of Applied Mechanics*, vol 17, September 1950, pp. 327–333.

2 Discussion of Ref. 1 above, by M. Yachter, *Journal of Applied Mechanics*, vol. 18, January 1951, pp. 114–116.

3 "A Theory of Unstable Combustion in Liquid Propellant Rocket Motors," by M. Summerfield, JOURNAL OF THE AMERICAN ROCKET SOCIETY, vol. 21, September 1951, pp. 108–114.

(*Continued on page 322*)

Aerodynamic Forces on a Cylinder for the Free Molecule Flow of a Nonuniform Gas

S. BELL[1] and S. A. SCHAAF[2]

University of California, Berkeley, Calif.

The aerodynamic forces on a cylinder which is small compared to the mean free path are calculated for the case of an incident gas flow which is in non-Maxwellian equilibrium. This nonequilibrium condition is associated with the presence of viscous stress and heat flux terms. It is shown that the shear stress and normal heat flux give rise to lift forces on the cylinder, while the tangential heat flux and the deviation of the normal stresses from the hydrostatic pressure give rise to additional drag forces. A modified version of the interaction of gas molecules and surfaces is introduced which involves three reflection coefficients governing the average transfer of energy and normal and tangential momentum.

Nomenclature

dA = element of surface area
C_D = drag coefficient, Equation [3.4]
C_L = lift coefficient, Equation [3.5]
$C_{Dp_{xx}}$, $C_{L\tau_{xy}}$, etc. = partial drag and lift coefficients proportional to term indicated in subscript, Equations [3.4], [3.5]
dE_i, dE_r, dE_w = energy fluxes incident, reflected, and diffusely reflected from dA, Equation [2.7]
F_D = drag force per unit length of cylinder
F_L = lift force per unit length of cylinder
$\vec{dF}$ = force on dA
$\vec{dF_i}$ = component of $\vec{dF}$ due to incident molecules
$\vec{dF_r}$ = component of $\vec{dF}$ due to reflected molecules
f = molecular velocity distribution function, Equation [2.5]
f° = Maxwellian distribution, Equation [2.4]
I_0, I_1 = modified Bessel functions of zero and first order
k = thermal conductivity
M = Mach number
m = molecular mass
N_w = number of molecules incident on dA per unit time per unit surface area
p = pressure
p_i, p_r, p_w = pressure on dA due to incident, reflected, and diffusely reflected molecules, respectively, Equation [2.10]
p_{xx}, p_{yy}, p_{zz} = normal stress deviation terms, Equations [2.5], [2.6]
q_x, q_y, q_z = heat flux terms, Equations [2.5], [2.6]
r = cylinder radius
R = gas constant
s = molecular speed ratio, Equation [3.3]
s_w = molecular speed ratio referred to cylinder temperatures, Equation [3.3] (s_w assumed equal to s in computations)
T = gas temperature
T_i = temperature of incident molecules, Equation [2.13]
T_w = cylinder temperature
u, v, w = molecular velocity component in x, y, z-direction, Fig. 1
U, V, W = gas velocity components
u', v', w' = molecular velocity components in x', y', z'-directions, Fig. 1
x, y, z = co-ordinates referred to flow direction, Fig. 1
x', y', z' = co-ordinates referred to surface element, Fig. 1
α = thermal accommodation coefficient, Equation [2.7]
γ = ratio of specific heats
μ = viscosity coefficient
θ = angle between surface normal and flow direction, Fig. 1
ρ = gas density
σ, σ' = reflection coefficients for tangential and normal momentum transfer, Equations [2.9], [2.10]
τ_i, τ_r, τ_w = shear stress due to incident, reflected, and diffusely reflected molecules, respectively, Equation [2.9]
τ_{xy}, τ_{xz}, τ_{yz} = shear stress terms, Equations [2.5], [2.6]

Received February 25, 1953.

[1] Research Mathematician, Department of Engineering.

[2] Associate Professor of Engineering Science.

1.0 Introduction

THE forces exerted upon a body in free molecule flow, i.e., on a body whose characteristic dimension is small compared to the molecular mean free path, have been determined theoretically by Tsien (1),[3] Stalder and Zurick (2), and others (10 to 12). Experiments by Stalder, Goodwin, and Creager (3), and by Kane and Estermann (4) have provided general confirmation of the theoretical developments.

These investigations have been confined to the case in which the gas flow past the body is in Maxwellian equilibrium. This restriction is satisfactory for free flight considerations but not for what may, perhaps, prove to be one of the most important applications of free molecule flow analyses. This is wind tunnel measurement of the velocity, and perhaps other flow variables, of a gas stream by means of small "free molecule flow" probes. The possibilities are especially promising in connection with hypersonic or supersonic wind tunnels operating at low test section densities (13). These probes might be of either the heat transfer or aerodynamic force type, or perhaps both. It is clear, however, that for probing boundary layers or shock waves or other characteristic parts of a flow field, the instrument will often be exposed to a gas stream which is not in Maxwellian equilibrium. The occurrence of a large shear stress in a boundary layer, for example, produces a departure of the molecular velocity distribution from the Maxwellian. As will be seen below, this nonuniformity gives rise to additional force terms.

Approximate analyses of the forces on bodies in such non-Maxwellian free molecule flows have been made by Einstein (5) and Epstein (6) in connection with the radiometer problem. In their discussions the nonuniformity was confined to the case of a local heat flux, and in any case the results were only of order-of-magnitude validity.

In the present report a more detailed analysis of the free molecular flow of a nonuniform gas is made. The results are

[3] Numbers in parentheses refer to the References on page 317.

general enough to include arbitrary (small) stress and heat flux. The body geometry has been confined to that of a right circular cylinder oriented perpendicular to the gas flow velocity, and it is assumed the body's thermal conductivity is so large that it is at uniform temperature. Only the aerodynamic force characteristics are determined. The extensions to the determination of heat transfer characteristics, to other body geometries and to the case of very low internal conductivity, will be presented in subsequent reports. The method, however, will be apparent from the present paper.

2.0 Method of Analysis

2.1 The Incident Molecules

The general method followed is a direct extension of the method for the Maxwellian case used by Tsien (1) and Stalder and Zurick (2), and was suggested by Goodwin. The force per unit area $\vec{dF}/dA$ on a surface element dA is broken up into a part $\vec{dF_i}/dA$ due to the incident molecules, and a part $\vec{dF_r}/dA$ due to the reflected or re-emitted molecules. Total force characteristics are obtained by integration over the surface of the body.

The force $\vec{dF_i}/dA$ is analyzed in terms of the component p_i normal to the surface (pressure) and the component τ_i tangential to the surface (shear stress). See Fig. 1. These

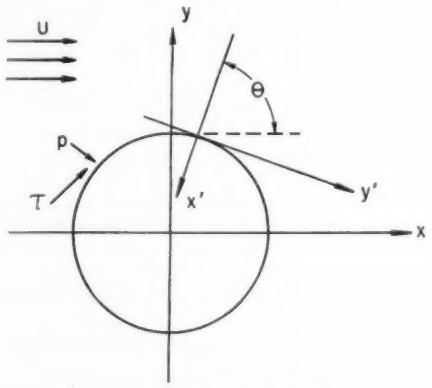

FIG. 1 CO-ORDINATE SYSTEM

quantities are obtained in terms of the molecular velocity distribution function, $f(u, v, w)$, which is the number density per unit volume of phase space of molecules with velocity components, u, v, w. One has

$$p_i = m \int_{-\infty}^{\infty} \int_{-\infty}^{\infty} \int_{0}^{\infty} u'^2 f du' dv' dw' \quad \ldots\ldots [2.1]$$

$$\tau_i = m \int_{-\infty}^{\infty} \int_{-\infty}^{\infty} \int_{0}^{\infty} u'v' f du' dv' dw' \quad \ldots\ldots [2.2]$$

where m is the molecular mass. The velocity components u, v, w and u', v', w' are related (see Fig. 1) by

$$\left.\begin{aligned} u &= -u' \cos\theta + v' \sin\theta \\ v &= -u' \sin\theta - v' \cos\theta \\ w &= w' \end{aligned}\right\} \quad \ldots\ldots [2.3]$$

where θ is the angle between the (outward) normal to the surface and the x (flow)-direction.

The function f is given in the Maxwellian case by

$$f(u, v, w) = f^\circ = \frac{\rho}{m(2\pi RT)^{3/2}} e^{-((u-U)^2 + v^2 + w^2)/2RT} \quad [2.4]$$

where ρ, T, U, R are the gas density, temperature, flow velocity, and the gas constant, respectively. For the non-Maxwellian case, one uses the distribution function considered by Maxwell (7) and Grad (8)

$$f = f^\circ \left[1 + \frac{1}{2pRT} \left\{ p_{xx}(u-U)^2 + p_{yy}v^2 + p_{zz}w^2 - 2\tau_{xy}(u-U)v - 2\tau_{xz}(u-U)w - 2\tau_{yz}vw - 2\left(1 - \frac{(u-U)^2 + v^2 + w^2}{5RT}\right)(q_x(u-U) + q_y v + q_z w) \right\} \right] \quad \ldots [2.5]$$

where p_{xx}, τ_{xy}, q_x, etc., are the viscous stress and heat flux components. These quantities, together with ρ, U, and T, are treated as constants throughout the region occupied by the cylinder. For the equilibrium case, and for small gradients of velocity and temperature, these terms are related to the velocity and temperature by the Navier-Stokes relations

$$\left.\begin{aligned} p_{xx} &= -2\mu \left[\frac{\partial U}{\partial x} - \frac{1}{3}\left(\frac{\partial U}{\partial x} + \frac{\partial V}{\partial y} + \frac{\partial W}{\partial z} \right) \right] \\ \tau_{xy} &= \mu \left[\frac{\partial U}{\partial y} + \frac{\partial V}{\partial x} \right] \\ q_x &= -k \frac{\partial T}{\partial x} \end{aligned}\right\} \quad \ldots [2.6]$$

For rapid processes (e.g., shock waves) or for large gradients of temperature and velocity, more complicated relations exist; see (8) for details. In the present report, the results will be obtained in terms of the variables listed in Equation [2.5], so that they are independent of whether or not Equations [2.6] are valid. It should also be mentioned that for sufficiently nonuniform situations the approximation of Equation [2.5] itself becomes poor. Additional terms in the expression for the molecular velocity distribution would then be required and would contribute to the gross force exerted upon the body. The relative dependence upon the parameters p_{xx}, τ_{xy}, q_x, etc., however, would be unchanged.

2.2 The Reflected Molecules

The determination of $\vec{dF_r}$, the force on dA due to the re-emitted molecules, requires a specification of the nature of the interaction of the impinging molecules with the surface. The treatment of this question will be somewhat generalized in this report from the usual treatment of Maxwell (7) which has been followed in the subsequent work of Tsien (1), Stalder and Zurick (2), and others. Traditionally, the interaction has been described in terms of two parameters, the thermal accommodation coefficient α and the specular reflection coefficient σ. The quantity α is defined by

$$\alpha = \frac{dE_i - dE_r}{dE_i - dE_w} \quad \ldots\ldots [2.7]$$

where dE_i, dE_r, and dE_w are the energy fluxes, respectively, incident on and re-emitted from the surface, and the flux which would be re-emitted if all incident molecules were re-emitted with a Maxwellian distribution corresponding to the surface temperature T_w. The quantity α then is a measure of the degree to which the incident molecules are "accommodated" to the surface. Measured values of α are usually slightly less than unity (9). It will be observed that all quantities on the right side of Equation [2.7] are well-defined and can be either calculated or measured.

The definition of σ, however, is somewhat less satisfactory. It is supposed that the incident molecules are either reflected "specularly" (i.e., with simple reversal of normal velocity) or "diffusely" (which for some applications can be just "randomly," but eventually must be defined more precisely as Maxwellian corresponding to a temperature T_r which is not necessarily the same as T_w). The coefficient σ is then defined as the fraction of diffusely reflected molecules, $1 - \sigma$ being the fraction which is specularly reflected. The definition in this

form of the quantity σ thus becomes meaningless unless the actual interaction with the surface is of the type specified. As measured values of σ have actually been determined, however, this difficulty has been avoided because only gross tangential forces are dealt with. Thus, according to the definition of σ, one has

$$\sigma = \tau_i - \tau_r/\tau_i \quad \ldots\ldots [2.8]$$

where τ_i and τ_r are the incident and reflected fluxes of tangential momentum (shear stress). For all practical purposes, Equation [2.8], rather than the specular-diffuse model, has been the defining equation for σ. The two definitions are in agreement if the interaction actually is of the specular-diffuse type (which, of course, it almost certainly is not), otherwise Equation [2.8] defines σ. Equation [2.8] may be written also, for symmetry with Equation [2.7], in the form

$$\sigma = \tau_i - \tau_r/\tau_i - \tau_w \quad \ldots\ldots [2.9]$$

where τ_w is defined as the tangential momentum flux which would be reflected from the surface if all incident molecules were re-emitted with a Maxwellian distribution corresponding to the surface temperature T_w. Clearly $\tau_w = 0$.

Thus the difficulty inherent in the original definition of σ is avoided, in so far as the determination of tangential forces. However, it occurs again in the determination of normal forces, and again recourse has been taken in (1) and (2), for example, to the specular-diffuse model. If the actual interaction is different, then the determination of heat transfer, tangential force, and normal force in terms of just the two parameters α and σ would yield results which one would expect to be mutually inconsistent. This difficulty can be avoided if an additional parameter σ', say, is defined by

$$\sigma' = p_i - p_r/p_i - p_w \quad \ldots\ldots [2.10]$$

where p_i, p_r, and p_w are, respectively, the incident and reflected fluxes of normal momentum (pressure), and the flux which would be re-emitted if all the incident molecules were re-emitted with a Maxwellian distribution corresponding to the surface temperature T_w.

The quantity p_w is given (2) by

$$p_w = N_w m \sqrt{\frac{\pi RT_w}{2}} \quad \ldots\ldots [2.11]$$

where N_w is the number of molecules per unit time incident on a unit surface area It is given by

$$N_w = \int_{-\infty}^{\infty}\int_{-\infty}^{\infty}\int_{0}^{\infty} u' f du' dv' dw' \quad \ldots\ldots [2.12]$$

For completely specular reflection one has $\alpha = \sigma = \sigma' = 0$. For completely diffuse reflection, $\alpha = \sigma = \sigma' = 1$. For the hypothetical partly diffuse, partly specular interaction, and for a surface at rest with respect to the gas, one would have

$$\sigma' = \frac{\sigma\sqrt{T_i} - \sqrt{\sigma(\sigma - \alpha)T_i + \sigma\alpha T_w}}{\sqrt{T_i} - \sqrt{T_w}} \to \alpha \text{ as } T_w \to T_i \quad \ldots [2.13]$$

However, in general, for actual physical interaction the three parameters would be independent. They are sufficient, however, to determine free molecule flow heat transfer and aerodynamic force characteristics.[4]

[4] Strictly speaking, it would be logical for completeness to introduce two additional interaction parameters, one for possible asymmetry in the momentum transfer in the direction mutually perpendicular to the normal and tangential directions, and the other to allow for possible net mass interaction, i.e., ingassing or outgassing. It is tacitly assumed in the present report that such additional phenomena are not present.

2.3 *The Combined Expressions*

The total force on a unit of surface area is analyzed into a normal component p and a tangential component τ given by

$$\left.\begin{aligned} p &= p_i + p_r \\ \tau &= \tau_i - \tau_r \end{aligned}\right\} \quad \ldots\ldots [2.14]$$

With the help of Equations [2.9] and [2.10] these reduce to

$$\left.\begin{aligned} p &= (2 - \sigma')p_i + \sigma' p_w \\ \tau &= \sigma\tau_i \end{aligned}\right\} \quad \ldots\ldots [2.15]$$

In terms of f, using Equations [2.11], [2.12], [2.1], and [2.2], one has

$$\left.\begin{aligned} p &= m\int_{-\infty}^{\infty}\int_{-\infty}^{\infty}\int_{0}^{\infty} f\left[(2 - \sigma')u'^2 + \sigma'\sqrt{\frac{\pi RT_w}{2}}\,u'\right] du'dv'dw' \\ \tau &= \sigma m\int_{-\infty}^{\infty}\int_{-\infty}^{\infty}\int_{0}^{\infty} u'v' f du'dv'dw' \end{aligned}\right\} \quad \ldots [2.16]$$

The total force on a unit length of the cylinder is obtained in terms of the drag force F_D and the lift force F_L. These are given by

$$\left.\begin{aligned} F_D &= \int_0^{2\pi} (-p\cos\theta + \tau\sin\theta) r d\theta \\ F_L &= \int_0^{2\pi} (-p\sin\theta - \tau\cos\theta) r d\theta \end{aligned}\right\} \quad \ldots\ldots [2.17]$$

Combining Equations [2.17], [2.16], [2.5], and [2.3], one has finally

$$F_D = \frac{\rho}{(2\pi RT)^{3/2}}\int_0^{2\pi}\int_{-\infty}^{\infty}\int_{-\infty}^{\infty}\int_0^{\infty}\left\{\left(-\left[(2 - \sigma')u'^2 + \sigma'\sqrt{\frac{\pi RT_w}{2}}\,u'\right]\cos\theta + \sigma u'v'\sin\theta\right)\times e^{-\frac{(-u'\cos\theta + v'\sin\theta - U)^2 + (-u'\sin\theta - v'\cos\theta)^2 + w'^2}{2RT}}\left(1 + \frac{1}{2pRT}\left[p_{xx}(-u'\cos\theta + v'\sin\theta - U)^2 + p_{yy}(-u'\sin\theta - v'\cos\theta)^2 + p_{zz}w'^2 - 2\tau_{xy}(-u'\cos\theta + v'\sin\theta - U)(-u'\sin\theta - v'\cos\theta) - 2\tau_{xz}(-u'\cos\theta + v'\sin\theta - U)w' - 2\tau_{yz}(-u'\sin\theta - v'\cos\theta)w' - 2\left(1 - \frac{(-u'\cos\theta + v'\sin\theta - U)^2 + (-u'\sin\theta - v'\cos\theta)^2 + w'^2}{5RT}\right)\times\left(q_x(-u'\cos\theta + v'\sin\theta - U) + q_y(-u'\sin\theta - v'\cos\theta) + q_z w'\right)\right]\right)\right\} r du'dv'dw'd\theta \quad \ldots [2.18]$$

$$F_L = \frac{\rho}{(2\pi RT)^{3/2}}\int_0^{2\pi}\int_{-\infty}^{\infty}\int_{-\infty}^{\infty}\int_0^{\infty}\left\{-\left(\left[(2 - \sigma')u'^2 + \sigma'\sqrt{\frac{\pi RT_w}{2}}\,u'\right]\sin\theta + \sigma u'v'\cos\theta\right)\times e^{-\frac{(-u'\cos\theta + v'\sin\theta - U)^2 + (-u'\sin\theta - v'\cos\theta)^2 + w'^2}{2RT}}\left(1 + \frac{1}{2pRT}\left[p_{xx}(-u'\cos\theta + v'\sin\theta - U)^2 + p_{yy}(-u'\sin\theta - v'\cos\theta)^2 + p_{zz}w'^2 - 2\tau_{xy}(-u'\cos\theta + v'\sin\theta - U)(-u'\sin\theta - v'\cos\theta) - 2\tau_{xz}(-u'\cos\theta + v'\sin\theta - U)w' - 2\tau_{yz}(-u'\sin\theta - v'\cos\theta)w' - 2\left(1 - \frac{(-u'\cos\theta + v'\sin\theta - U)^2 + (-u'\sin\theta - v'\cos\theta)^2 + w'^2}{5RT}\right)\times\left(q_x(-u'\cos\theta + v'\sin\theta - U) + q_y(-u'\sin\theta - v'\cos\theta) + q_z w'\right)\right]\right)\right\} r du'dv'dw'd\theta \quad \ldots [2.19]$$

3.0 Results

Performing the integration indicated in Equations [2.18] and [2.19], one obtains

$$F_D = \rho r U^2 \left\{ \frac{(4 - 2\sigma' + \sigma)\sqrt{\pi} e^{-s^2/2}}{6S} \left[(3 + 2s^2) I_0\left(\frac{s^2}{2}\right) + (1 + 2s^2) I_1\left(\frac{s^2}{2}\right) \right] + \frac{\sigma' \pi^{3/2}}{4 s_w} + \frac{(4 - 2\sigma' + \sigma)\sqrt{\pi} e^{-s^2/2}}{60S} \times \left[\frac{6 q_x}{pU} \left(I_0\left(\frac{s^2}{2}\right) - I_1\left(\frac{s^2}{2}\right) \right) + \frac{5 p_{xx}}{p} \left(2 I_0\left(\frac{s^2}{2}\right) + \left(2 + \frac{1}{s^2}\right) I_1\left(\frac{s^2}{2}\right) \right) + \frac{5 p_{yy}}{p} \left(I_0\left(\frac{s^2}{2}\right) + \left(1 - \frac{1}{s^2}\right) I_1\left(\frac{s^2}{2}\right) \right) \right] \right\} \quad [3.1]$$

$$F_L = \rho r U^2 \frac{(4 - 2\sigma' + \sigma)\sqrt{\pi} e^{-s^2/2}}{60S} \left\{ \frac{10\, \tau_{xy}}{p} \left[I_0\left(\frac{s^2}{2}\right) + \left(1 - \frac{1}{s^2}\right) I_1\left(\frac{s^2}{2}\right) \right] + \frac{6 q_y}{pU} \left[I_0\left(\frac{s^2}{2}\right) + I_1\left(\frac{s^2}{2}\right) \right] \right\} \quad [3.2]$$

where I_0 and I_1 are the modified Bessel functions, and s is the molecular speed ratio

$$s = \frac{U}{\sqrt{2RT}} = \sqrt{\frac{\gamma}{2}}\, M \quad [3.3]$$

It will be observed that the drag force for the nonuniform case differs from that for the uniform case by terms proportional, respectively, to the heat flux in the x-direction and to the deviation of the normal stresses from the hydrostatic. The lift force, which is zero for the uniform case, contains terms proportional to the shear stress and the heat flux in the y-direction.

Equations [3.1] and [3.2] may be rewritten in the form

$$C_D \equiv \frac{F_D}{\rho U^2 r} = C_{D_0} + \frac{q_x}{pU} C_{Dq_x} + \frac{p_{xx}}{p} C_{Dp_{xx}} + \frac{p_{yy}}{p} C_{Dp_{yy}} \quad [3.4]$$

$$C_L \equiv \frac{F_L}{\rho U^2 r} = \frac{\tau_{xy}}{p} C_{L\tau_{xy}} + \frac{q_y}{pU} C_{Lq_y} \quad [3.5]$$

The indicated partial lift and drag coefficients, $C_{L\tau_{xy}}$, C_{Dq_x}, etc., correspond to the contribution to the total lift or drag arising from the nonuniformity denoted in the subscript. These results are presented graphically in Figs. 2 and 3 for the case of diffuse reflection. It should also be mentioned that the results of Equations [3.1] and [3.2] agree with those of (2) for the uniform case.

Inspection of Figs. 2 and 3 reveals that the partial lift and drag coefficients corresponding to the nonuniform terms are all small compared to the coefficient for the uniform case C_{D_0}. Unless a gas flow is very nonuniform, i.e., if the flow itself is in the continuum or slip flow region, the quantities p_{xx}, p_{yy}, and τ_{xy} are small compared to p. It follows that the contribution to the total force on the cylinder arising from these viscous stress terms will be small compared to the force due to the uniform flow (of the order of a few per cent or less). These quantities might thus be neglected in connection with use of the cylinder as a probe.

The relative importance of the forces arising from the heat flux terms, however, depends on the magnitude of the ratio of q_x or q_y to pU. At high flow velocities these forces will thus be negligible compared to the force for the uniform case. At very low velocities they will not. In a stagnation region such forces constitute the entire force on the cylinder.

4.0 Conclusions

4.1. In the free molecule flow of a nonuniform gas (i.e., one in which heat flux or viscous stresses are present) past a cylinder, both the lift and drag forces will be affected by the nonuniformity.

4.2. Force contributions due to stress and heat flux terms are, in general, small compared to the force for the uniform case, except in regions of low flow velocity where the forces arising from the heat flux terms become important.

5.0 References

1 "Superaerodynamics, Mechanics of Rarefied Gases," by H. S. Tsien, *Journal of the Aeronautical Sciences*, vol. 13, December 1946, pp. 643–664.

(*Continued on page 322*)

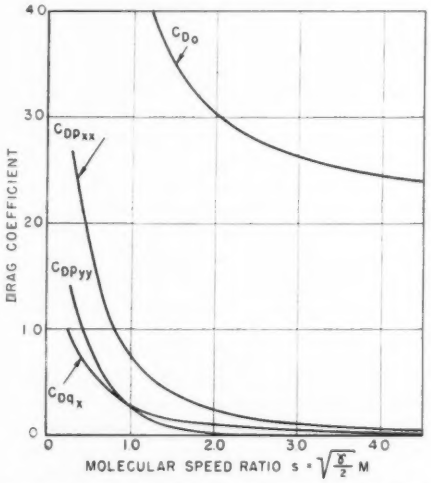

FIG. 2 PARTIAL DRAG COEFFICIENT FOR NONUNIFORM FREE MOLECULE FLOW PAST A CYLINDER (DIFFUSE REFLECTION)

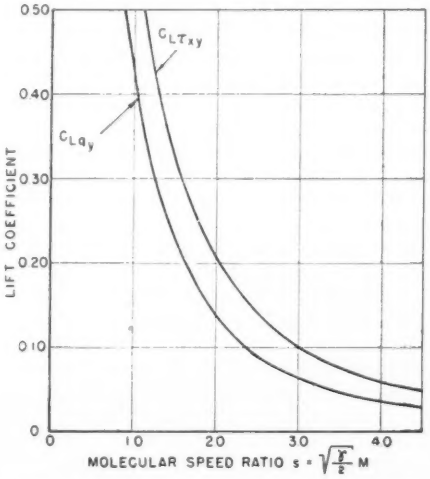

FIG. 3 PARTIAL LIFT COEFFICIENT FOR NONUNIFORM FREE MOLECULE FLOW PAST A CYLINDER (DIFFUSE REFLECTION)

$$C = \frac{\tau_{xy}}{p} C_{L\tau_{xy}} + \frac{q_y}{p \cdot U} C_{Lq_y}$$

Jet Propulsion News

ALFRED J. ZAEHRINGER, Thiokol Corporation, *Acting Editor*

JOSEPH C. HOFFMAN, General Electric Corporation, *Contributor*

Rockets

THE Navy Bureau of Aeronautics announced that smokeless JATO units are now in full production with deliveries currently being made to the Navy and the Air Force.

IT HAS been reported that the Chrysler Corporation has received a contract for the production of the "Redstone" surface-to-surface missile at Detroit, Mich. The missile was developed at the Army Ordnance Redstone Arsenal at Huntsville, Ala., by a group of former German engineers from the V-2 group at Peenemuende. The group is headed by Wernher von Braun.

FAIRCHILD'S "Lark" guided missile is shown (Fig. 1) leaving the launcher on the Navy's guided missile ship, the *USS Norton Sound*. This photograph is the first cleared for public release and shows the firing of this anti-aircraft type guided missile from a Navy vessel. The Lark is produced

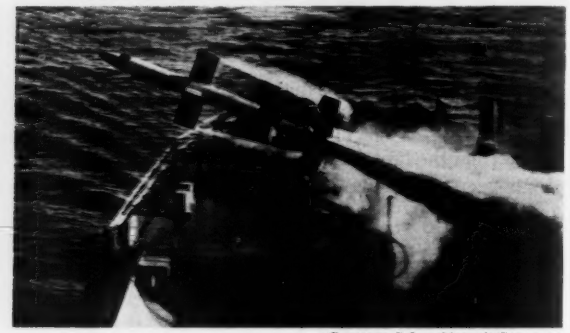

Courtesy Solar Aircraft Company

FIG. 1 SHIPBOARD LAUNCHING OF FAIRCHILD "LARK"

by the Guided Missiles Division of the Fairchild Engine and Aviation Corporation at Wyandanch, Long Island, N. Y. Currently Larks are being flown by all three branches of the Armed Services in their training and evaluation programs. Design of the missile was begun under a Navy project during the latter months of World War II as a defense against Japanese suicide planes. Under the Lark project in the years after the war, Fairchild engineers developed a homing system considered one of the most advanced yet devised. The cloud of smoke partially obscuring the stern of the ship is emitted by the booster rockets which push the "bird" to flight speed and then drop off as the missile continues under the thrust of its own rocket motors.

A TOTAL of 100 launchings of the Aerojet-General "Aerobee" have been conducted from White Sands Proving Ground, Holloman Air Development Center, and the *USS Norton Sound*. An additional quantity is on hand to be launched in the near future, and production of new units will continue this year. At the present time, a new program is under way to further extend the altitude and range of the Aerobee. Although the design performance of the new "Aerobee-Hi" is classified, it is expected that a substantial gain will be made in general utility permitting an even wider use.

THE Air Force is modifying 6 Martin B-61 Matador pilotless missiles for testing and training programs associated with the Hughes "Falcon," and also for ground-to-air weapons, pilotless missiles, and rockets.

AN all-rocket power plant producing 6000 lb of thrust and weighing only 210 lb has been announced by Reaction Motors, Inc. The rocket engine, designated as 1500N4C by RMI, burns alcohol and liquid oxygen. Similar units have powered jet-fighter aircraft of the Navy and Air Force and single-stage missiles.

PRODUCING 1000 lb of thrust for 14 sec, the Aerojet-General Corporation 14AS-1000G-1 solid propellant JATO has been certified by CAA for use in commercial aircraft.

Novel Jet Devices

THE Nagler Helicopter Company of Westchester County Airport, N. Y., has been using rocket motors in autogyro applications. The rocket motors, located at the hub of the blades, are discharged through a nozzle at the tip of the blades. Two models have been displayed. One is called a Convertiplane, an Aeronca light plane fitted with rocket-powered autogyro blades. Another is called the Heliglider, a one-man lifting unit. The strap-on unit, weighing 65 lb, will lift a man off the ground at 2700 fpm climb rate to a ceiling of 2700 ft. Range is about 5 miles.

ANOTHER novel use for reaction engines involves the use of the pulsejet engine which was used on the German V-1 "buzz-bomb." Devenco of New York uses the pulsejet engine to atomize insecticides and fumigants, to produce smokes and fogs, and for use as a blowtorch to kill weeds or to remove snow and ice.

Turbojet Engines

A JET thrust reverser, developed by the French national aircraft engine facility at Snecma, has been flight-tested in a de Havilland Vampire in France. Reverse thrust is said to be about half the normal positive thrust of the engine. A compressor bleed of air is injected into the center of the engine exhaust flow. The exhaust flow is thus forced into a series of 20 annular deflector vanes placed concentrically along the thrust line at the tailpipe. The flow is thus turned. A requirement of about 2 per cent of the engine air flow is needed to produce the negative thrust which acts as a brake. However, as much as 10 per cent thrust reduction has been experienced when the device is not in operation due to air bleeding through the annular vanes.

A DEVICE to make the operation of high-speed jet aircraft easier and safer has been announced by Solar Aircraft Company of San Diego, Calif. Called the Microjet, it directly senses engine pressures and replaces complex electronic equipment. Although most details are under security restrictions, the device is stated to be pneumatically operated. It computes what the turbine discharge pressure should be under all flight conditions, and at the same time notes any error between the actual engine pressure and what

it should be. If there is an error, electrical signals are automatically sent out to other engine controls which correct the pressure conditions.

THE Westinghouse Electric Corporation and Rolls-Royce, Ltd., of Derby, England, have signed an agreement providing for technical co-operation between the two companies for a period of ten years. The agreement includes exchange of information in the design, development, and production of gas turbine and aero-engines. The first application will be in the collaboration of Rolls-Royce with Westinghouse in future development of Westinghouse jet engines.

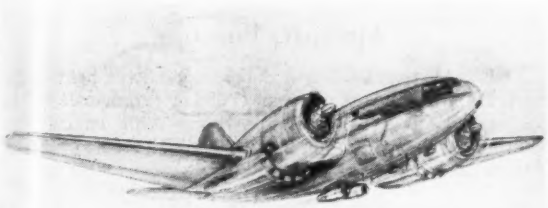

Courtesy El Al Israel Airlines

FIG. 2 EL AL ISRAEL AIRLINES' CURTISS C-46 SHOWING TWIN JETS INSTALLED UNDERNEATH THE FUSELAGE

DR. ERICH SCHATZKI, aeronautical engineer and designer, suggested that the installation of jet engines as thrust boosters on Curtiss C-46 aircraft, developed by him for El Al Israel Airlines, might offer the most promising solution in improving C-46 performance in compliance with CAA regulations. Curtiss C-46 aircraft would be equipped with two Marbore II engines each. Both engines would be housed in individual, interchangeable pods (Fig. 2) underneath the fuselage. No structural modifications are necessary.

IT IS understood that Allison is preparing to flight-test its J-71 turbojet engine in a B-45 flying test bed. The J-71 is a 9600-lb thrust engine having a 16-stage axial-flow compressor and a three-stage turbine. This engine has recently completed a 200-hr test run in an altitude test chamber of the NACA. Reports in the press state the J-71 will be used in the Douglas B-66, the Republic F-105, the Northrop F-89, and the McDonnell F-3H.

THE de Havilland Aircraft Company is reported to have developed a new lightweight jet engine, "Gyron," said to be Britain's first in the 15,000-lb to 20,000-lb thrust class. This engine employing a seven-stage, single-spool compressor was developed for around $2.5 million under a joint de Havilland-General Electric private venture.

ROLLS-ROYCE has installed "teeth" around the perimeter of a jet engine tailpipe and has reduced low-frequency noise normally encountered in engine tests, although there has been some increase reported in high-frequency noise.

Aircraft, United States

THE Strategic Air Command has disclosed that the B-47B Stratojet recently flew more than 12,000 miles nonstop in 24 hours. Aerial refueling techniques were employed.

PRATT & Whitney's J-57 axial-flow gas turbines will power Boeing's new prototype jet transport. The engines are similar to the J-57's used on the B-52 long-range bomber. Boeing expects its jet transport to be in the air by mid-1954. Called Project X by Boeing, the four-engine, swept-wing jet liner is now called Model 707. The aircraft is expected to have performance characteristics which will give it a definite speed and power edge over the de Havilland Comet. The 707 is to carry 100 passengers at a speed of nearly 600 mph.

THE first flight of the North American YF-100 has been reported to have taken place at Edwards AFB, Calif. Sweepback is said to be 45 deg. Other features are a streamline external fuel tank of new design, canopy design for high speed, and a lowered horizontal tail fin. The F-100 has been ordered into quantity production by the USAF. The weight is expected to be around 24,000 lb. Power is supplied by a Pratt & Whitney J-57 engine delivering 15,000-lb thrust with an afterburner.

FIG. 3 shows a view of the XA3D, the Navy's new swept-wing jet attack aircraft now being built by the Douglas Aircraft Company. It is powered by two jets, each slung in a pod under the wing outboard of the fuselage. It will be in the 600 to 700-mph class and will carry a crew of three. As in other carrier aircraft, the wing of the A3D will fold to permit easier handling and more compact storage aboard aircraft carriers. Detailed performance data are secret, but no known airplane of comparable size, now in service or contemplated for early service introduction, can carry an equivalent bomb load as high and as fast as the A3D.

Courtesy U. S. Navy

FIG. 3 THE XA3D, THE NAVY'S NEW SWEPT-WING JET ATTACK AIRCRAFT

A NEW world speed record made on July 16 is claimed for the F-86D which flew 715.7 mph. A General Electric J47-17 turbojet engine powered the Air Force's North American Sabre Jet. The J47-17 engine is equipped with electronic controls and an afterburner which utilizes additional fuel for extra thrust.

FIG. 4 shows the new F-94C Starfire, all rocket-armed interceptor now rolling off Lockheed Aircraft Corporation production lines. Besides the standard 24 rockets housed in its sleek nose, the USAF plane now carries a dozen 2.75-in.

Courtesy Lockheed Aircraft Corporation

FIG. 4 LOCKHEED'S NEW F-94C PRODUCTION LINE

rockets on each wing in pods visible on the plane at left, where a workman is ready to install the rocket launcher's white plastic breakaway cover. The stovepipe apparatus behind each F-94C is a silencer to muffle engine sound during ground tests.

FIG. 5 shows standard HVAR 5-in. rockets mounted in the launching position on the rotary bomb door developed by Martin for the XB-51 tactical bomber. The new preloaded

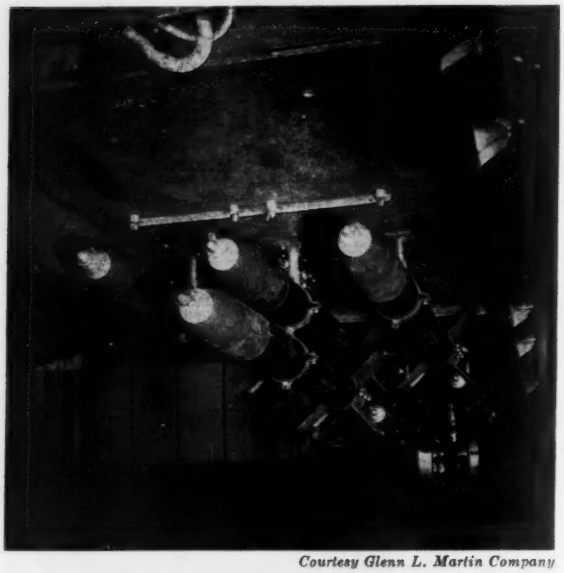

Courtesy Glenn L. Martin Company

FIG. 5 HVAR 5-IN. ROCKETS MOUNTED IN LAUNCHING POSITION ON ROTARY BOMB DOOR

door rotates 180 deg just prior to bomb or rocket release. Through use of this door, a jet bomber traveling at high speed is just as stable a platform as one flying at World War II speeds, and U. S. military aircraft will not have to slow down to make a successful bomb or rocket release as they have in the past.

REPUBLIC Aircraft Corporation has disclosed details on two of its aircraft. The first of the new aircraft is the Thunderstreak, a sleek new high-speed swept-wing F-84F jet fighter, which is being produced in quantity for the U. S. Air Force and NATO countries. Although much of the F-84's performance is classified, it is listed as a plane of more maneuverability and higher speed than the Thunderjet. General data: span 33 ft, 6 in.; length 43 ft, 4 in.; height 14 ft, 4 in. at rudder tip; speed 600 mph plus; combat radius: not disclosed but exceeds F-84G, which with external tanks is more than 1000 miles; service ceiling 45,000 ft plus; armament six 0.50-caliber machine guns plus externally mounted rockets, bombs, and napalm; power Wright-Sapphire J-65 turbojet engine developing 7200-lb thrust. The Republic XF-91 (Fig. 6) is a high-speed, high-altitude intereceptor fighter which has made several flights at speeds faster than sound to become the first combat-type aircraft with this achievement. Incorporating several radical features, the XF-91 is powered by a General Electric J-47 5200-lb thrust turbojet engine plus afterburner, and emergency power is supplied by a 6000-lb thrust rocket engine built by Reaction Motors. An unusual wing design features inverse taper, sweptback wings, also a variable incidence of the wing permitting changes in angle of attack.

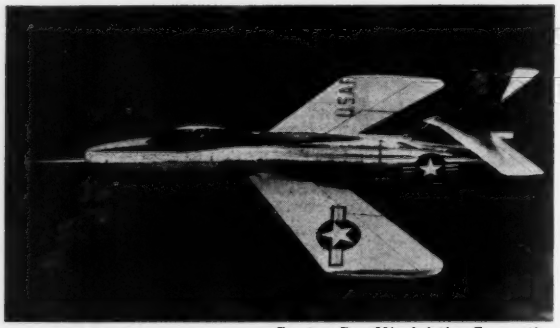

Courtesy Republic Aviation Corporation

FIG. 6 REPUBLIC XF-91, HIGH-ALTITUDE INTERCEPTOR FIGHTER

Aircraft, Foreign

THE RAF recently flew a Supermarine Swift fighter, the Swift F.4, which boasts more power and more armaments than the early Swift F.1. The Rolls-Royce Avon engine with afterburner has a thrust of about 9000 lb. Carried are four 30-mm cannon.

A COMET jet airliner, the first to visit the North American continent, arrived at Ottawa on May 29, having flown from London across the Atlantic via Iceland and Labrador. The total flying time for the journey of 3550 miles was 10 hr, 48 min.

RECENT movies show launchings of the British-made Fairey vertical take-off aircraft at the Woomera missile range in Australia. This delta wing craft is powered by a Fairey Beta I rocket engine having two 900-lb thrust motors. A booster assisted take-off is produced by two 600-lb thrust rockets. Additional information on the rocket propulsion system or the flight test data is not available at this time.

THE Jindivik pilotless aircraft, which is radio-controlled and is used as a target drone, has been placed into operation at the Woomera rocket range. Take-off is from a tricycle dolly, landing with a retractable skid. The aircraft is 23 ft long and has a wing span of 19 ft; powered by an Armstrong-Siddeley turbojet engine, two models are disclosed, one having a thrust of 1000 lb, another 1600 lb. Use is as a target for other weapons now in development at Woomera.

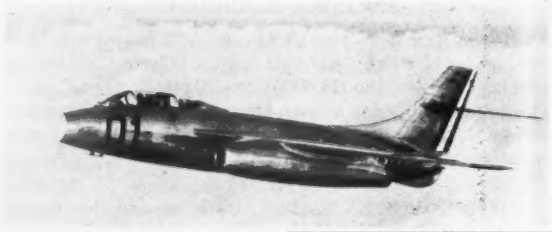

Courtesy Aviation Week Magazine

FIG. 7 THE SUD-OUEST S.O. 4050 VAUTOUR

THE French Sud-Ouest S.O. 4050 Vautour is shown in Fig. 7. Two 5500-lb thrust Atar jets mounted in underwing nacelles give it sonic-speed capabilities in level flight.

FLIGHT tests are reported to be under way with a new Leduc ramjet aircraft, the Leduc 021 which is being fostered by the French Air Ministry. The craft is said to weigh about 11,000 lb and capable of a speed of Mach 0.95 in level flight. New features include retractable outrigger wheels with tandem main wheels, tiptanks, and a jettisonable cockpit located upstream from the air inlet.

THE French Sncase S.E. 5000 Baroudeur jet ground-attack plane is capable of taking off from a small field without a runway by means of a rocket-propelled sled which is jettisoned after the craft is airborne. Take-off space is thus claimed to be under 700 yards. Landing is with retractable skids. The wings of the plane are sweptback 35 deg, which is expected to allow sonic flight capabilities with its Atar 101 power plant of 6000-lb thrust.

High Altitude and Extraterrestrial Research

TO determine the effects of cosmic radiation at altitudes of 50,000 to 100,000 ft, the Air Research and Development Command is sending fruit flies, sealed in pressurized tubes, aloft in controlled balloons. Launchings will be from the West Coast and drifts will be eastward across the U. S. Data from these tests are expected to aid our knowledge of the effects of cosmic radiation for high-altitude aircraft.

THE U. S. Navy operating in Baffin Bay, Northern Greenland, has launched rockets from balloons to secure cosmic radiation data. "Deacon" type solid propellant rockets weighing about 300 lb are launched from "Skyhook" balloons and have attained altitudes of about 40 miles.

ANOTHER high-altitude project using the Viking rocket calls for the study of the Aurora Borealis from the *USS Norton Sound* in co-operation with Norwegian scientists at Tromso. Dr. H. Newell is in charge of the program.

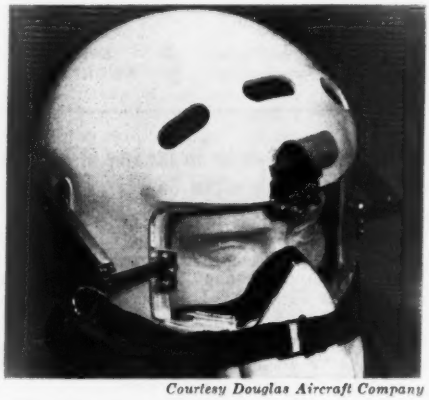

Courtesy Douglas Aircraft Company

FIG. 8 HELMET DESIGNED FOR EMERGENCY ESCAPE FROM AIRCRAFT FLYING AT SUPERSONIC SPEEDS

DEVELOPMENT of a new slotted helmet designed to protect pilots forced to bail out from their aircraft while traveling at supersonic speeds, was announced by the U. S. Air Force Research and Development Command (see Fig. 8). Engineers of the Douglas Aircraft Company, Santa Monica Division, who designed and built the helmet, said the slots or vents which are cut into the forward crown section of the headgear greatly reduce wind shock and air lift and keep the helmet secure on the pilot's head. The helmet has been successfully tested in an outdoor wind tunnel at simulated speeds up to Mach 1.04.

SAINT Louis University will become one of the first institutions in the world to offer a program of graduate study dealing with the problems of space travel. The program will be offered through Saint Louis University's Parks College of Aeronautical Technology. The first phase of the program will be a seminar offered to senior students in aeronautical engineering and will deal with rocket stability and design. Faculty members of Saint Louis University will conduct the seminar, but it is anticipated that leading authorities in the field will be brought in as guest lecturers.

THE Naval Aero Medical Laboratory at Philadelphia has tested its new "space suit" and will soon conduct tests aloft. Made of rubber with a large plexiglas helmet fastened to the neck, the suit has been successfully tested at simulated altitudes up to 70,000 ft.

Facilities and Equipment

HUGHES Aircraft Company is reported to have avionics (electronics in aviation) contracts totaling $200 million per year with a $600 million backlog. Research and development on the Hughes air-to-air Falcon missile, F-98 (carried by the Convair F-102 interceptor), led to development of avionic control and guidance systems such as the radar fire-control system used with the F-86D, F-89D, and F-94C, the F2H-4, and the Canadian CF-100.

NACA has disclosed details of its new 8-ft wind tunnel at Langley Field, Va. Capabilities are reported to be Mach 1.4 with variable speed, temperature, and air pressure. It is expected that the tunnel will be in normal operation in about a year. Also at Langley is the new Gas Dynamics Laboratory used to gain insight into the physics of high-speed flight. Flight speeds up to Mach 9.0 or at altitudes of about 200,000 ft can be simulated.

G. M. GIANNINI & Co., designers and manufacturers of precision instruments used in guided missiles and radar control, plans to build a new 24,000-sq ft assembly plant in Pasadena, Calif.

ENGINEERING Research Associates has been made a division of Remington Rand, Inc. The country's largest manufacturers of electronic computers have facilities at St. Paul, Minn., and Arlington, Va.

CONSOLIDATED Engineering Corporation of Pasadena, Calif., is planning a 20-acre "Instrument Park" in the Hastings Ranch area of Pasadena. The Corporation is a manufacturer of electronic analytical instruments.

REACTION Motors of Rockaway, N. J., has announced ground-breaking for a new plant site. In addition, it was revealed that a backlog of over $5.5 million exists.

CONSTRUCTION proceeded from the roof down on Boeing's new B-52 hangar at Seattle. The roof structure, 90 ft above ground level, rested on wood towers while supporting steel columns were built beneath it. Another feature is its 785 ft long, 65 ft high door—the largest unobstructed door in the country. Four of the all-jet B-52's can be housed in the hangar.

PRODUCTION of 8 to 12-ton capacity liquid oxygen and nitrogen transfer, storage, and transport units has been announced by Hofman Laboratories, Newark, N. J. A semi-trailer consists primarily of a liquid storage vessel and an outer shell which also functions as part of the chassis. All components are attached to the container for accessibility and easy operation. A vacuum space between the container walls maintains high thermal efficiency. While the trailer is at rest the evaporation loss will not exceed 250 lb per day. An electric-motor-driven centrifugal liquid-oxygen pump, capable of transferring 100–150 gal of liquid oxygen per min, is installed at the rear of the trailer with all other controls.

THE Components Development Section of the Aircraft

Courtesy General Electric Company

FIG. 9 SHOCK TUBE FOR STUDYING JET ENGINE COMBUSTION PROCESSES

Gas Turbine Division of the General Electric Corporation (Evendale, Ohio) is using shock waves to study combustion processes (Fig. 9). The effect of such waves is studied in a miniature shock tube. Development on jet engine combustion and the effect of shock waves are becoming increasingly important, G. E. engineers explain, since the combustion chamber is one of the most important sections of a jet engine.

MATHIESON Chemical Corporation has announced it is producing hydrazine at its new three-million-dollar plant at Lake Charles, La. The principal use of the hydrazine will be by the armed forces in various rocket programs. Hydrazine will be prepared by a modified Raschig Process which utilizes the reaction of ammonia with sodium hypochlorite to form monochloramine; the latter is reacted with ammonia to form hydrazine. Hydrazine, a powerful reducing agent, now sells for about $3 per lb; the price is expected to fall to about $0.50 per lb with large-scale production and improved techniques.

THE Armour Research Foundation of the Illinois Institute of Technology, Chicago, Ill., is currently engaged in several jet projects. These include: effects of explosions in jet-engine test cells, analysis of forces and surface pressures in jet-engine fuel pumps, instrumentation and resistance probe for true free-air thermometer, guided missile warheads, rocket-assist artillery ammunition, physical constants of propellant materials, and a bent-nozzle isotope separator.

High-Frequency Combustion Instability in Rocket Motor with Concentrated Combustion

(*Continued from page 313*)

4 "Aspects of Combustion Stability in Liquid Propellant Rocket Motors, Parts I, II," by L. Crocco, JOURNAL OF THE AMERICAN ROCKET SOCIETY, vol. 21, November 1951, pp. 163–178; vol. 22, January–February 1953, pp. 7–16.

5 "High Frequency Combustion Instability in Rockets With Distributed Combustion," by L. Crocco and Sin-I Cheng, paper presented at the Fourth Symposium on Combustion, September 1952.

6 "Supercritical Gaseous Discharge with High Frequency Oscillation," by L. Crocco, paper presented at the Eighth International Congress of Applied Mathematics and Mechanics, August 1952.

7 "The Transfer Functions of Rocket Nozzles," by H. S. Tsien, JOURNAL OF THE AMERICAN ROCKET SOCIETY, vol. 22, May–June 1952, pp. 139–143.

Aerodynamic Forces on a Cylinder for the Free Molecule Flow of a Nonuniform Gas

(*Continued from page 317*)

2 "Theoretical Aerodynamic Characteristics of Bodies in a Free Molecule Flow Field," by J. R. Stalder and V. J. Zurick, *NACA Technical Note* 2423, 1951.

3 "A Comparison of Theory and Experiment for High Speed Free Molecule Flow," by J. R. Stalder, G. Goodwin, and M. O. Creager, *NACA Technical Note* 2244, 1950.

4 "A Torsion Balance for Measuring Forces in Low Density Gas Flows," by I. Estermann and E. D. Kane, *Journal of Applied Physics*, vol. 20, June 1949, pp. 608–610.

5 "Zur Theorie der Radiometerkräfte," by A. Einstein, *Z. Physik*, vol. 27, 1924, p. 1.

6 "Zur Theorie des Radiometers," by P. Epstein, *Z. Physik*, vol. 54, 1929, p. 537.

7 "On Stresses in Rarefied Gases Arising from Inequalities of Temperature," by J. C. Maxwell, *Transactions of the Royal Society of London*, vol. 170, 1879, p. 231.

8 "On the Kinetic Theory of Rarefied Gases," by H. Grad, *Communications on Pure and Applied Mathematics*, vol. 2, 1949, pp. 331–407.

9 "Kinetic Theory of Gases," by L. B. Loeb, McGraw-Hill Book Co., Inc., New York, N.Y., 1934.

10 "Theory of Drag in Highly Rarefied Gases," by M. Heineman, *Communications on Pure and Applied Mathematics*, vol. 1, 1948, pp. 259–273.

11 "Applications of the Theory of Free Molecule Flow to Aeronautics," by H. Ashley, *Journal of the Aeronautical Sciences*, vol. 16, 1949, pp. 95–104.

12 "Transport Phenomena in Very Dilute Gases," by C. S. Wang Chang, NORD 7924-U17H-3-5, 1950.

13 "Wind Tunnel Testing Problems in Superaerodynamics," by H. S. Tsien, *Journal of the Aeronautical Sciences*, vol. 15, Oct. 1948, p. 577.

American Rocket Society News

H. K. WILGUS, *Associate Editor*

Successful ARS Summer Meeting at Los Angeles, July 2, Draws Record Attendance

Southern California Section Acts as Host

IN conjunction with the ASME Summer Meeting held at the Statler Hotel, Los Angeles, Calif., June 30–July 2, 1953, the American Rocket Society sponsored two technical sessions and a luncheon on the last day of the meeting. More than 150 ARS members registered, with the Southern California Section acting as unofficial host and participating in the program.

Morning Session

The morning technical session, at which four papers were presented, attracted more than 100 members. The chairman and co-chairman for this session were R. D. Geckler, chief technical specialist, Aerojet-General Corporation, Azusa, Calif., and Leon Green, Jr., senior engineer, Solid Engine and Chemical Division, Aerojet-General Corporation.

The following are brief summaries of the papers presented:

"Rocket-Powered Wind Tunnel" by F. Kreith, P. B. Stewart, and E. S. Starkman, University of California, Berkeley, Calif. Aerodynamic performance testing sometimes requires large capacity, high velocity, and subatmospheric pressures. Not many large-scale installations are available which satisfy such requirements, primarily because of the cost of the blowers and evacuating pumps required. A low-cost design is proposed which uses the exhaust from rocket engine thrust chambers as motive fluid for jet pumps built integrally into the wind tunnel. Configurations, estimated performance, and cost analysis were presented for a large, high subsonic wind tunnel capable of operating at altitude conditions from 5000 ft to about 60,000 ft.

"Correlation of Experimental Data on the Disintegration of Liquid Jets" by C. C. Miesse, Aerojet-General Corporation, Azusa, Calif. The paper summarized the various theories of jet disintegration, from Rayleigh's first analysis to contemporary theories, evaluating them according to their ability to effect a correlation of the wave length, maximum drop size, and breakup-length data obtained from over 60 photographs of jet disintegration. These photographs included tests with two different liquids (water and liquid nitrogen), two different types of nozzles, and a wide range of nozzle diameters and jet velocities.

"New Instruments for Rocket Motor Testing" by R. B. Bowersox, R. A. Buchanan, and J. R. Zweizig, Jet Propulsion Laboratory, California Institute of Technology, Pasadena, Calif. The paper described three instruments developed at the Jet Propulsion Laboratory to meet special operating requirements in rocket motor operation and research tests. These instruments are: (1) a ten-channel recording potentiometer which makes 20 measurements per sec with an accuracy of ±0.3 per cent, and has input-voltage ranges of 10, 50, and 100 millivolts; (2) a chopper-stabilized d-c amplifier having negligible drift and fixed gains of 10, 25, 50, 100, or 200; (3) a rocket motor performance computer which computes mixture ratio and characteristic velocity continuously during a motor test with an accuracy of ±0.5 per cent.

"Effect of Wave Propagation in Feed Lines on Low Frequency Rocket Instability" by R. H. Sabersky, California Institute of Technology, Pasadena, Calif. This paper analyzed a liquid monopropellant rocket system for low frequency instability, taking into account the compressibility of the fluid in the propellant line. The propellant is assumed to turn into gas at a fixed time interval after entering the chamber, this time interval being taken to be independent of pressure or temperature. A numerical example was given, illustrating that the effect of compressibility may become important for practical cases.

Major Yeager Speaks at ARS Luncheon

More than 250 members and guests, including many representatives of the West Coast aircraft industries, attended the ARS Luncheon, held in the Golden State Room of the Statler Hotel, to hear Major C. E. ("Chuck") Yeager of the AF Experimental Flight Test Center, Edwards AF Base, Calif.

B. L. Dorman of the Southern California Section, manager of the Test and Field services Division, Aerojet-General Corporation, was the presiding chairman. J. H. Kindelberger, chairman of the Board, North American Aviation, introduced Major Yeager who spoke on the topic, "Experiences in Rocket-Propelled Aircraft." Major Yeager was the first man to penetrate the sound barrier (to fly faster than sound).

Afternoon Session

The afternoon technical session, at which three papers were presented, was presided over by S. K. Hoffman, president of the Southern California Section, and chief of the Propulsion Section, Aerophysics Department, North American Aviation. The co-chairman for the session was L. E. Stocking of Douglas Aircraft.

The first paper presented was "An Air-Transportable Liquid-Oxygen Generator —Its Operation and Application" by C. A. Bleyle, R. B. Hinckley, and C. L. Jewett, Arthur B. Little, Inc., Cambridge, Mass. It discussed the design and operation of a lightweight air-transportable liquid-oxygen generator, constructed for the U. S. Air Force. This plant, which operates on a low-pressure cycle, separates oxygen from air at the rate of 10 tons per day. Unique design features include a special type of heat exchanger, aluminum construction, gas-turbine-driven air compressor, and skid-mounted sections for loading into standard cargo aircraft.

The second paper was "Solid Propellant Rockets—Basic Concepts, Present Status, and Trends in Development" by Charles E. Bartley, Grand Central Aircraft Company, Pacoima, Calif. Only the unclassified sections of this paper were discussed.

"Take-Off from Satellite Orbit," by H. S. Tsien, California Institute of Technology, Pasadena, Calif., appeared in the JOURNAL, July-August 1953, pp. 233–236.

Note: Due to lack of space, news of ARS Sections will appear in the next issue of the JOURNAL.

THE LUNCHEON OF THE ARS SUMMER MEETING, HELD IN THE GOLDEN STATE ROOM, STATLER HOTEL, LOS ANGELES, CALIF., JULY 2, 1953

Book Reviews

H. S. SEIFERT, California Institute of Technology, *Associate Editor*

RAUMFAHRTFORSCHUNG, H. Gartmann, editor, R. Oldenbourg Co., Munich, 1952, 199 pp. $3.

Reviewed by FRED WOLF
California Institute of Technology
Jet Propulsion Laboratory

With the co-operation of the Stuttgart Society for Space Research the editor has arranged for a number of specialists to write a series of rather loosely connected essays in German on arbitrarily selected topics in the field of space travel.

Willy Ley, author of the first section, starts with the successful flight of the two-stage Bumper rocket, which in his opinion represents a major historical event. Then he reaches into mythological antiquity to trace in 20 pages the idea of space travel throughout history. He surveys the scientific thought immediately preceding the modern development of rockets, which he dates as beginning with Oberth's book on space travel in 1923. He then roams backward through time and fictional literature searching for the beginning of the idea of space travel.

In the second chapter Werner Schaub gives a good 80-page summary of celestial mechanics from an astronautical viewpoint. Building up from fundamental dynamics, Professor Schaub develops the possible orbits and the equations of the two- and three-body problem in simple steps, interpreting the concise mathematical formulation in clear uncramped German. Discussion of periodic orbits of the restricted three-body problem leads to direct applications in astronautics.

In the third chapter Rolf Engel, U. T. Bödewadt, and Kurt Hanisch describe a multistep rocket for the purpose of supplying a satellite space station. The design considers two possible orbits for the space station, one at 346-mile altitude and the other at 1040 miles. The authors briefly discuss the effects of altitude and the inclination of the orbital plane with the ecliptic on the field of view and illumination of the station. Apart from this, the main emphasis is laid on the supply vehicle itself, its trajectory of ascent, structural vehicle efficiency, and optimization under the numerous conditions imposed on the flight. Conservative assumptions have been made for the propellant performance, and the data of the aircraft industry on structures were used to arrive at the gross weight. The authors also consider the recovery of the first stage by means of human pilot-controlled descent with a rocket-motor brake and give some thought to the return trip from the satellite station, based on Dr. Sanger's ideas, on a large-wing glider in a "skipping" trajectory, circling the earth several times to brake the velocity gradually. In a final cost estimate the authors envision a satellite station for experimental and research purposes with a structural weight of 180 tons and 330 tons of equipment. This total could be transported in three hundred supply vehicles of which every fifth would be a return glider. Three years would be required to build the satellite at a total cost of 500 million dollars, including the ground-station organization and its personnel of 1600.

The plan for the space station itself and its possibilities for use are treated in the fourth chapter by Herman Oberth. The author shows his own tentative schematic layout and a picture of Ross and Smith's proposal, and lets his fancy run the whole gamut from conservative research to speculative conjecture. However, the student of astronautics, engaged in the tedious footwork of slow and sober preparatory techniques, may welcome an occasional boost of morale with such a quick glance into the future!

In the fifth and final chapter by Heinz von Diringshofen, medical problems of extraterrestrial travel are classified in two groups—the well-known effects of high acceleration on the human body and other recent experiences related to high-speed flight; and the totally unknown reaction of man to exposure of his delicately balanced physical and mental equilibrium to removal of gravity. Only the most rudimentary glance at this vast unexplored field is given, together with an optimistic belief in ultimate success which is based on very scant evidence.

The book closes with an enumeration of various societies for space research, the International Astronautical Federation, and its members. Also a historical bibliography on space travel is added which goes back to Goddard's work in 1919.

REFRACTORY HARD METALS, by P. Schwarzkopf, R. Kieffer, and Associates, The Macmillan Co., N. Y., 1953, 447 pp., 92 illus. $10.

Reviewed by POL DUWEZ
California Institute of Technology
Jet Propulsion Laboratory

This book deals with the structure, preparation, and properties of refractory carbides, nitrides, silicides, and borides. The authors, who are leading authorities in the field, present a critical evaluation of our knowledge of these extremely important high-temperature materials. The book will be particularly welcomed by those interested in fundamental research. Since the work of Becker published in 1933 (Hochschmelzende Hartstoffe), there has not been a book covering the field, and many of the original papers published in the intervening period (especially those on borides) have not been easy to find. The really thorough literature coverage presented in this book will be greatly appreciated and will help in planning future research programs.

The applications are dealt with in each chapter covering each individual material. In addition, however, the last part of the book is a comprehensive summary of the present position of the carbides, nitrides, silicides, and borides in the field of high-temperature materials, especially in view of their application to gas turbines. The comparison of the physical properties of these materials with the more conventional high-temperature alloys is particularly useful.

Erratum Note: The editor of this section regrets that the price of this book was incorrectly listed as $7.50 in the May-June issue of the JOURNAL.

QUANTUM CHEMISTRY, by K. S. Pitzer, Prentice-Hall, Inc., N. Y., 1953, 529 pp. $10.

Reviewed by DAVID ALTMAN
California Institute of Technology
Jet Propulsion Laboratory

The book is an outgrowth of many original papers by the author on various phases of quantum mechanics and of several years of teaching a course on this subject matter at the University of California, which this reviewer was fortunate enough to attend. Briefly, the book presents the essentials of quantum theory of interest to chemists and treats many classical problems in sufficient detail to provide a working knowledge of the principles. In keeping with the author's opinion that it is not necessary to employ advanced mathematics to gain a basic understanding of the fundamentals of quantum mechanics, this book has been written mainly for exposition of basic principles rather than formulation of mathematical techniques for detailed solution of problems. There are 24 appendixes for treatment of specific topics of more mathematical interest. The underlying approach of the presentation is contained in the following statement by the author: "Many persons, the writer included, tend to think first in terms of qualitative physical phenomena and to follow with the mathematics appropriate to the model so conceived. Such individuals should not discard models but rather remind themselves frequently of the distinction between the concepts established by experiment and the parts which are only figments of imagination."

The book contains thirteen chapters of which the first seven are devoted mainly to the development of the principles of the quantum theory, and the second six chapters to a more or less detailed discussion of many practical problems of interest to the chemist. The first part of the book which treats the general theory is adequate, although it adds very little to the treatments which have already been given in the many other books on this subject. The second half of the book, however, contains much valuable information on such topics as chemical bonds and valences, spectra of polyatomic molecules and statis-

tical thermodynamic calculations concerning them, properties of crystalline solids, imperfect gasses, and electrical and nuclear phenomena. This discussion is interspersed with numerous practical examples which are very instructive for indicating the method of treating the problem. In addition the book has problem sets at the end of each chapter which make it well-suited for use in a teaching course on quantum chemistry.

In general, the book has a sufficient volume of new and interesting material which cannot be found in any other single published source but which would recommend it to the chemist or practical physicist working the field. Although the price of $10 is not inconsistent with the subject matter contained in the book, it appears that the quality of the binding and the paper could be improved at this price.

MECHANICAL ENGINEERING THERMODYNAMICS, by D. A. Mooney, Prentice-Hall, Inc., N. Y., 1953, 540 pp. $9.35.

Reviewed by R. S. WICK
California Institute of Technology
Jet Propulsion Laboratory

This textbook is written for junior or senior engineering students and consists of essentially two parts. The first deals with general thermodynamics, and the second with engineering applications. Although the title implies that this textbook was written primarily for mechanical engineering students, the first part of the text is sufficiently general for a first course in thermodynamics in other curricula. The first twelve chapters deal with the first and second laws and their applications, the properties of pure substances, steam, gases and gaseous mixtures. The thirteenth chapter treats process calculations for stationary systems. These chapters could very well form a first-semester course in thermodynamics. The final twelve chapters cover the usual engineering applications such as steam and gas cycles, turbine, compressor, refrigeration, air conditioning, internal-combustion-engine cycles, and combustion processes.

This well-written text is designed for the student who wants to know not only "how" but "why" when it comes to engineering thermodynamics. Because of its clearness and conciseness, it is also recommended to those interested in a self-study or review course in thermodynamics.

INTERNAL BALLISTICS, F. R. W. Hunt, editor, Philosophical Library, Inc., N. Y., 1951, 311 pp. $12.

Reviewed by A. J. ZAEHRINGER
Thiokol Corporation

This book, which is a collective work on internal ballistics and its application to guns, was sponsored by the Scientific Advisory Council of the British Ministry of Supply. Although primarily a treatise on gun ballistics, there is much which is applicable to solid rocket propellants. The first five chapters of the book are devoted to the chemical, thermal, and ballistic properties of propellants, and two ballistic equations are derived relating to the mode and rate of burning. Numerical tables are given for thermochemical computations. The gun is introduced in Chapters VI and VII, and the energy equation and the equation of motion of the shot are deduced.

In Chapter VIII a solution of the ballistic equations for a linear law of burning is given, and Chapter IX is devoted to other solutions of the same problem. Solutions for nonlinear law of burning are given in Chapter X. Chapter XI is devoted to a number of approximations which are frequently used. Chapters XII and XIII deal with the measurement of velocity and pressure, and the subject of cordite proof is treated in Chapter XIV. Chapter XV gives an outline of the application of statistical methods to cordite production and proof; Chapter XVI reviews the results of recent experimental work in America, Germany, and England.

Appendix I deals extensively with the theory of leaking guns into which category falls the recoilless gun (which may be considered as a rocket and gun built together). The book closed with a bibliography of theoretical works on internal ballistics.

Although the greater part of the book deals with guns, the early sections are of general theoretical interest to those in the solid rocket propellant field. For example, thermochemical computations are treated, and together with the tables furnished, basic parameters for single- and double-base rocket propellants may be calculated. Also the sections on pressure measurements and statistical methods are of value to those engaged in the testing and analysis of solid-propellant rocket motors. One should not, however, expect to find much carry-over of quantitative information from one field to the other, as the ranges of variables involved differ by orders of magnitude.

THEORY OF THE INTERIOR BALLISTICS OF GUNS, by J. Corner, John Wiley & Sons, N. Y., 1950, 443 pp. $8.

Reviewed by JACK LORELL
California Institute of Technology
Jet Propulsion Laboratory

This is a textbook on theoretical interior ballistics of guns, written by one of the foremost British authorities on the subject. The emphasis is on methods rather than magnitudes. Thus examples of typical data are included, but there are no extensive tables of ballistic magnitudes. The subject matter is very definitely limited to interior ballistics, with little of any tie-in either to gun design techniques or to exterior ballistics.

In theoretical interior ballistics, the problem of determining muzzle velocity and peak pressure when the characteristics of shot, charge, and gun are known motivates the entire subject. This problem, known as the central problem of interior ballistics, forms the theme for the book, to which are related discussions of topics ranging from ballistic methods proper to the chemistry of propellants.

In Chapter I, the scope of the book is laid out, and a short discussion of experimental ballistics is included. Chapters II and III are devoted to gun propellants. Topics such as flame propagation in one dimension, bulk burning rates in guns, propellant erosion, and the thermochemistry of propellants are discussed in some detail. Chapters IV, V, and VI describe the various ballistic theories that are used in attacking the central problem of interior ballistics. Chapters VII and VIII involve the ballistics of special types of guns, for which the methods of the previous chapters must be modified. Of particular interest to the rocket engineer, perhaps, is the theory of the recoilless gun, which uses the rearward thrust of part of the gases from the combustion chamber released through a nozzle to balance the recoil. Chapter IX discusses hydrodynamic problems in guns. The main difference between the gas flow in rockets and guns is, of course, that in the former the flow is steady-state, whereas in the latter it is nonsteady. As a consequence, supersonic velocity can be reached in a straight gun tube, whereas a throat is required in order to obtain supersonic velocity in a rocket motor. Chapter X is a discussion of heat transfer in guns. In addition to the text there are three appendixes providing aids for numerical ballistic calculations, a name index, and a subject index.

As a text in the theory of the interior ballistics of guns, this book is excellent. However, its use to the rocket engineer may be limited since the theories of rocket and gun ballistics, though superficially closely related, diverge widely when it comes to quantitative calculations. For example, in guns, pressures are of the order of 50,000 psi, which is perhaps two orders of magnitude higher than those used in rockets. As a result, the thermodynamics of the powder gases, for instance, are entirely different in the two cases.

Books

Structure of Metals. Crystallographic Methods, Principles, and Data (Metallurgy and Metallurgical Engineering Series), by C. S. Barrett, McGraw-Hill Book Co., Inc., N. Y., 1952 (second edition), 661 pp. $10.

Titanium—Its Occurrence, Chemistry and Technology, by J. Barksdale, Ronald Press Co., N. Y., 1949, 591 pp. $10.

Introduction to the Theory of Probability and Statistics, by N. Arley and K. R. Buch, John Wiley & Sons, Inc., N. Y., 1950, 236 pp. $4.

Small Particle Statistics, by G. Herdan (with a Guide to the Experimental Design of Particle Size Determinations, by M. L. Smith), Elsevier Press, Houston, Texas 1953, 520 pp. $12.

Detonation in Condensed Explosives, by J. Taylor, Oxford University Press, N. Y.; Oxford, at the Clarendon Press, 1952, 196 pp. $5.

Organic Chemistry, by R. Q. Brewster, Prentice-Hall, Inc., N. Y., 1953, 855 pp. $9.35.

Advances in Geophysics, Vol. I, H. E. Landsberg, editor, Academic Press, Inc., N. Y., 1952, 362 pp. $7.80.

Elements of Cartography, by A. H. Robinson, John Wiley & Sons, Inc., N. Y., 1953, 254 pp. $7.

Vision Through the Atmosphere, by W. E. K. Middleton, University of Toronto Press, Toronto, Canada, 1952, 250 pp. $8.50.

The Comets and Their Origin, by R. A. Lyttleton, Cambridge University Press, N. Y., 1953, 173 pp. $5.

Technical Literature Digest

M. H. SMITH and M. H. FISHER

The James Forrestal Research Center, Princeton University, Princeton, N. J.

Jet Propulsion Engines

A Note on the Performance of Ducted Fans, by Bryan Thwaites, *Aeron. Q.*, vol. 4, part II, Feb. 1953, pp. 179–185.

Theory and Practice of Gas Turbine Power Plants for Helicopters, by Igor B. Bensen, *Amer. Helicopter*, vol. 30, May 1953, pp. 6–10, 13.

Hydraulic Regulation of Feeding of Turbomachines, by Basile Demtchenko (in French), *France, Ministére de l'Air. Pub. Sci. Tech.*, no. 277, 1953, 182 pp.

Analysis of the Performance Characteristics of Turbojet Engines as a Function of Operating Conditions, by Ludovico Pascuci (in Italian), *Aerotecnica*, vol. 33, Feb. 1953, pp. 94–99.

Possibilities of Turbojets and Ramjets at Supersonic Speeds, by Gaspare Santangelo (in Italian), *Aerotecnica*, vol. 33, Feb. 1953, pp. 114–117.

Research and Development Progress, Propulsion, by Abe Silverstein, *Aviation Age*, vol. 19, June 1953, pp. 182–189.

Flying Tests on Supersonic Ram Jet Tubes at Low Subsonic Speed, by Irene Sänger-Bredt (in German), *VDI-Forschungsheft*, no. 437, 1953, pp. 40–60.

Physical Fundamentals of Jet Propulsion, by Eugen Sänger (in German), *VDI-Forschungsheft*, no. 437, 1953, pp. 5–25, 46 references.

Specialization in Turbojet Engine Design, by Bill Krase and Bob Neitzel, *Aero Digest*, vol. 66, June 1953, pp. 74, 76, 78–80, 82, 84, 86, 88–95.

Research on Aerodynamic Noise from Jets and Associated Problems, by E. J. Richards, *J. Roy. Aeron. Soc.*, vol. 57, May 1953, pp. 318–342, 25 references.

Some NACA Research on Centrifugal Compressors, by I. A. Johnsen, and Ambrose Ginsburg, *Trans. ASME*, vol. 75, July 1953, pp. 805–817.

Periodic Flow Regenerator—a Summary of Design Theory, by J. E. Coppage and A. L. London, *Trans. ASME*, vol. 75, July 1953, pp. 779–787.

The Rotary Regenerative Air Preheater for Gas Turbines, by A. T. Bowden and W. Hryniszak, *Trans. ASME*, vol. 75, July 1953, pp. 767–777.

Ramjet Possibilities, *Flight*, vol. 114, July 3, 1953, pp. 7–12.

Aircraft Powerplant Seals, by Norman F. Rooke, *SAE J.*, vol. 61, July 1953, pp. 23–29.

Exhaust Augmented Engine Cooling, *Shell Aviation News*, no. 179, May 1953, pp. 19–20.

Theory and Practice of Gas Turbine Power Plants for Helicopters, part II, by Igor B. Bensen, *Amer. Helicopter*, vol. 31, June 1953, pp. 10–13, 16.

Tailpipe "Teeth" Cut Jet Engine Noise, *Aviation Week*, vol. 59, July 6, 1953, pp. 28–29.

Heat Transfer and Fluid Flow

On the Noise Emanating from a Two-Dimensional Jet Above the Critical Pressure, by Alan Powell, *Aeron. Q.*, vol. 4, part II, Feb. 1953, pp. 103–122, 12 references.

Heat Transfer to Bodies in a High-Speed Rarefied-Gas Stream, by Jackson R. Stalder, Glen Goodwin, and Marcus O. Creagor, *NACA Rep.*, no. 1093 (supersedes *NACA TN* 2438), 1952, 9 pp.

Physical Phenomena in Gas Jets. Final Report, by Maryland University, Institute for Fluid Dynamics and Applied Mechanics, Oct. 1952, 53 pp. Contents: Optical Study of Compressible Jets, by D. Bershader and B. Cary, pp. 1—20; On Supersonic Flow of a Two-Dimensional Jet in Uniform Stream, by S. I. Pai, pp. 21–32 (*J. Aero. Sci.*, vol. 19, Jan. 1952, pp. 61–65); Problems in the Study of Turbulence, by R. Betchov, pp. 44–53; Axially Symmetrical Jet Mixing of a Compressible Fluid, by S. I. Pai, pp. 33–43 (*Q. Appl. Math.*, vol. 10, July 1952, pp. 141–148).

Shape and Thickness of Shock Fronts in Argon, Hydrogen, Nitrogen, and Oxygen, by E. F. Greene, and D. F. Hornig, *J. Chem. Phys.*, vol. 21, April 1953, pp. 617–623.

Flow Changes in Gases in Which Mass and Impulse are Conserved, by L. G. Dawson, *Aeron. Q.*, vol. 4, part II, Feb. 1953, pp. 193–204.

A Note on the Theory of the Constant-Area Mixing of Compressible Flows as Applied to High-Speed Wind Tunnel Design, by F. G. Irving, *Aeron. Q.*, vol. 4, part II, Feb. 1953, pp. 164–178.

On the Stability of the Flow of Gas out of a Compressor, by J. M. Stephenson, *J. Roy. Aeron. Soc.*, vol. 57, May 1953, pp. 345–346.

Schlieren Analysis of Supersonic Three-Dimensional Flows, by Claude Picard (in French), *Recherche Aeron.*, no. 32, March-April 1953, pp. 15–19.

Calculation of a Nozzle and of a Profile in the Hodograph Approximation, by A. Gilles (in French), *Recherche Aéron.*, no. 32, March-April 1953, pp. 1–10.

Calculation of Cascade Flows by a Field of a Series of Whirls, by A. Betz (in German), *Z. Angew. Math. Mech.*, vol. 33, no. 4, April 1953, pp. 113–116.

A Visualization Study of Secondary Flows in Cascades, by Arthur G. Hanson, *NACA TN* no. 2947 (formerly *RM* no. E52F19), May 1953, 93 pp.

Measurement of Heat Transfer and Skin Friction at Supersonic Speeds; Preliminary Results of Measurements on Flat Plate at Mach Number of 2.5, by J. E. Johnson and R. J. Monoghan, *Gt. Brit. Aeron. Res. Council, Current Paper*, no. 59 (formerly *ARC TR* 12,483, *RAE TN* Aero 1994), 1951, 18 pp., 17 figs.

One-Dimensional High-Speed Flows, by J. Kestin and S. K. Zaremba, *Aircr. Engng.*, vol. 25, June 1953, pp. 172–175, 179; 19 references.

Flows Through Nozzles and Related Problems of Cylindrical and Spherical Waves, by Yu Why Chen, *Comm. Pure Appl. Math.*, vol. 6, May 1953, pp. 179–228; 22 references.

Pulsed Surface Heating of a Semi-Finite Solid, by J. C. Jaeger, *Q. Appl. Math.*, vol. 11, April 1953, pp. 132–137.

Subsonic Flow of Air Through a Single-Stage and Seven-Stage Compressor, by Chung-Hua Wu, *NACA TN*, no. 2961, June 1953, 32 pp.

Experimental Investigation of the Mixing Loss Behind the Trailing Edge of a Cascade of Three 90° Supersonic Turning Passages, by Luke L. Luccini, *NACA RM* L50F21a, Aug. 1950 (declassified from Confidential 4/13/53), 31 pp.

A Method for Stabilizing Shock Waves in Channel Flow by Means of a Surge Chamber, by Stanford E. Neice, *NACA TN* no. 2694, June 1953, 46 pp.

Theoretical and Experimental Investigation of the Flow in a Duct of Varying Cross-Section, with Particular Application to the Design of Ducts for Free Flight Ground-Launched Model Tests, by C. H. E. Warren, R. E. Dudley, and P. J. Herbert, *Gt. Brit. Aeron. Res. Council, Current Paper* no. 60 (formerly *ARC TR* no. 13,726, *RAE TN* Aero 2064), 1951, 25 pp., 12 figs.

Radial-Axial Heat Flow in Regions Bounded Internally by Circular Cylinders, by J. H. Blackwell, *Can. J. Phys.*, vol. 31, May 1953, pp. 472–479.

Efficiency and Drag of an Axial-Flow Compressor Stage, by J. M. Stephenson, *Aircr. Engng.*, vol. 25, June 1953, pp. 158–160.

Preliminary Analysis of Axial-Flow Compressors Having Supersonic Velocity at the Entrance of the Stator, by Antonio Ferri, *NACA RM* no. L9G06, Sept. 1949 (declassified from Confidential 4/13/53), 36 pp.

Theoretical and Experimental Analysis of Low-Drag Supersonic Inlets Having a Circular Cross Section and a Central Body at Mach Numbers of 3.30, 2.75, and 2.45, by Antonio Ferri and Louis Nucci, *NACA RM* L8H13, Nov. 1948 (declassified from Confidential 4/13/53), 89 pp.

Combustion

Factors Controlling the Combustion of Zirconium Powders, by Holger C. Anderson, Lawrence H. Belz, *J. Electrochem. Soc.*, vol. 100, May 1953, pp. 240–249.

A Theoretical Model of a Gaseous Combustion Wave Governed by a First-Order Reaction, by Raymond Friedman and Edward Burke, *J. Chem. Phys.*, vol. 21, April 1953, pp. 710–714.

Aerothermodynamics and Combustion Theory, by Theodore von Kármán, *Aerotecnica*, vol. 33, Feb. 1953, pp. 80–86.

Radical Reactions of Nitric Acid in Flames, by G. K. Adams, W. G. Parker, and H. G. Wolfhard, *Discussions Faraday Soc.*, no. 14, 1953, pp. 97–103.

Free Radicals in Explosions Studied by Flash Photolysis, by R. G. W. Norrish, *Discussions Faraday Soc.*, no. 14, 1953, pp. 16–22.

The Mode of Action of Lead Tetraethyl

EDITOR'S NOTE: This collection of references is not intended to be comprehensive, but is rather a selection of the most significant and stimulating papers which have come to the attention of the contributors. The readers will understand that a considerable body of literature is unavailable because of security restrictions. We invite contributions to this department of references which have not come to our attention, as well as comment on how the department may better serve its function of providing leads to the jet propulsion applications of many diverse fields of knowledge.

as an Inhibitor of Combustion Processes, by G. H. N. Chamberlain, D. E. Hoare, and A. D. Walsh, *Discussions Faraday Soc.*, no. 14, 1953, pp. 89–96.

A Slot Burner Method for Studying Combustion Wave Instability, by G. H. Markstein and L. H. Somers, *J. Chem. Phys.*, vol. 21, May 1953, p. 941.

Burning Velocity Measurement, by Dorothy M. Simon and Edgar L. Wong, *J. Chem. Phys.*, vol. 21, May 1953, p. 936.

Reaction Processes Leading to Spontaneous Ignition of Hydrocarbons, by Charles E. Frank and Angus U. Blackham, *NACA TN* no. 2958, June 1953, 27 pp.

Flame Propagation Rates and the Chemical Nature of the Attachment Surface, by L. Lapidus, J. B. Rosen, and R. N. Wilhelm, *Princeton Univ., Forrestal Res. Center, Chemical Kinetics Project, TR* no. 1, April 1953, 23 pp., 12 figs.

The Thermodynamics of Combustion Gases: Temperatures of Methane-Air, Propane-Air, and Ethylene-Air Flames, by Robert W. Smith, Jr., John Manton, and Stuart R. Brinkley, Jr., *Bureau of Mines. Report of Investigations* 4983, June 1953, 21 pp.

Studies on the Spontaneous Ignition of Fuels Injected into a Hot Air Stream. V. Ignition Delay Measurements of Hydrocarbons, by B. P. Mullins, *Fuel*, vol. 32, July 1953, pp. 363–379.

Studies on the Spontaneous Ignition of Fuels Injected into a Hot Air Stream. IV. Ignition Delay Measurements on Some Gaseous Fuels at Atmospheric and Reduced Static Pressures, by B. P. Mullins, *Fuel*, vol. 32, July 1953, pp. 343–362.

Spontaneous Ignition of Fuels Injected into a Hot Air Stream. III. Effect of Chemical Factors upon the Ignition Delay of Kerosene-Air Mixtures, by B. P. Mullins, *Fuel*, vol. 32, July 1953, pp. 327–342.

Analytical (Power Series) Solutions to the Equations of Flame Propagation, by J. O. Hirschfelder and Edwin S. Campbell. *Wisconsin Univ. Naval Res. Lab.* CM-784, May 1953, 117 pp.

Fuels, Propellants and Materials

Heat Capacities, Latent Heats and Entropies of Fluorine from 13° to 85°K; Heats of Transition, Fusion, Vaporization, and Vapor Pressures of the Liquid, by Jih-Heng Hu, David White, and Herrick L. Johnston, *Ohio State Univ. Res. Foundation, TR* no. 283–23, April 1953, 11 pp.

An Investigation of Boron Carbide, by Frank W. Glaser, David Moskowitz, and Benjamin Post, *J. Appl. Phys.*, vol. 24, June 1953, pp. 731–733.

Determination of Excessive Sludge Formation in Mixed Acid Storage Drums, by Arthur E. Lenehan, *Naval Air Rocket Test Sta. Rep.* no. 29, Feb. 1953, 8 pp.

Optical Absorbance of the Ternary System of Nitric Acid-Nitrogen Dioxide-Water, by Scott Lynn, David M. Mason, and B. H. Sage, *Calif. Inst. Tech. Jet Propulsion Lab. Progress Rep.* no. 20-187, Jan. 1953, 22 pp.

Storage and Handling of Nitrogen Oxides, by F. T. Selleck, H. H. Reamer, and B. H. Sage, *Indust. Engng. Chem.*, vol. 45, April 1953, pp. 814–819.

Studies on Hydrazine. Technical Report No. 1. The Photolysis of Ammonia at 1849Å in a Flow System, by C. C. McDonald, A. Kahn, and H. E. Gunning, *Illinois Inst. Tech. Department of Chemistry*, Feb. 1953 (declassified from Restricted June 23, 1953), 20 pp.

Effect of Prestraining on Recrystallization Temperature and Mechanical Properties of Commercial, Sintered, Wrought Molybdenum, by Kenneth C. Dike and Roger A. Long, *NACA TN* 2973, July 1953, 25 pp.

Investigation of Effects of Grain Size upon Engine Life of Cast AMS 5385 Gas Turbine Blades, by Charles A. Hoffman and Charles A. Gyorgak, *NACA RM* no. E53D06, July 1953, 21 pp.

Behavior of Materials Under Conditions of Thermal Stress, by Samuel S. Manson, *NACA TN* no. 2933, July 1953, 105 pp.

Physical-Chemical Topics

Analytical Procedures for Rocket Propellants. VII. Mixed Acid, by John D. Clark, *Naval Air Rocket Test Sta. Rep.* no 24, Sept. 1952, 18 pp.

Kinetics of Two Exchange Reactions Involving Diborane, by P. Calvin Maybury and W. S. Koski, *J. Chem. Phys.*, vol. 21, April 1953, pp. 742–747.

The Thermal Decomposition of Nitrous Oxide, by Lewis Friedman and Jacob Bigeleisen, *J. Amer. Chem. Soc.*, vol. 75, May 5, 1953, pp. 2215–2217.

The Reactivity of Free Radicals, *Discussions Faraday Soc.* no. 14, 1953, 256 pp.

Free Radicals by Mass Spectrometry. Part II. The Thermal Decomposition of Ethylene Oxide, Propylene Oxide, Dimethyl Ether, and Dioxane, by F. P. Lossing, K. U. Ingold, and A. W. Tickner, *Discussions Faraday Soc.* no. 14, 1953, pp. 34–44.

Studies of Free Radical Reactivity by

the Methods of Flash Photolysis; the Photochemical Reaction Between Chlorine and Oxygen, by George Porter and Franklin J. Wright, *Discussions Faraday Soc.* no. 14, 1953, pp. 23–34.

The Absorption Spectrum of Free NH_2 Radicals, by G. Herzberg and D. A. Ramsay, *Discussions Faraday Soc.* no. 14, 1953, pp. 11–16.

Infra-Red Spectrum of Nitric and Deuteronitric Acid Vapour. Completion of the Identification of the Fundamental Frequencies. Entropy of Nitric Acid. Barrier Resisting Rotation of the Hydroxyl Group, by Henry Cohn, C. K. Ingold, and H. G. Poole, *J. Chem. Soc.*, Nov. 1952, pp. 4272–4282.

Molecular Sound Velocity and Molecular Compressibility of Liquid Mixtures, by Otohiko Nomoto, *J. Chem. Phys.*, vol. 21, May 1953, pp. 950–951.

Kinetics of Reaction Between Ammonia and Oxygen in a Quartz Vessel, by Henry Wise and Maurice F. Frech, *J. Chem. Phys.*, vol. 21, May 1953, pp. 948–949.

The Normal Boiling Points of Oxygen on the Thermodynamic Scale, by J. G. Aston and G. W. Moessen, *J. Chem. Phys.*, vol. 21, May 1953, p. 948.

Monometric Determination of the Density of Liquid Ozone, by Callaway Brown and Karl D. Franson, *J. Chem. Phys.*, vol. 21, May 1953, pp. 917–919.

Applied Chemical Kinetics. VI. Determination of Kinetic Constants. c. Parallel reactions, by J. C. Jungers and A. Giraud (in French), *Rev. Inst. français Pet. Am. Combust. Liquides*, vol. 8, April 1953, pp. 152–168.

Contribution to the Theory of Fast Reaction Rates, by R. DeVogelaere and M. Boudart, *Princeton Univ. James Forrestal Res. Center. Chemical Kinetics Project, TR* no. 3, July 1953, 40 pp.; 6 figs.

Kinetics and Mechanisms of the "Water-Gas" Reactions, by W. M. Graven and F. J. Long, *Princeton Univ. James Forrestal Res. Center. Chemical Kinetics Project, TR* no. 2, May 1953, 27 pp., 10 figs.

Frictional Behavior of Polyethylene, Polytetrafluoroethylene and Halogenated Derivatives, by R. C. Bowers, W. D. Clinton, and W. A. Zisman. *Naval Res. Lab. Rep.* no. 4167, May 1953, 21 pp.

Transport Properties of Gases Obeying a Modified Buckingham (Exp-Six) Potential, by Edward A. Mason, *Wisconsin Univ. Naval Res. Lab. Rep.* ONR-1, June 1953, 64 pp.

Instrumentation and Experimental Techniques

Meter Measures Fuel Flow in Pounds (Gavco Corp., Mass Flowmeter), *Aviation Week*, vol. 58, April 6, 1953, pp. 62, 64, 66.

Temperature Measurement; the Use of Heat-Sensitive Colour-Changing Pigments, *Aircr. Prod.*, vol. 15, May 1953, p. 184.

Apparatus for the Measurement of the Particle Content of Air (in High Speed Wind Tunnels), by P. Durrenberger (in French), *Recherche Aéron.*, no. 32, March-April 1953, p. 14.

Microsecond Photography of Rockets in Flight, by E. Barkofsky, R. Hopkins, and S. Dorsey, *Electronics*, vol. 26, June 1953, pp. 142–147.

Frequency Modulated Magnetic Tape Recording and Playback Instrumentation System, by Joseph Petes, *Naval Ordn. Lab. Rep.* no. 1167, pp. 75–136; *Navord Rep.* no. 2713, Feb. 1953.

Development of an Inductance Type Accelerometer for Use in a Frequency Modulated Recording System, by Benjamin Sussholz, *Naval Ordn. Lab. Rep.* no. 1167, pp. 21–67; *Navord Rep.* no. 2712, Feb. 1953.

Three-Dimensional Liquid Analog for the Determination of Temperature Distribution, by G. A. Sterbatzel and J. L. Beal, *Project Squid, TM* no. CAL-44, Oct. 1952, 22 pp., 14 figs.

The Teopler Schlieren Apparatus, by D. W. Holder and R. J. North, *Gt. Brit. Aeron. Res. Council, Reps. and Mem.* no. 2780 (formerly *ARC TR* no. 13,068), 1953, 13 pp., 6 figs.

A Variable High Frequency Light Synchronized with a High-Speed Motion-Picture Camera to Provide Very Short Exposure Times, by Walter Frank Lindsey and Joseph Burlock, *NACA TN* no. 2949, May 1953, 17 pp.

Possibility of Simulation of a Flying Structure With Free Control Surfaces by a Servomechanism, by G. Coupry and R. Valid (in French), *Recherche Aéron.*, no. 32, March-April 1953, pp. 29–34.

A Small Pirani Gage for Measurements of Non-Steady Flow Pressures, by Miroslav John Pilney, *NACA TN* no. 2946, June 1953, 36 pp.

Experiments with Static Tubes in a Supersonic Air-Stream. Parts I and II, by D. W. Holder, R. J. North, and A. Chinneck, *Gt. Brit. Aeron. Res. Council, Reps. and Mem.* no. 2782 (formerly *ARC TR* no. 13,269 and 13,268), 1953, 14 pp., 13 figs.

Measurement and Registration of Short Time Intervals, by Jan Groeneveld (in German), *Z. Phys.*, vol. 134, April 17, 1953, pp. 645–647.

An Instrument for the Direct Measurement of Intense Thermal Radiation, by Robert Gardon, *Rev. Sci. Instrum.*, vol. 24, May 1953, pp. 366–370.

A Method of Control of a Predetermined Flow Rate, by H. H. Reamer and B. H. Sage, *Rev. Sci. Instrum.*, vol. 24, no. 5, May 1953, pp. 362–366.

A High Temperature Thermo-Regulator, by F. Rosebury, *Rev. Sci. Instrum.*, vol. 24, no. 5, May 1953, pp. 398–399.

Continuous Recording of Pressures for Supersonic Wind-Tunnel Calibration, by L. P. Gieseler, *Navord Rep.* no. 2744, Jan. 1953, 14 pp., 7 figs.

Measurement by Times Spark Shadowgraphs of Shock Velocities in the Shock Tube, by Herbert L. Hoover, *Lehigh Univ. Inst. of Res. TR* no. 3, July 1953, 24 pp.

A Modern Jet Engine Test Plant (Standard Motors, Coventry), *Aeroplane*, vol. 84, May 15, 1953, p. 643.

Terrestrial Flight, Ballistics, and Vehicle Design

Ghost Jets in the Sky (United Air Lines research on simulated jet flight service), *Aviation Age*, vol. 19, May 1953, pp. 6–9.

The Air Force and Guided Missiles, by E. P. Mechling, *Ordnance*, vol. 37, March-April 1953, pp. 789–790.

The Case for Pod-Mounted Jet Engines, by David A. Anderton, *Aviation Week*, vol. 58, May 18, 1953, pp. 29–30, 32–34, 37–38.

The Case for the Underslung Nacelle on the Jet Transport, by B. T. Salmon, *Aviation Age*, vol. 19, May 1953, pp. 84–91.

Properties and Tables of Generalized Rocket Functions for Use in the Theory of Rockets with a Constant Slow Spin, by J. Barkley Rosser and R. J. Walker, Cornell Univ., 1953, 111 pp.

An Experimental Solution to the Lagrange Ballistic Problem, by A. E. Seigel, *Navord Rep.* 2693 (Aeroballistic Research Rep. 80), Sept. 1953, 9 pp.

Guided Missiles—Comments on Surface Based Antiaircraft Missiles, by Henry H. Porter, *Aero. Engng. Rev.*, vol. 12, July 1953, pp. 24–29.

Parachute Recovery of Ryan "Firebee" Jet Propelled Target Aircraft, *Shell Aviation News*, no. 179, May 1953, pp. 21.

More about Jindivik, *Aeroplane*, vol. 84, June 1953, pp. 790.

Recent Developments in Rockets and Guided Missiles in the United States, by Norman J. Bowman, *J. Space Flight*, vol. 5, May 1953, pp. 1–9.

U. S. Turboprop Transport Future, by C. R. Smith, *Aero Digest*, vol. 66, June 1953, pp. 17–19.

Space Flight

The Food and Atmosphere Control Problem on Space Vessels. Part I. Chemical Purification of Air, by Norman J. Bowman, *J. Brit. Interplan. Soc.*, vol. 12, May 1953, pp. 118–123.

Optimum Conditions for Multi-Stage Rockets Rising Vertically in a Gravitational Field, by Irene Sänger-Bredt (in German), *VDI-Forschungsheft*, no. 437, 1953, pp. 26–39.

Astrophysics, Aerophysics, and Atomic Physics

Table of Isotopes, by J. M. Hollander, I. Perlman, and G. T. Seaborg, *Revs. Mod. Phys.*, vol. 25, April 1953, pp. 469–651.

The Energy Levels and the Structure of Light Nuclei, by D. R. Inglis, *Revs. Mod. Phys.*, vol. 25, April 1953, pp. 390–450.

Light Pulses from the Night Sky, by J. V. Jelley and W. Galbraith, *Phil. Mag.*, vol. 44, June 1953, pp. 619–622.

Cloud-Chamber Observations of the Heavy Charged Unstable Particles in Cosmic Rays, by H. S. Bridge, C. Peyron, B. Rossi, and R. Safford, *Phys. Rev.*, vol. 90, June 1, 1953, pp. 921–933.

Ratio of Neutral to Charged Particles in the Nuclear Interacting Component of Cosmic Rays, by K. Greisen and W. D. Walker, *Phys. Rev.*, vol., 90, June 1, 1953, pp. 915–920.

Cosmic Radiation Intensity-Time Variations and their Origin. I. Neutron Intensity Variation Method and Meteorological Factors, by J. A. Simpson, W. Fonger, and S. B. Treiman, *Phys. Rev.*, vol. 90, June 1, 1953, pp. 934–950.

The Instability of a Layer of Fluid Heated Below and Subject to Coriolis Forces, by S. Chandrasekhar, *Proc. Roy. Soc.*, vol. 217A, May 7, 1953, pp. 306–327.

The Coriolis Force of a Sphere in a Flow, by Friederich Bayer-Helms and Heinz Pick (in German), *Z. Phys.*, vol. 134, April 17, 1953, pp. 582–595.

Fluctuations and Latitude Effect of Cosmic Rays at High Altitudes and Latitudes, by H. V. Neher, V. Z. Peterson, and E. A. Stern, *Phys. Rev.*, vol. 90, May 15, 1953, pp. 655–674.

The Penetrating Component of Cosmic Radiation in the Upper Atmosphere, by J. D. Pullar and E. G. Dymond, *Phil. Mag.*, vol. 44, June 1953, pp. 565–577.

General Topics

From Dirigibles to Missiles, by G. A. Crocco (in Italian), *Aerotecnica*, vol. 33, Feb. 15, 1953, pp. 6–9.

The Birth of an Engine; British Practice in Aviation Engine Procurement and Development, by F. R. Banks, *Aero. Engng. Rev.*, vol. 12, June 1953, pp. 31–43.

Aeronautical Acoustics, *Flight*, vol. 63, June 12, 1953, pp. 755–758.

Wright Brothers *pioneers in piston power in 1903*

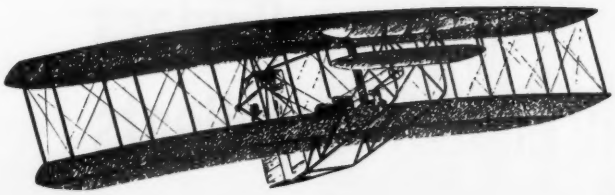

PROGRESS
50TH ANNIVERSARY OF POWERED FLIGHT
SECURITY

marquardt *pioneers in jet power in 1953*

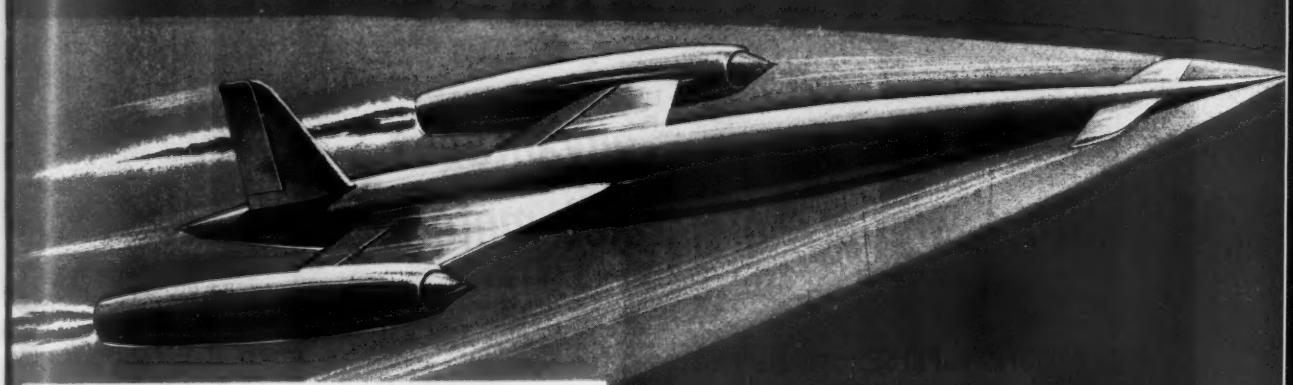

The Institute of Aeronautical Sciences selected Marquardt engineers to produce the replica of the original Wright Brothers engine for permanent display at their Durand Aeronautical Museum.

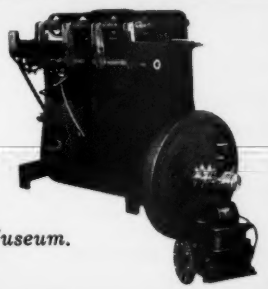

Aviation has come a long way from the piston powered craft in 1903, pioneered by the Wright Brothers, to ramjet speeds of mach 4. Marquardt has been the pioneer in the research and development of ramjets, afterburners, air turbine accessory drives and thrust controls of advanced design. These units are currently in production to meet your requirements. Let us send you our illustrated engineering manuals.

marquardt AIRCRAFT CO.

ATTENTION ENGINEERS—Write today for full information concerning your future with Marquardt.

Van Nuys, California

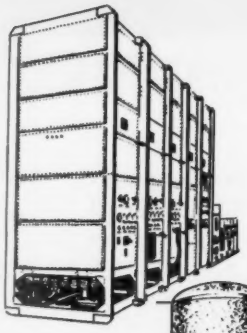

LIQUID OXYGEN GENERATORS
An air-transportable plant for the separation of high-purity oxygen from the air.

LIQUEFIED-GAS STORAGE CONTAINERS
Containers for the storage or transport of liquefied gases such as liquid hydrogen or oxygen.

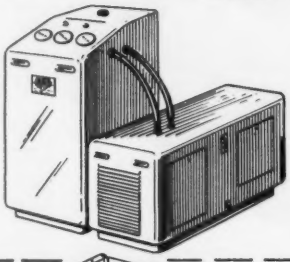

LIQUID OXYGEN PUMPS
A compact, noncontaminating unit for supplying high-pressure oxygen gas from low-pressure liquid oxygen storage containers.

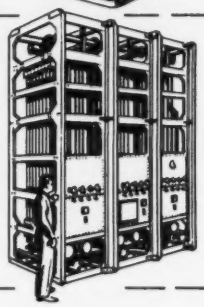

HEAT EXCHANGERS
A gas-to-gas heat exchanger with exceptional characteristics.

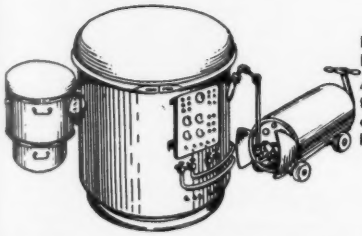

HELIUM REFRIGERATORS
A practical system for the prevention of evaporation loss in stored liquefied gases.

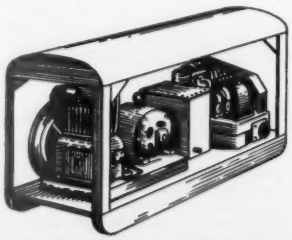

AIR COOLERS
A unit which provides cooled, compressed air which is free of dirt, oil, or entrained water.

THERMODYNAMICS • HEAT TRANSFER • REFRIGERATION TO MINUS 456°F • GAS LIQUEFACTION • VACUUM ENGINEERING • ELECTROMAGNETISM • MECHANICAL DESIGN • VIBRATION

UNIQUE
PROTOTYPE DEVELOPMENT

Arthur D. Little, Inc. has blended its scientific and engineering skills in the Mechanical Division to provide industry with a unique service . . .

Scientists in the fields of chemistry, physics, metallurgy, mathematics, biology, electronics and technical economics regularly engaged in diversified research and development projects join with our engineers in prototype development of equipment requiring a high level of engineering skills.

Our staff is experienced in interpreting the ideas of industry and following through with the perfection of specialized equipment.

ADL
Mechanical Division

WRITE FOR BROCHURE RJ28-5

MECHANICAL DIVISION
Arthur D. Little, Inc.
30 MEMORIAL DRIVE — CAMBRIDGE 42, MASS.
Offices in New York, St. Louis, and Mexico City

CREATIVE TECHNOLOGY SINCE 1886

multiply your engineering manpower!

* EQUATION SOLVING
SYSTEM SIMULATION
TESTING

do it with EASE*

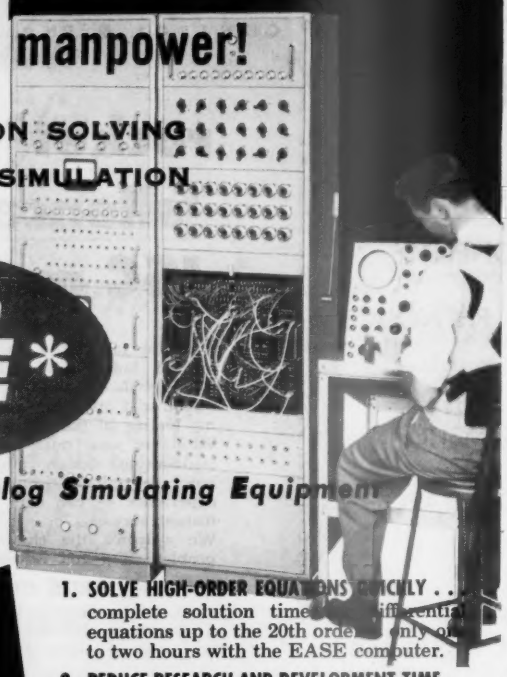

***Electronic Analog Simulating Equipment**

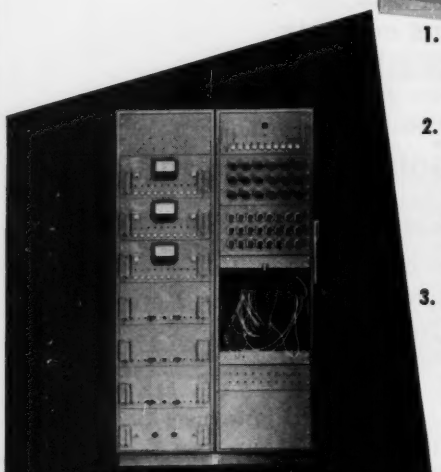

EASE 30-channel linear computer

1. **SOLVE HIGH-ORDER EQUATIONS QUICKLY . . .** complete solution time for differential equations up to the 20th order in only one to two hours with the EASE computer.
2. **REDUCE RESEARCH AND DEVELOPMENT TIME . . .** functioning of an entire dynamic system can quickly be simulated on the EASE. Effects of changing loads, forces, conditions and other variables can be determined rapidly and accurately—at a fraction of the time and cost of operational testing.
3. **SPEED PRODUCTION TESTING . . .** coupled with voltage transducers, the EASE computer can be channeled to physical systems, subsystems or components. By substituting for, and simulating, associated equipment it provides substantial savings in test time.

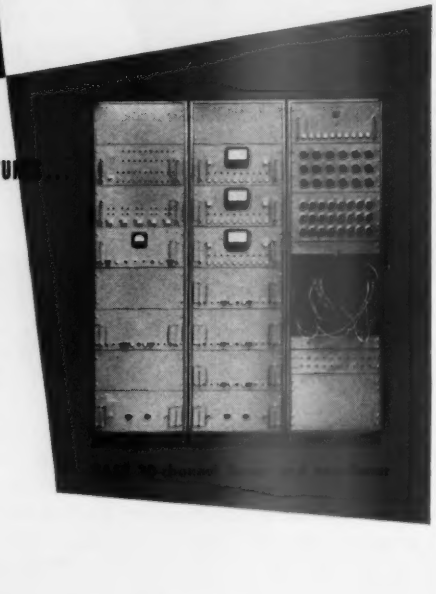

INVESTIGATE THESE IMPORTANT EASE FEATURES

SIMPLE TO OPERATE AND MAINTAIN . . . any engineer or mathematician who can write the equation can solve it on the EASE computer with only a few hour's training.

COMPACT, COMPLETELY SELF-CONTAINED . . . the entire unit requires less than 8 sq. ft. of floor space, is complete with its own regulated power supply . . . you simply plug it in to a 20 ampere, 110 v. a.c. line!

LOW COST . . . the EASE is the world's first high-quality computer to be mass-produced in practical commercial form. The result is low cost without sacrifice in utility or quality.

For complete data, please request Bulletin F-9

Berkeley *division*
BECKMAN INSTRUMENTS INC.
2200 WRIGHT AVE., RICHMOND, CALIF.

How Tight is LEAKPROOF?

CIRCLE-SEAL provides *dead tight* sealing at pressures • as low as 1" H_2O • as high as proof pressure.

Dead tight means NO bubbles, NO dripping.

200 SERIES combines low cracking pressure, high strength. Well suited to both high pressure pneumatic systems and low pressure pneumatic and vacuum service.

800 SERIES provides physical and functional characteristics comparable to swing check valves—insures zero leakage even with fuel or fuel vapor—can be mounted in any position.

	200 Series	800 Series
Pressures:	0 to 3000 psi	0 to 600 psi
Temperatures:	—65° F to 280° F	—65° F to 170° F
Cracking Pressure:	normally less than 1 psi	6" to 8" H_2O
Sizes:	¼" to ¾" Tube	¼" to 1" Tube
Suitability:	air, carbon dioxide, nitrogen, helium, oxygen, etc.	air, carbon dioxide, alcohol, water, aircraft and jet fuel, fuel vapor, etc.

CIRCLE SEAL
precision check valves

JAMES-POND-CLARK
2181 E. Foothill Blvd., Pasadena 8, Calif.
Engineering data sent free of charge on request

Index to Advertisers

SUPERIOR PERFORMANCE

On 3 Cycles to 20 Megacycles

The LA-239 C Oscilloscope

DATA

1. Wider Bandwidth: Complex waves from 5 Cycles to 15 Megacycles. Sine waves from 3 Cycles to 20 Megacycles.

2. Extended Sweep Frequencies: Linear from 10 Cycles to 20 Megacycles internally synchronized. Triggered sweep, from single random impulses to irregular pulse-intervals up to as high as 6 Megacycles.

3. Square Wave Response: Rise time 0.042 Microseconds; only 5% droop on flat-topped pulses as long as 30,000 Microseconds duration.

4. Greater Stability: Electronically regulated power supplies throughout to maintain accuracy and constant operation under varying line conditions or line surges. You can display surges on the line from which Model LA-239C is being powered without distortion of the trace!

5. Higher Signal Sensitivity: Maximum sensitivity without Probe: 10.4 millivolts. With Probe: 100 millivolts. (Maximum signals, 125 V. Peak and 450 V. Peak respectively.)

6. Timing Markers: Interval Markers of 0.2; 1; 5; 20; 100; 500; or 2,000 Microseconds may be superimposed on the trace for the accurate measurement of the time base.

7. Voltage Calibration: Signal amplitude is compared against a 1,000 cycle square wave (generated internally) the amplitude of which is controlled by a step-and-slide attenuator calibrated in peak volts. (A jack is provided to deliver 40V Peak for use in calibrating other instruments.)

8. Sweep Delay: Any portion of the sweep longer than a 10 Microsecond section may be expanded by 10:1 for detailed study of that portion of the signal.

9. Power Source: 110 to 130 V AC; from 50 to 1,000 cycles. 295 Watts. (Fused at 4 Amperes.)

10. Dimensions: In Bench Cabinet: 19½ in. Wide; 15¼ in. High; 16¾ in. Deep. In Rack Mounting (With cabinet removed to fit standard relay rack): 19½ in. Wide; 14 in. High.

THE LAVOIE MODEL LA-239C has been designed to surpass the high performance of the TS-239A/UP, which has been the standard test oscilloscope for the Armed Services since its introduction. Model LA-239C is the result of a long period of research and development which has included the study of new tubes, new circuits, and new techniques. Rugged design has been combined with functional simplicity to produce an instrument as attractive as it is efficient.

To create a circuit that will produce a certain complex wave form, or study transients and pulse phenomena, no better precision instrument is available today.

Lavoie Laboratories take pride in offering this precision oscilloscope as the combination of engineering perfection and manufacturing skill.

UHF

Lavoie Laboratories, Inc.

MORGANVILLE, NEW JERSEY

DESIGNERS AND MANUFACTURERS OF ELECTRONIC EQUIPMENT